DEEP Report 5.01
Salford Energy House

Fabric Performance Testing

Prepared by Energy House Labs Research Group, University of Salford

David Farmer
Grant Henshaw
Dr Christopher Tsang
Benjamin Roberts
Prof. Richard Fitton
Prof. Will Swan

Contents

Executive Summary

One of the objectives of the Department for Energy Security and Net Zero (DESNZ) Demonstration of Energy Efficiency Potential (DEEP) Retrofit Project was to investigate the unintended consequences of fabric retrofit. The primary objective of the Energy House DEEP fabric performance tests was to assess the potential benefits of a whole house approach to retrofit against 'typical' retrofit practice that follows a piecemeal approach. The research involved in performing a staged whole house fabric retrofit of the Energy House that replicated a piecemeal retrofit. The Energy House's thermal elements were then adapted to be representative of a retrofit that had been performed following whole house approach retrofit principles. Fabric thermal performance testing took place at each stage of the retrofit process to assess the benefit and unintended consequences of applying retrofit measures individually and in combination.

The primary benefit of a whole house approach to retrofit was found to be the reduction in risk of surface condensation and mould growth at junctions. At the baseline stage, measurements indicated that 75% of the Energy House's junctions presented a risk. Following the piecemeal approach retrofit, 33% of the junctions were still considered to pose a risk. Despite reducing the risk at most junctions, the piecemeal approach retrofit created a risk at a ground floor junction. Following work to convert the piecemeal retrofit to a whole house approach retrofit, only the eaves was considered at risk. The residual risk present from the baseline stage was attributed to difficulty installing a piecemeal retrofit measure rather than issues with the design of the whole house approach retrofit or the conversion process. The whole house approach retrofit measures underperformed by 5% and external wall insulation (EWI) by 17%. This demonstrates that the whole house approach depends not only on design but also material performance, buildability, and workmanship to ensure its principles are realised in practice.

The whole house approach retrofit reduced the heat transfer coefficient (HTC) of the Energy House by 51% from baseline. However, it was not significantly different to the 50% HTC reduction from baseline achieved by the piecemeal retrofit. A 53% HTC reduction would have been achieved if the whole house approach measures had performed as predicted. As a result, the whole house approach retrofit would not result in significantly lower space heating energy bills than the piecemeal retrofit. Furthermore, the work required to convert the piecemeal retrofit to a whole house retrofit increased the cost of the retrofit by 61%. Although some of the additional cost can be attributed to converting a pre-existing piecemeal retrofit, the additional time and complexity inherent to whole house retrofit means that its additional cost is unlikely to be recouped via payback models that rely on energy bill savings alone. Fabric retrofit funding models must also consider the occupant health as well as energy and carbon reductions.

The EWI system was responsible for 78% of the HTC reduction and removed the risk of surface condensation and mould on the surface of walls and from the greatest number and length of junctions. However, the EWI system did not remedy the significant pre-existing risk along the eaves junction. The whole house approach measure of extending the eaves to link the loft insulation with the EWI was extremely effective at removing the risk, but significantly increases the cost of an EWI installation. The openings did not pose a risk following a piecemeal retrofit, so moving them in line with EWI was unnecessary in this instance. As funding for whole house approach measures through energy saving payback schemes is unlikely to be viable, their application should be targeted according to requirement. Survey tools are required to specify the appropriate whole house approach measures for a retrofit.

1 Introduction

This report provides findings from the fabric thermal performance tests that took place at the University of Salford (UoS) Energy House test facility during the Department for Energy Security and Net Zero (DESNZ) Demonstration of Energy Efficiency Potential (DEEP) Retrofit Project. The test programme was designed to compare the following approaches to the full fabric retrofit of solid wall dwellings:

1. **Piecemeal approach**. A piecemeal approach retrofit only considers reducing plane elemental heat losses. The piecemeal retrofit process is often cumulative and involves retrofitting individual elements in isolation. Retrofits typically occur sporadically and are not designed as part of a coordinated programme of works. Measures required to treat interfaces between elements (junctions) are omitted if they involve additional complexity and cost. Any improvements in thermal performance at junctions during a piecemeal retrofit process can be considered incidental.

2. **Whole house approach[1].** The "whole house approach" is a way of thinking about retrofit in manner that is holistic and risk based[2]. It seeks improve building fabric energy efficiency while minimising the risks posed to the health of occupants and the structure of a building. The whole house approach is incorporated within the PAS 2035:2019 standard[3]. Improvements in the thermal performance of junctions are intentional and designed to reduce the risk of surface condensation and mould growth.

The research involved sequentially retrofitting the Energy House's thermal elements to simulate a piecemeal retrofit. The Energy House's thermal elements were then adapted to be representative of a retrofit that had been performed following whole house approach retrofit principles. Fabric thermal performance measurements were performed at each stage the test programme. The aims of the test programme were to:

1. **Assess the benefits and drawbacks of a whole house approach retrofit**. The initial piecemeal retrofit provided a benchmark representative of 'typical' retrofit practice.

2. **Identify unintended consequences resulting from each retrofit approach**. The staged retrofit enabled the impact of individual measures to be assessed and to identify points during the retrofit process where risks either emerge or are addressed.

3. **Inform the conversion of pre-existing piecemeal retrofits**. By performing whole house approach measures after the piecemeal retrofit, the test programme provided insight into converting pre-existing piecemeal retrofits to whole house approach retrofits.

4. **Assess the repeatability of fabric retrofit measures**. Apart from the external wall insulation (EWI), all elements were retrofitted and measured at least twice during the test programme. Findings were also compared with previous Energy House retrofits.

It must be noted that work presented should be regarded as a case study and that findings and recommendations contained within this report may not be applicable to all dwellings.

---

[1] Whole house approach has been abbreviated as WHA in graphs, tables, and figures.
[2] STBA (2016), What is the Whole House Approach to Retrofit (https://stbauk.org/whole-house-approach/)
[3] BSI (2019), PAS 2035/2030:2019 Retrofitting dwellings for improved energy efficiency - specification and guidance, British Standards Institution, London

2 Methodology

2.1 Test subject

2.1.1 The Salford Energy House test facility

Testing was performed at the Salford Energy House test facility (Figure 1). It contains the Energy House, a replica Victorian solid wall end-terrace house constructed within an environmental chamber capable of replicating external air temperatures between -12 °C and +30 °C. It was built using reclaimed materials and traditional construction methods and can be retrofitted to most fabric thermal performance standards. The Energy House has a conventional hydronic central heating system with radiators in each room that can be served by a domestic gas condensing combination boiler or an air source heat pump. It has an infrared heating system and can also accommodate other forms of electric space heating. The Energy House shares a party wall with a similar building, referred to as the conditioning void. Environmental conditions in the chamber and conditioning void can be controlled and repeated across multiple test periods. This makes it possible to measure the impact of changes to the Energy House's building fabric and space heating provision with greater confidence and speed than houses in the field[4]. Please refer to Appendix A for more details of the Energy House construction and Appendix B for floor plans.
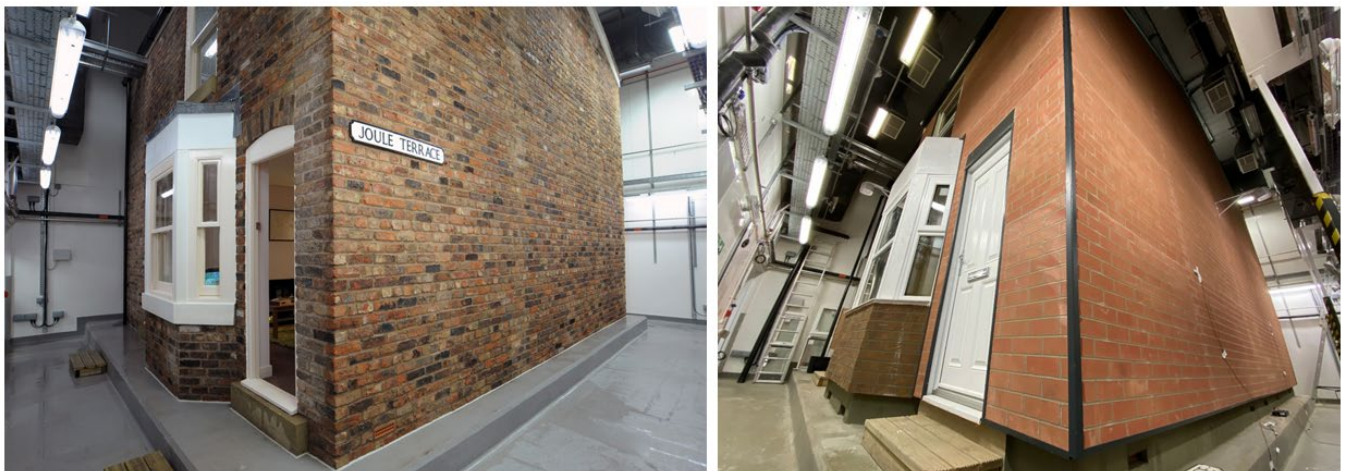
Figure 1: The Salford Energy House test facility pre-retrofit (left) and post-retrofit (right)

2.1.2 Previous Energy House whole house approach retrofits

Two previous whole house approach retrofits have been performed on the Energy House in 2013[5] and 2014[6]. Both retrofits were performed by Saint-Gobain and undertaken for

---

[4] The Energy House is frequently modified for test purposes. Therefore, baseline measurements of fabric and heating system performance are undertaken at the commencement of each project.

[5] For more details refer to: Farmer, D., Gorse, C., Swan, W., Fitton, R., Brooke-Peat, M., Miles-Shenton, D. & Johnston, D. (2017). Measuring thermal performance in steady state conditions at each stage of a full fabric retrofit to a solid wall dwelling. Energy and Buildings. 156. 10.1016/j.enbuild.2017.09.086.

[6] For more details refer to: Centre of Refurbishment Excellence (2015) Mark Weaver, Richard Fitton and Dave Farmer - Salford Energy House. [online video] Available at: https://youtu.be/l1WlL5NEqP4

commercial purposes according to 'best practice' retrofit principles. Where applicable, publicly available findings have been compared with findings from the Energy House DEEP retrofit to provide context. The Saint Gobain 2013 whole house approach retrofit provides the most useful comparator to the DEEP retrofit as the configuration of the fabric at the baseline and whole house approach full retrofit stages were similar.

2.1.3 Energy House DEEP baseline fabric configuration

The Energy House's thermal elements were adapted to provide a baseline that can be considered representative of the thermal performance of most English solid wall dwellings. 88% of which have uninsulated external walls, 87% have full double glazing, and 61% have less than 200 mm of loft insulation[7]. The timber sash windows were replaced with Window Energy Rating (WER) 'E' rated double glazed units (DGUs) in uninsulated uPVC frames to represent pre-2010 installations. The timber doors were replaced with Door Energy Rating (DER) 'E' rated uninsulated uPVC doors and frames, also simulating historical installations[8]. In the absence of robust data detailing the typical quality and depth of existing loft insulation in UK homes, 100 mm of correctly installed loft insulation was selected to represent baseline performance. Table 1 provides the DEEP baseline configuration of the Energy House's thermal elements and compares baseline elemental U-values calculated[9] in accordance with BRE 443[10] and ISO 6946[11] with RdSAP[12] assumed U-values.

Table 1: DEEP baseline configuration of the Energy House's thermal elements and calculated and RdSAP assumed U-values

Thermal element	Baseline construction	Area (m²)	Calculated U-value (W/m²K)	RdSAP assumed U-value (W/m²K)
External walls	Solid wall – 223 mm brick arranged in English bond (5 courses) with 9 mm lime mortar and 10.5 mm British Gypsum Thistle hardwall plaster with a 2 mm Thistle Multi-Finish final coat. The ground and intermediate floor joists are built-in to the gable wall.	62.4	1.84	1.70
Roof	Purlin and rafter cold roof structure with 100 mm mineral wool insulation (λ 0.044 W/mK) at ceiling level between 100x50 mm ceiling joists. Ceiling joists run	28.4	0.45	0.40

---

[7] English housing data from Department for Levelling Up, Housing and Communities (2021) English housing survey 2020 to 2021: Headline report. London: Department for Levelling Up, Housing and Communities. Available at: gov.uk/government/statistics/english-housing-survey-2020-to-2021-headline-report

[8] The replacement doors and windows were new units and are likely to provide superior insulation and airtightness to units fitted prior to 2010 due to lack of material degradation.

[9] U-values calculated using Stroma FSAP software.

[10] Anderson, B. (2006) Conventions for U-value Calculations. BR 443. Watford: Building Research Establishment.

[11] British Standards Institution (2017) BS EN ISO 6946: Building Components and Building Elements – Thermal Resistance and Thermal Transmittance – Calculation Methods. Milton Keynes, British Standards Institution.

[12] BRE, SAP 2012. The Government's Standard Assessment Procedure for Energy Rating of Dwellings 2012, in, Building Research Establishment, UK, 2017.

Thermal element	Baseline construction	Area (m²)	Calculated U-value (W/m²K)	RdSAP assumed U-value (W/m²K)
	parallel to the gable wall at 400 mm centres above lath (6 mm) and plaster (17 mm) ceiling. Solid timber loft hatch			
Ground floor	Suspended timber ground floor above a ventilated underfloor void (20 mm depth). 150x22 mm floorboards fixed to 200x50 mm floor joists at 400 mm centres. Floor joists run between the gable and party wall with joists ends built into masonry walls.	28.4	0.68	0.68
Windows	4-20-4 'E' rated double glazing units in uninsulated uPVC frames.	9.9	-	2.60
Doors	Front – 'E' rated uPVC Rear – 'E' rated half glazed uPVC.	3.5	-	3.00
Party wall	Solid wall – as external walls but with plaster finish on both sides	37.4	-	0

2.2 Energy House DEEP fabric retrofits

2.2.1 DEEP retrofit test programme

The Energy House DEEP retrofit programme comprised three phases.

1. **Phase 1 – piecemeal retrofit approach** (Stages 1-5). Thermal elements were retrofitted sequentially to simulate a 'typical' piecemeal full retrofit process. Sequencing of elemental retrofits was undertaken in ascending order of financial cost. Testing at each stage of the piecemeal retrofit process allowed the cumulative impact of successive retrofits to be measured.

2. **Phase 2 – whole house retrofit approach** (Stages 6a-6d). Stage 6 of the test programme was intended to upgrade stages and replicate a whole house approach retrofit[13]. It involved performing staged modifications to the fabric after the final piecemeal retrofit stage (Stage 5). The final configuration of the fabric (Stage 6d) was

---

[13] The DEEP retrofit test programme was designed prior to the introduction of PAS 2035:2019. Therefore, the whole house approach retrofit was not implemented to this specification.

designed to be indistinguishable from a whole house approach retrofit. Testing at each stage allowed the cumulative impact of successive whole house approach measures to be measured.

3. **Phase 3 – individual retrofit measures** (Stages 10-16). Only one thermal element was retrofitted at Phase 3 test stage. Phase 3 was not intended to replicate 'real world' retrofit scenarios. It was designed to disaggregate the impact of multiple retrofit measures, assess the repeatability of loft and ground floor retrofits, and measure the performance of the external wall/ground floor junction without ground floor retrofit measures.

At each stage, the Energy House was subject to thermal performance measurements and qualitative building performance evaluation (BPE) investigation. Findings from each retrofit were compared with baseline measurements of thermal performance, to quantify the change in thermal performance characteristics resulting from an individual or combination of retrofit measures.

Figure 2 shows the configuration of the Energy House fabric at each DEEP fabric test stage

Test programme phase	Test stage	Elemental retrofit				Whole house approach details			
		Roof	Openings	Ground floor	External walls	EWI below DPC	Bay window	Extend eaves	Openings into EWI
1 - Piecemeal retrofit	1 (Phase 1 *baseline*)								
	2	✓							
	3a	✓	✓						
	3b	✓	Low U-value						
	4	✓	✓	✓					
	5 (*piecemeal full retrofit*)	✓	✓	✓	✓				
2 - Whole house approach retrofit	6a	✓	✓	✓	✓	✓			
	6b	✓	✓	✓	✓	✓	✓		
	6c	✓	✓	✓	✓	✓	✓	✓	
	6d (*WHA full retrofit*)	✓	✓	✓	✓	✓	✓	✓	✓
3 - Individual retrofit measures	10 (Phase 3 full retrofit)	✓	✓	✓	✓				
	11				✓				
	12		✓						
	13			✓					
	14	✓							
	15a			Unsealed					
	15b			Sealed					
	16 (Phase 3 baseline)								

Figure 2: Energy House DEEP retrofit sequence and fabric test stage identifiers[14]

Measurements of space heating (gas combination boiler and air source heat pump central heating) performance and occupant thermal comfort metrics were also measured throughout the test programme. Please refer to DEEP Report 5.02 Salford Energy House Heating Systems Testing.

2.2.2 Piecemeal retrofit measures (Phase 1)

Elemental retrofits were designed to meet the limiting values in Approved Document Part L1b 2018[15] of the Building Regulations. Retrofit performance was based on improvement to calculated baseline performance (refer to Table 1) using conventional insulating materials. Retrofits to openings exceeded the requirements of Part L1b. This was intended to

---

[14] Stages not shown relate to non-fabric test stages (refer to DEEP Report 5.02).
[15] HM Government, UK Building Regulations. Part L1B: Conservation of Fuel and Power in Existing Dwellings in, RIBA Publishing Ltd, London, 2018.

compensate for the original window frames being retained for practical purposes. Table 2 provides the calculated retrofit design U-values and details of the primary thermal components of each retrofit.

Table 2: Retrofit measures and design U-values at each piecemeal retrofit stage

Test stage	Element retrofitted	Thermal component	Retrofit design U-value (W/m^{2}K)
2	Roof	Additional 170 mm mineral wool perpendicular to pre-existing insulation and joists. Total 270 mm mineral wool (λ 0.044 W/mK). 100 mm PIR (0.022 W/mK) applied to loft hatch.	0.16
3a	Openings	'A' rated argon filled low emissivity DGUs (in original frames) and 'A' rated composite doors	1.60[16]
3b	High performance glazing (installed for Stage 3b only)	Crystal Units C.U.in glazing units (in original frames) and 'A' rated composite doors. CU.in contain a film within the inert gas filled cavity of a low emissivity DGU.	n/a
4	Ground floor	150 mm mineral wool (λ 0.044 W/mK) between joists supported on vapour permeable vapour control layer	0.24[17]
5	External walls	Steel frame EWI system. 102 mm mineral wool (λ 0.033 W/mK). EWI applied to gable wall to ridge level.	0.30

2.2.3 Whole house approach details (Phase 2)

Design details for the whole house approach measures were decided by the EWI contractor (walls below damp proof course (DPC) level and relocation of openings) and building contractor (bay window and eaves). Contractors were briefed on the principles of the whole house approach measures and asked to design and construct the details as they would for retrofit projects in the field.

---

[16] Whole window U-value.
[17] Building Regulations Part L1b ground floor limiting U-value is 0.25 W/m^{2}K.

Remedial works were requested during the Stage 6 tests to simulate a retrofit that had been performed in one coordinated programme of work as some measures degraded the performance of previous retrofit measures (refer to Sections 2.3.2.1 and 3.3.2).

Details of the whole house approach measures pre- and post-installation are contained within Table 3. Images of the whole house approach retrofit works are provided in Figure 3 and Figure 4.

Table 3: Whole house approach details at each stage

Test stage	Detail	Condition at full piecemeal retrofit stage (Stage 5)	Whole house approach measure
6a	Walls below DPC	223 mm solid brick. EWI only applied above ground floor level	45 mm XPS boards (λ 0.034 W/mK) to external walls of underfloor void
6b	Bay window	Walls treated with 100 mm XPS boards (λ 0.034 W/mK) during Stage 5 EWI retrofit. Stone mullions and lintel uninsulated. Flat roof uninsulated	Mullions and lintel treated with 45 mm XPS boards (λ 0.034 W/mK). Flat roof treated with 150 mm mineral wool (λ 0.04 W/mK)
6c	Eaves	EWI applied up to facia board level at eaves level resulting in discontinuity between EWI and loft insulation	Eaves extended beyond EWI. 100 mm mineral wool (λ 0.04 W/mK) connecting loft insulation with EWI
6d	Position of openings	Original location	Openings moved in line with EWI. Bay side windows replaced with smaller DGUs

Figure 3: Whole house approach retrofit works. Extruded polystyrene (XPS) being applied to walls below DPC level at Stage 6a (left) and to bay window mullions at Stage 6b (right)

Figure 4: Whole house approach retrofit works. Eaves being extended over EWI at Stage 6c (left) and window moved in line with EWI at Stage 6d (right)

2.2.4 Individual retrofit measures (Phase 3)

It was not possible to test the whole house approach measures in isolation due to their integration with the EWI system. Whole house approach measures were removed prior to Stage 10, and the full retrofit for Phase 3 (Stage 10) replicated the Phase 1 piecemeal full retrofit (Stage 5).

Phase 3 enabled the performance of repeat installations of each retrofit to be measured, except for the EWI due to cost and time constraints. Repeat installations were performed using the same retrofit specification and installers. Test Stage 12 was introduced to enable additional heating system tests with Stage 3 fabric configuration, this enabled the loft insulation to be installed three times. To assess the impact of the ground floor membrane during Stage 15, the ground floor was initially tested with the membrane unsealed at the perimeter (Stage 15a), then tested following perimeter sealing (Stage 15b).

2.2.5 Predicted heat transfer coefficients

The heat transfer coefficient (HTC) is the rate of heat loss (fabric and ventilation) in watts (W) from the entire thermal envelope of a building per kelvin (K) of temperature differential between the internal and external environments and is expressed in W/K. Figure 5 shows the predicted HTC at each Phase 1 and Phase 2 test stage. The predicted HTC was calculated using pre- and post-retrofit calculated U-values for each element, ventilation heat losses derived from SAP assumed infiltration rates[18], and thermal bridging heat losses based on the RdSAP assumed y-value of 0.15 W/m^{2}K[19].
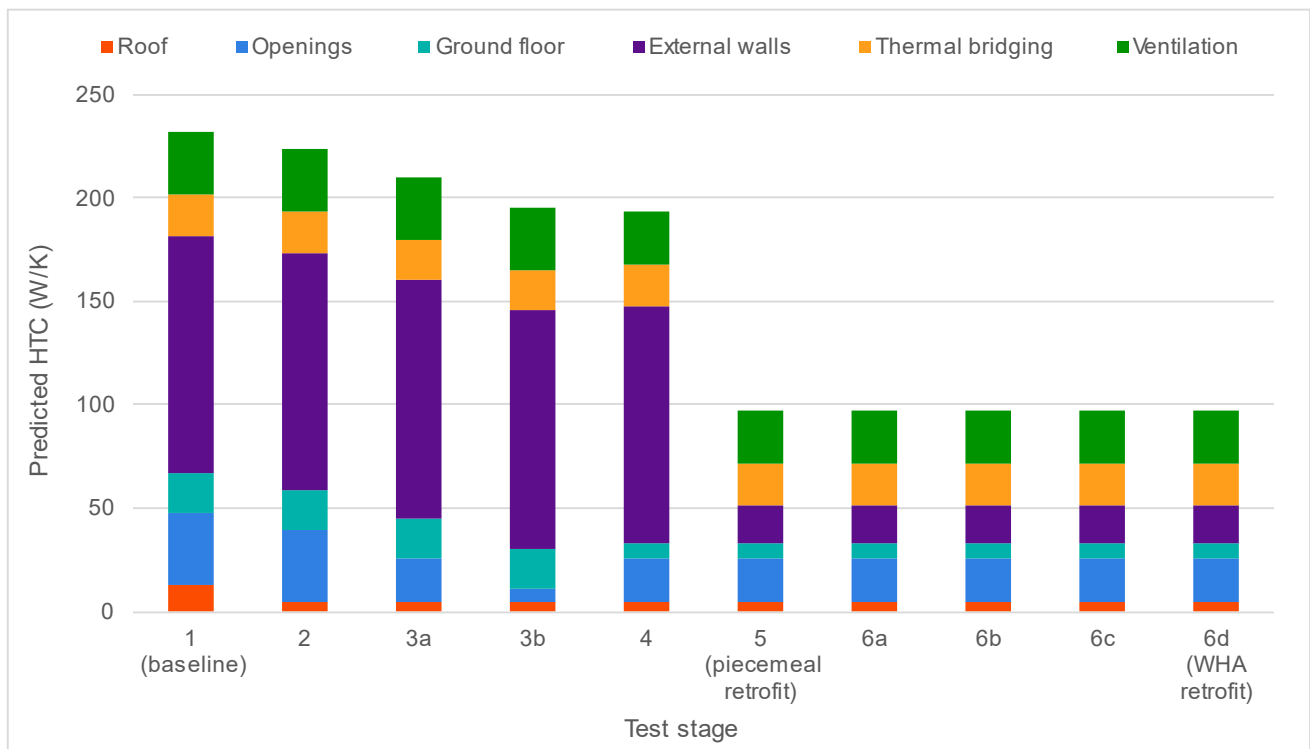
Figure 5: Energy House predicted HTC at each Phase 1 and Phase 2 test stage

The baseline (Stage 1) predicted HTC of the Energy House was 231.7 W/K. The predicted HTC for the full piecemeal (Stage 5) and whole house approach retrofits was 97.4 W/K, a 134.3 W/K (58%) reduction from baseline. The reason for the piecemeal and whole house approach predicted HTCs being the same is due to RdSAP assuming the same thermal bridging heat losses throughout the retrofit process. The only change in SAP assumed infiltration rate occurs at Stage 4 with floor sealing reducing the infiltration rate from 0.2 ACH to 0.1 ACH. The EWI applied at Stage 5 was predicted to result in the single greatest HTC reduction from any previous retrofit stage (50%). The 96 W/K EWI HTC reduction is 72% of the total predicted reduction in HTC resulting from the full retrofit. This is because the external walls are the greatest heat loss area (47% of total heat loss area) and the 84% (1.54 W/m^{2}K) predicted reduction in U-value resulting from their retrofit.

---

[18] Excludes intentional ventilation points sealed during testing.
[19] In the context of RdSAP, a simplified thermal bridging factor called the y-value is used to determine heat loss from non-repeating thermal bridges in existing homes. The RdSAP method sets a default y-value at 0.15 W/m^{2}K.

2.2.6 Retrofit installation practice

The installation of retrofit measures was intended to simulate typical retrofit practice rather than showcase best practice retrofit. The building contractor and EWI contractor were instructed to perform the retrofit works as they would in the field. However, installers were asked to make provision for the removal of retrofit measures at the end of the test (e.g. reduce mechanical fixings where possible). The research team observed the retrofit process but did not instruct the retrofit installers.

2.3 Building performance evaluation methods

This section details the methods used to measure fabric thermal performance at each stage of the test programme.

2.3.1 Steady state thermal performance measurements

2.3.1.1 Steady state test environment

Building fabric performance is typically characterised using steady state heat transfer metrics. The Energy House test facility allows these metrics to be measured at near steady state. No recognised standards currently exist for steady state fabric thermal performance measurement (whole house or elemental) using an indoor full-scale test facility. Therefore, measurements of steady state fabric performance in DEEP were based on existing in-situ measurement methods adapted for the test environment.

Table U1 of SAP10 was used to select external temperatures representative of the UK average during the winter months (December to February). The chamber HVAC system was set to maintain approximately 4.5 °C during each measurement period. The Energy House and conditioning void were maintained at 20 °C throughout each steady state measurement period using electric resistance heaters connected to PID controllers with PT-100 RTD temperature sensors. This temperature was selected as it is the average central heating thermostat setpoint for homes in England[20]. Air circulation fans were used to increase air temperature homogeneity within the Energy House. Fans remained in the same location and at the minimum speed setting during each steady state measurement period.

Compliance with ISO 9869-1[21] was deemed as the minimum threshold by which to assess whether heat transfer could be considered at steady state. Each steady state measurement period was a minimum of 72 hours in duration. Each measurement period concluded once the building heat transfer coefficient (HTC) measured during three successive 24-hour periods differed by less than ± 5% from that measured during the final 24-hour period. The uncertainty associated with the HTC measurement during the final 24-hour period had to fall within ± 5% of the HTC for heat transfer to be considered steady state. Reported values for steady state metrics are based on measurements during the final 24-hour period of each measurement period.

---

[20] Shipworth, M., Firth, S., Gentry, M., Wright, A., Shipworth, D. & Lomas, K. (2010) 'Central heating thermostat settings and timing: building demographics', Building Research & Information, 38, (1) 50-69.
[21] BSI (2014) BS ISO 9869-1 Thermal insulation. Building elements. In-situ measurement of thermal resistance and thermal transmittance. Heat flow meter method. London. British Standards Institution.

2.3.1.2 Building heat transfer coefficient (HTC) measurement

HTC measurements were used to quantify the change in whole house heat loss of Energy House resulting from retrofits to its thermal elements. The change in HTC captures the aggregate change in plane element, thermal bridging, and unintentional ventilation (air infiltration and leakage) heat losses from the Energy House.

At the start of DEEP testing, no formally recognised standard existed for the in-situ HTC measurement. The 2013 version of the Leeds Metropolitan (now Beckett) University Whole House Heat Loss Test Method[22] was adapted for HTC measurements in the DEEP project. The principal differences being the reduction in test duration and analysis of test data.

A coheating test typically assumes the steady state whole house energy balance in Equation 1.

Equation 1: Typical coheating test whole house energy balance[23]
$$Q + A_{sw}.q_{sw} = (H_{tr} + H_v).\Delta T$$

Where:

Q = Power input (W)

A_{sw} = Solar aperture (m^2)

q_{sw} = Solar irradiance (W/m^2)

H_{tr} = Transmission heat transfer coefficient (W//K)

H_v = Ventilation heat transfer coefficient (W/K)

ΔT = Internal to external temperature difference (K)

HTC measurements at Salford Energy House test facility can be performed without solar gains, so the terms A$_{sw}$ and q$_{sw}$ can be removed from the whole house energy balance, and the equation rearranged to show how at steady state, the HTC can be calculated from measurements of only Q and ΔT. Equation 2 shows the HTC calculation in the DEEP Energy House tests.

Equation 2: Energy House DEEP HTC calculation
$$HTC = \frac{Q}{\Delta T}$$

Where:

HTC = H_{tr} + H_v (W/K)

Q = 24-hour mean power input[24] (W)

---

[22] Johnston, D., Miles-Shenton, D., Farmer, D. & Wingfield, J. (2013) Whole House Heat Loss Test Method (Coheating), Leeds Metropolitan University, 2013, June 2013.
[23] Adapted from Everett, R. (1985). Rapid Thermal Calibration of Houses, Technical Report, Open University Energy Research Group, Milton Keynes, UK, 1985, ERG 055.
[24] Based on total cumulative energy input to the Energy House over 24-hour period

ΔT = 24-hour volume weighted average internal air temperature (T_{i_vw}) minus the 24-hour average chamber air temperature (T_e)

Please refer to Appendix E for details of the HTC uncertainty calculation.

2.3.1.3 Alternative HTC measurement methods

The test programme also provided the opportunity to compare commercial rapid HTC test methods against the coheating test. Saint-Gobain QUB[25] and Veritherm perform dynamic HTC measurements of unoccupied dwellings over one night, as opposed to the coheating test that typically requires a test period of 2-3 weeks. However, their effectiveness for assessing improvement in fabric thermal performance post-retrofit is relatively untested, notably in the case of the Veritherm test method.

Both are dynamic test methods that involve a stabilisation period of constant internal temperature, followed by a heating period with constant power input, then a cooling period. They both use assumptions of fabric performance to calculate the power input required for the test. Both also use integrated hardware and software to control heat input, monitor power input and environmental conditions, and perform data analysis. The main difference in equipment between the two methods is that Veritherm also uses air circulation fans during the test.

2.3.1.4 In-situ heat flux and U-value measurement

In-situ U-value measurements of each thermal element were undertaken in accordance with ISO 9869-1. The measurements were primarily intended to compare the predicted and measured change in U-value resulting from the retrofit of each element, thus enabling the identification and quantification of any building fabric performance gap. RdSAP assumptions were used as a baseline to specify the performance of retrofit materials to meet the limiting U-values in Part L1b of the Building regulations. However, for performance gap identification, the post-retrofit target U-value for each element was baselined against its pre-retrofit in-situ U-value. Post-retrofit target U-values were calculated in accordance with ISO 6946 and BRE 443 by using the measured baseline in-situ thermal resistance (R-value)[26] of the thermal element plus the additional R-value of the retrofit materials. In-situ U-value measurements were also used to disaggregate change in fabric and ventilation heat losses from the changes in HTC, compare RdSAP assumed U-values with pre-retrofit baseline U-values, and to identify whether the retrofit of an element impacts the U-value of other elements.

The thermal transmittance of a building element (U-value) is defined in ISO 7345[27] as the *"Heat flow rate in the steady state divided by area and by the temperature difference between the surroundings on each side of a system"*. To account for thermal storage and release, ISO 9869-1 uses a cumulative moving average of the heat flow rate and ΔT to calculate in-situ U-values. However, steady state conditions at the Energy House during DEEP allowed in-situ U-values to be calculated as defined by ISO 7345 using Equation 3.

[25] Alzetto, F., Pandraud, G., Fitton, R., Heusler, I. and Sinnesbichler, H. (2018) QUB: A fast dynamic method for in-situ measurement of the whole building heat loss. Energy and Buildings 174:124-133; DOI: 10.1016/j.enbuild.2018.06.002

[26] $R = \frac{1}{U}$

[27] ISO (1987) ISO 7345: Thermal insulation –Physical quantities and definitions. Geneva, Switzerland, International Organization for Standardisation.

Equation 3: Energy House DEEP in-situ U-value calculation

$$U = \frac{q}{\Delta T}$$

Where: U = in-situ U-value (W/m²K)

      q = 24-hour mean heat flow rate (W/m²)

      ΔT = 24-hour mean internal to external air temperature difference (K)

Please refer to Appendix F for details of the in-situ U-value uncertainty calculation.

Measurements of heat flux density (heat flow rate), from which in-situ U-values were calculated, were taken at 74 locations on the thermal elements of the Energy House and conditioning void using heat flux plates (HFPs). Figure 6 shows HFPs on the external walls of bedroom 1.

Figure 6: HFPs on the external walls of bedroom 1 measuring heat flux density

The ground floor had a disproportionate allocation of HFPs for its surface area as heat transfer is known to vary across the surface area of suspended timber ground floors[28]. A HFP was placed on each element of the conditioning void to assess whether retrofits to the Energy House have any impact on the neighbour. A HFP was placed on an external wall >1000 mm from the Energy House to act as a control for the Energy House external wall U-value measurements. Table 4 provides the allocation of HFPs on each thermal element. Schematics of HFP locations can be found in Appendix D.

---

[28] Pelsmakers, S, Fitton, R, Biddulph, P, Swan, W, Croxford, B, Stamp, S, Calboli, F, Shipworth, D, Lowe, R, & Elwell, C (2017), 'Heat-flow variability of suspended timber ground floors: Implications for in-situ heat-flux measuring', Energy and Buildings, 138, pp. 396-405

Table 4: Energy House DEEP HFP allocation

Element	HFPs at non-bridged locations	HFPs at bridged locations	Total HFPs
Roof	5 + 1 loft hatch	5 (inc. 1 joist)	11
Windows	3 (centre pane)	-	3
Doors	1	-	1
Ground floor	18	5 (inc. 1 joist)	23
External walls	10	17	27
Party wall	5	-	5
Conditioning void	4	-	4

HFPs were positioned, with the aid of thermography, in locations considered to be representative of the whole element. The HFPs were fixed to surfaces using adhesive tape and thermal contact paste. Care was taken to ensure that HFPs were not unduly influenced by excessive air movement by positioning air circulation fans in such a way that air was not blown directly on to the HFPs.

Only measurements of heat flux density obtained from locations that were not likely to be significantly influenced by thermal bridging at junctions with neighbouring thermal elements (typically at distances greater than 1000 mm) were used to calculate the average in-situ U-value for each thermal element. The average in-situ U-value of each thermal element was calculated using spatial linear interpolation of individual U-value measurements across an element and corrected to account for repeating thermal bridges (e.g. joists).

In-situ measurements of heat flux density were also obtained from locations on thermal elements affected by thermal bridging and thermal anomalies. They were normalised for comparative purposes using Equation 3. These measurements were intended to provide additional insight into thermal performance and cannot be considered representative of plane element thermal transmittance.

The ΔT for each in-situ U-value measurement was calculated using the internal and external air temperature differential measured in the vicinity of each HFP. The high number of HFP locations meant that it was not practicable to mount surface temperature thermocouples alongside each HFP, hence the air-to-air ΔT.

2.3.1.5 Alternative in-situ U-value measurement method

The external wall U-value of the living room was measured in its pre- and post-retrofit conditions using Heat3D. It is an iOS mobile application used for rapid in-situ U-Value

measurements (in comparison to ISO 9869) across a predefined area of an external wall. Heat3D uses both Apple augmented reality (AR) kit, the FLIR One Pro mobile thermal camera, and reflective and air temperature targets to create a 3D thermal model of a room.

Heat3D requires a room to be pre-heated using a convective heater with PID controller at a constant temperature for a period of up to 12 hours prior to a one-hour period in which timelapse infrared thermography is used to estimate heat flux and U-value. Figure 7 shows the location of the Heat3D external wall U-value measurement and the DEEP external wall HFPs in the living room (EW1 and EW2).

Figure 7: Heat3D external wall U-value measurement. Yellow square denotes Heat3D measurement area and red circles the location of HFPs EW1 and EW2

2.3.1.6 Ventilation heat transfer coefficient (H_v)

The air infiltration/leakage ventilation rate (n) from which the ventilation heat transfer coefficient was calculated was obtained using:

Blower door test results. Blower door test n_{50} values (refer to section 2.3.2.1) were used to derive n using the $n_{50}/20$ 'rule of thumb'[29]. The derivation includes the correction factor for dwelling shelter factor contained within SAP 2012[30].

CO_2 tracer gas test results. A mass flow controller was used to dispense 100 l of CO_2 into the centre of the Energy House (staircase) during steady state measurement periods. The CO_2 decay rate was measured in the Living Room and Bedroom 1. n was calculated using the averaged method detailed in ASTM E741-11[31].

The n values were multiplied by the internal volume of the Energy House and by the specific heat capacity of air (0.33 Wh/m^{3}K) to determine H_v.

2.3.1.7 In-situ temperature factor (f_{Rsi}) measurement

The temperature factor (f_{Rsi}) is a dimensionless metric of thermal performance used to assess the potential risk of surface condensation and mould growth. Surfaces in dwellings with a f_{Rsi} below the critical temperature factor (f_{CRsi}) of 0.75 are considered to pose a risk of surface condensation and mould growth[32]. The in-situ f_{Rsi} of each element and junction was derived from in-situ measurements using Equation 4.

Equation 4: fRsi calculation

$$f_{Rsi} = \left(\frac{T_{si} - T_e}{T_i - T_e}\right)$$

Where:

T_{si} = 24-hour mean internal surface temperature

T_e = 24-hour mean external air temperature

T_i = 24-hour mean internal air temperature

To account for the DEEP f_{Rsi} measurement uncertainty of ±0.03 and surface temperatures only being measured at one location on each junction, the f_{CRsi} of 0.75 was expanded to include values between 0.70-0.79. f_{Rsi} <0.70 is deemed high risk and ≥0.80 is considered low risk. Please refer to Appendix G for details of the in-situ f_{Rsi} uncertainty calculation and surface condensation and mould growth risk categorisation.

Thermography was used to identify representative locations on the surface of each element and at junctions between elements for the in-situ f_{Rsi} measurements. Surface temperature was measured using thermocouples fixed with aluminium tape. Twelve junctions were measured in the Energy House and two in the conditioning void. The conditioning void measurements were to assess whether retrofitting the Energy House had any unintended consequences for the neighbour. The identifier and location of each in-situ f_{Rsi} measurement is provided in Table 5.

---

[29] Kronvall, J. (1978). Testing of houses for air leakage using a pressure method. ASHRAE transactions, 84(1), 72-9.
[30] BRE (2019), The Government's Standard Assessment Procedure for Energy Rating of Dwellings: 2012 edition (updated October 2019). Building Research Establishment, Watford.
[31] American Society for Testing and Materials (Philadelphia, Pennsylvania). (2017). ASTM E741-11 (Reapproved 2017): Standard Test Method for Determining Air Change in a Single Zone by Means of a Tracer Gas Dilution. ASTM.
[32] Ward, T. (2006) Assessing the Effects of Thermal Bridging at Junctions and Around Openings. IP 1/06. Watford, Building Research Establishment

Table 5: Identifier and location of each in-situ f_{Rsi} measurement

Designation	Junction	Location
EW/GF (par)	External wall/ground floor with joists parallel	Kitchen
EW/GF (perp)	External wall/ground floor with joists perpendicular	Kitchen
EW/IF	External wall/intermediate floor	Living room
EW/RF (eaves)	External wall/roof at eaves	Kitchen
EW/RF (gable)	External wall/roof at gable	Bedroom 1
EW (corner)	External wall corner	Bedroom 1
EW/PW	External wall/party wall	Bedroom 1
Jamb	Window jamb with window frame	Bedroom 1
Sill	Windowsill with window frame	Bedroom 1
Lintel	Lintel with window frame	Bedroom 1
Bay lintel	Lintel with bay roof	Living room
PW/RF	Party wall with roof	Landing
PW/RF (CV)	Party wall with roof	Conditioning void
EW/PW (CV)	External wall/party wall	Conditioning void

2.3.2 Airtightness testing

2.3.2.1 Blower door tests

A blower door test (also referred to as a fan pressurisation test) was performed at each stage of the test programme to quantify the change in air permeability value at 50 Pa (AP_{50}) and air change rate at 50 Pa (n_{50}) resulting from each retrofit measure. Blower door tests were undertaken in accordance with ATTMA Technical Standard L1[33]. All intentional ventilation openings and wastewater services were sealed throughout the test programme.

2.3.2.2 Co-pressurisation tests

Co-pressurisation tests were conducted at two stages of the test programme to assess whether blower door test results were influenced by air movement between the Energy House and conditioning void. Blower door fans were installed in the doorway of each house and simultaneous measurements taken across a range of pressure differentials to provide AP_{50} and n_{50} values for the Energy House which do not include inter-dwelling air exchange. The results were subtracted from values obtained from conventional blower door tests performed on the Energy House to quantify inter-dwelling air exchange.

2.3.3 Thermal bridging calculations

Elemental thermal modelling using Physibel TRISCO thermal modelling software was conducted to calculate non-repeating linear thermal bridging heat losses in the Energy House at each test stage. The detailed modelling procedure can be found in Report 2.01 DEEP Methods. By modelling the Ψ-value (Psi-value) of junctions, it is possible to calculate the non-repeating thermal bridging heat loss (H_{TB}), excluding point thermal bridges. This can be achieved by multiplying the Ψ-value of each junction by its respective length at each test stage.

The y-value at each stage of the retrofit was derived by summing up all H_{TB} values for all junctions and dividing it by the total heat loss area, excluding the party wall. This information is valuable when assessing the suitability of default values in RdSAP for retrofit evaluation, particularly in terms of their impact on the whole house HTC.

For the Energy House, thermal bridging calculations were performed for all 25 unique junctions in both pre- and post-retrofit scenarios. Material properties were derived from default tabulated values and, where available, manufacturer data.

2.3.4 Qualitative data collection

2.3.4.1 Thermography

Thermographic surveys of the Energy House were undertaken throughout the test programme to identify changes in surface temperature distribution across test stages that could indicate regions of poor retrofit performance. Thermographic surveys were performed in accordance with the guidance set out in BSRIA Guide 39/2011[34]. The thermograms displayed in this report have been corrected to account for the environmental conditions present during the survey, as well as subject distance and emissivity.

---

[33] ATTMA (2021) ATTMA Technical Standard L1. Measuring the Air Permeability of Building envelopes (Dwellings). October 2021 Issue. Northampton, UK, Air Tightness Testing and Measurement Association
[34] Pearson, C. (2011) Thermal Imaging of Building Fabric. BG 39/2011. Bracknell, BSRIA.

2.3.4.2 Air leakage/infiltration identification

The conditions present during the blower door tests provided the opportunity for air leakage/infiltration identification to assess the effectiveness of retrofits at sealing points of uncontrolled air exchange with the external environment. During depressurisation, the elevated internal temperatures enabled infrared thermography to be used to observe and record areas of air infiltration. During building pressurisation, air leakage detection was performed using a handheld smoke generator.

2.3.4.1 Construction observations

A photographic record of the retrofit process was made. Installers were asked questions during the retrofit process about decisions made during the installation process and feedback requested on the reasons for any measured thermal underperformance of retrofit measures.

2.4 Energy House monitoring equipment

The findings provided in this report are based on measurements obtained using the equipment listed in Table 6. Measurements were recorded at one-minute intervals by the Energy House's monitoring system[35]:

Table 6: Measurement equipment used in the Energy House DEEP fabric performance tests

Measurement	Equipment	Uncertainty
Electricity consumption	Siemens 7KT PAC1200 digital power meter	±1%
Internal and chamber air temperatures	IC temperature sensor	±0.2 °C
Surface temperatures	Type-T thermocouple (calibrated to ±0.1 °C)	±0.1 °C
Heat flux density	Hukseflux HFP-01 heat flux plate	±3%
Air permeability	Retrotec 5100 Blower Door System	±2%[36]
CO_2 concentration	DataNab CO_2 sensor	±3%

---

[35] Refer to Appendix C for more details of the Energy House's monitoring system.
[36] The sheltered test environment allows measurement uncertainty to exclude wind-based errors, the ± 2% uncertainty value applies only to test apparatus.

3 Results

3.1 Airtightness and ventilation

3.1.1 Piecemeal and whole house approach retrofits

Table 7 provides the AP50 value measured using a blower door test at each Phase 1 and Phase 2 test stage.

Table 7: AP_{50} at each Phase 1 and Phase 2 test stage

Test stage	Retrofit (cumulative)	AP_{50} ($m^3.h^{-1}.m^{-2}$ @ 50 Pa)	AP_{50} change on previous stage ($m^3.h^{-1}.m^{-2}$ @ 50 Pa)	AP_{50} change on previous stage (%)	AP_{50} change on baseline ($m^3.h^{-1}.m^{-2}$ @ 50 Pa)	AP50 change on baseline (%)
1	Baseline	10.6 ±0.2	-	-	-	-
2	Roof	10.8 ±0.2	+0.2 ±0.3	+1	+0.2 ±0.3	+1
3	Openings	10.8 ±0.2	+0.1 ±0.3	+2	+0.2 ±0.3	+2
4	Ground floor	9.1 ±0.2	-1.8 ±0.3	-16	-1.5 ±0.3	-15
5	External walls	9.0 ±0.2	-0.1 ±0.3	-1	-1.6 ±0.3	-15
6a	Walls below DPC	9.2 ±0.2	+0.2 ±0.3	+2	-1.5 ±0.3	-14
6b	Bay window	9.2 ±0.2	+0.1 ±0.3	+1	-1.4 ±0.3	-13
6c	Extend eaves	9.3 ±0.2	+0.1 ±0.3	+1	-1.3 ±0.3	-12
6d	Openings into EWI	9.4 ±0.2	+0.1 ±0.3	+1	-1.2 ±0.3	-12

Figure 8 illustrates the AP_{50} value measured using a blower door test at each Phase 1 and Phase 2 test stage.
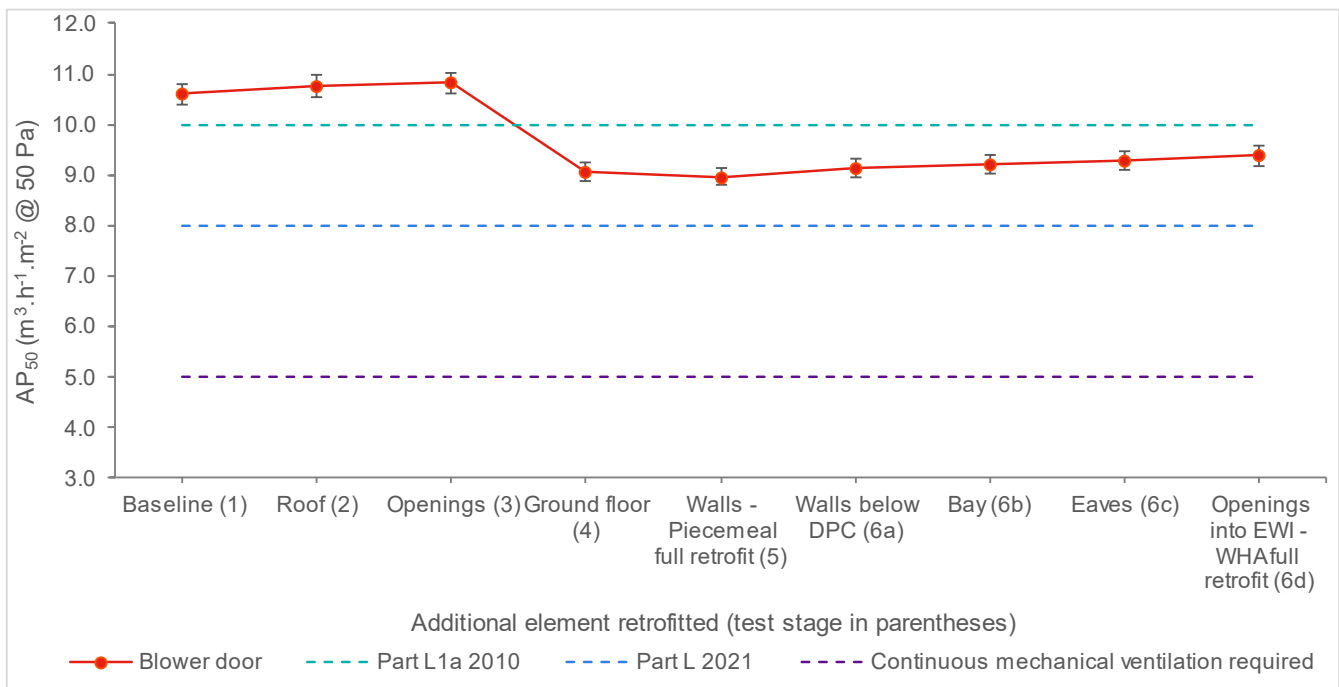
Figure 8: AP_{50} value at each Phase 1 and Phase 2 test stage

The Stage 1 baseline AP_{50} value of the Energy House was 10.6 (±0.2) $m^3.h^{-1}. m^{-2}$ @ 50 Pa, which is comparable with UK average[37] of 11.5 $m^3.h^{-1}.m^{-2}$ @ 50 Pa and suggests representative baseline performance. Retrofits to the loft and openings at Stages 2 and 3 did not result in any significant change to the baseline AP_{50} value. The ground floor retrofit delivered the only significant change in airtightness with a 16% reduction in AP_{50} measured between Stage 3 from Stage 4. At Stage 5 the AP_{50} value of the Energy House had been reduced by 15% on the Stage 1 baseline. Nonsignificant increases in AP_{50} were measured at each Stage 6 whole house approach test stage. The full whole house approach retrofit AP_{50} value measured at Stage 6d was 5% greater than that measured for the full piecemeal retrofit at Stage 5. Therefore, the findings suggest that the whole house approach measures selected for the Energy House DEEP test[38] may not provide any additional airtightness benefit over piecemeal approach measures and that the conversion process from a piecemeal retrofit to a whole house approach retrofit has the potential to reduce airtightness (refer to Section 3.1.6 for more details).

From Stage 4 onwards, the AP_{50} value was below the (upper) limiting value for permitted new-builds under Part L1a 2010 (10 $m^3.h^{-1}.m^{-2}$ @ 50 Pa). The AP_{50} value throughout the retrofit process was above that required to comply with Part L 2021 (8 $m^3.h^{-1}.m^{-2}$ @ 50 Pa). Therefore, the retrofits failed to provide the airtightness required to meet modern design standards for low

---

[37] Glew, D, Parker, J, Fletcher, M, Thomas, F, Miles-Shenton, D, Brooke-Peat, M, Johnston, D and Gorse, C (2021) Demonstration of energy efficiency potential: literature review of benefits and risks in domestic retrofit practice and modelling (BEIS Research Paper Number 2021/014). London: Department for Business Energy and Industrial Strategy.
[38] Airtightness only retrofit was not selected for the Energy House tests due to the requirement to return the Energy House to its original state post-DEEP, this precluded the use of foams and sealants.

carbon housing. The results show that the Energy House did not require continuous mechanical ventilation provision at any stage of the retrofit process.

3.1.2 Comparison with other Energy House whole house approach retrofits

Figure 9 compares the AP_{50} values resulting from the DEEP Energy House whole house approach retrofit with the Saint-Gobain whole house approach retrofits of the Energy House.
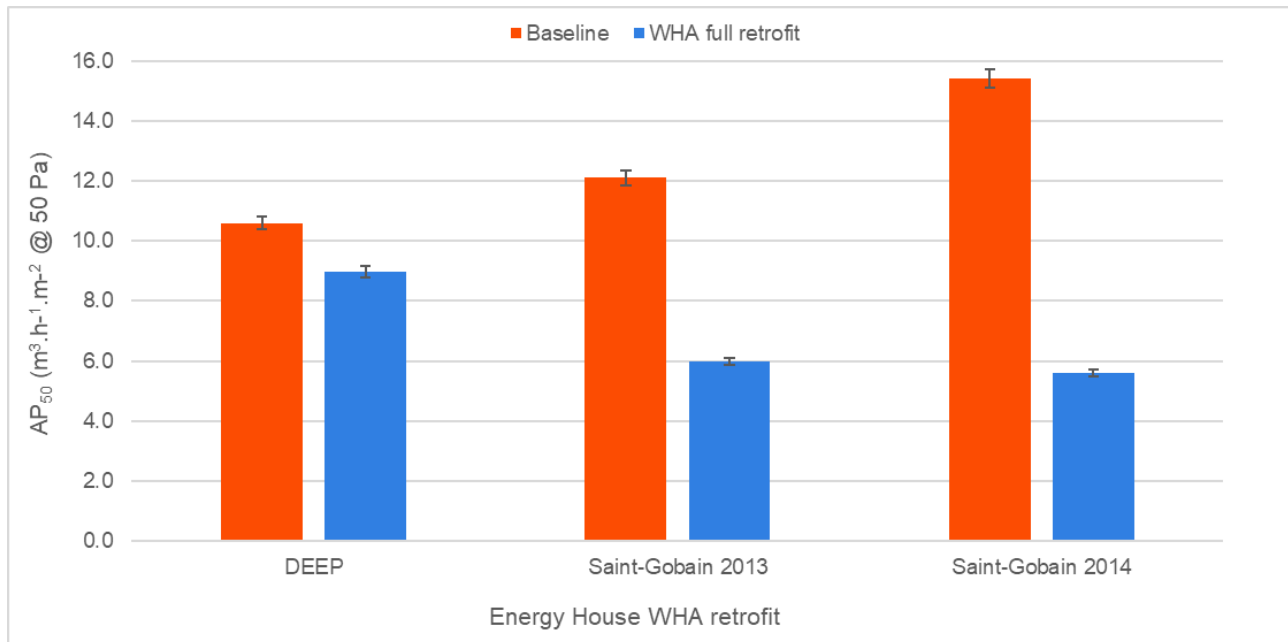
Figure 9: AP_{50} values following whole house approach retrofits to the Energy House

The 12% reduction in AP_{50} value resulting from the whole house approach retrofit in DEEP is significantly lower than the respective 50% and 64% AP_{50} value reductions from baseline achieved by the 2013 and 2014 Saint-Gobain whole house approach retrofits of the Energy House. However, it must be noted that both Saint-Gobain retrofits started from a higher baseline[39]. It is interesting to note that both Saint-Gobain post-whole house approach retrofit AP_{50} values were ~6 $m^3.h^{-1}.m^{-2}$ @ 50 Pa. The Saint-Gobain retrofits were undertaken for commercial purposes and followed 'best practice' installation that included remedial works following blower door air infiltration investigations. The Saint-Gobain findings could indicate that the lowest AP_{50} achievable from a 'best practice' whole house approach retrofit of the Energy House is ~6 $m^3.h^{-1}.m^{-2}$ @ 50 Pa. If that is the case, then the DEEP whole house approach AP_{50} value was ~60% worse than could be expected from a 'best practice' retrofit. The baseline configuration of the Energy House for DEEP and the Saint-Gobain 2013 test was almost identical, however there was a 13% difference in baseline AP_{50} value. These findings highlight the difficulty with making predictions about the pre-and post-retrofit airtightness of dwellings and the requirement for blower door testing.

---

[39] Variation in baseline AP_{50} values can be attributed to modifications to the Energy House between projects. The substantially higher baseline value for 2014 Saint-Gobain project is due to the presence of single glazed timber sash windows and timber doors which are characterised by poor airtightness.

3.1.3 Individual retrofit measures

Table 8 provides the AP_{50} value for each Phase 3 test stage where retrofits to individual measures were tested in isolation.

Table 8: AP_{50} value for each Phase 3 test stage

Test stage	Retrofit	AP_{50} ($m^3.h^{-1}.m^{-2}$ @ 50 Pa)	AP_{50} change on baseline ($m^3.h^{-1}.m^{-2}$ @ 50 Pa)	AP_{50} change on baseline (%)
10	Phase 3 piecemeal	10.9 ±0.2	-1.6 ±0.3	-13
11	External walls	12.4 ±0.2	-0.1 ±0.4	-1
12	Roof & openings	12.9 ±0.2	+0.4 ±0.4	+3
13	Openings	13.0 ±0.2	+0.5 ±0.4	+4
14	Roof	12.7 ±0.2	+0.2 ±0.4	+1
15a	GF (unsealed)	12.1 ±0.2	-0.4 ±0.3	-3
15b	GF (sealed)	11.4 ±0.2	-1.1 ±0.3	-9
16	Phase 3 baseline	12.5 ±0.2	-	-

The Phase 3 piecemeal retrofit (Stage 10) AP_{50} value was 1.9 (±0.3) $m^3.h^{-1}.m^{-2}$ @ 50 Pa greater than with the fabric in the same configuration in Phase 1 (Stage 5). The Phase 3 baseline (Stage 16) AP_{50} value was 1.7 (±0.3) $m^3.h^{-1}.m^{-2}$ @ 50 Pa greater than the Phase 1 baseline (Stage 1). The similar discrepancy is thought to be due to damage to the fabric of the Energy House during the deconstruction of the whole house approach measures prior to Phase 3. The sum of the individual retrofit changes in AP_{50} values from the Phase 3 baseline resulted in a reduction in AP_{50} of 0.6 (±0.7) $m^3.h^{-1}.m^{-2}$ @ 50 Pa. It was 1.0 $m^3.h^{-1}.m^{-2}$ @ 50 Pa lower than the 1.6 (±0.3) $m^3.h^{-1}.m^{-2}$ @ 50 Pa reduction for all measures combined. This could suggest that the combination of multiple retrofit measures in Phase 1 provided a greater airtightness benefit than the sum of individual measures. However, the ground floor retrofit had no connection with the roof or openings (other than at the interface with the doors) and external wall insulation had no significant impact on airtightness when applied in combination with other elements in Phase 1 or individually in Phase 3 (Figure 10). The cause for the discrepancy is thought to be due to inconsistency between repeat retrofit measures, namely the ground floor and openings (refer to Section 3.1.4).

3.1.4 Repeatability of retrofit airtightness

Figure 10 shows the change in AP_{50} value resulting from elemental retrofits in DEEP Phase 1 and Phase 3. Phase 1 is based on the change on change in AP_{50} value between successive

piecemeal retrofits stages. Phase 3 is based on the difference in AP_{50} value between the Phase 3 baseline (Stage 16) and the AP_{50} value resulting from retrofit measures applied in isolation. The only measure that was not a repeat installation in Phase 3 was the EWI (refer to Section 2.2.4).
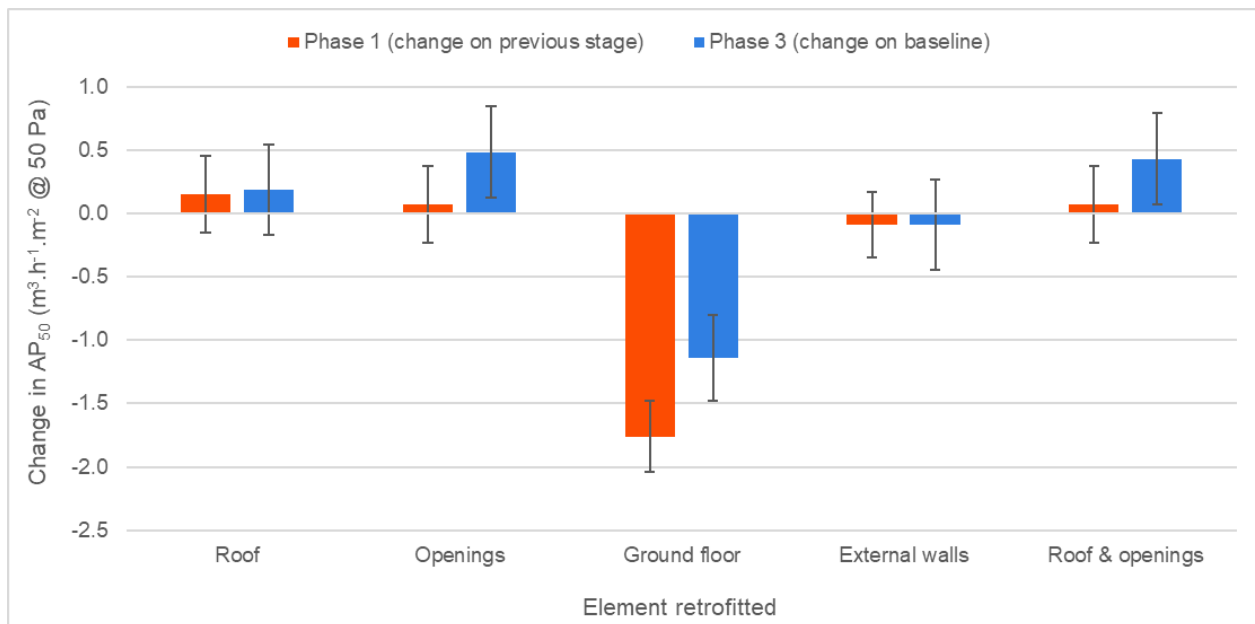
Figure 10: Change in AP_{50} value resulting from elemental retrofits in Phase 1 and Phase 3

The only significant difference between AP_{50} value change in Phase 1 and Phase 3 for each retrofit measure was the ground floor retrofit. In Phase 1 the ground floor resulted in a 1.8 (±0.3) $m^3.h^{-1}.m^{-2}$ @ 50 Pa (16%) reduction on the previous stage, whereas the Phase 3 retrofit resulted in a 1.1 (±0.3) $m^3.h^{-1}.m^{-2}$ @ 50 Pa (9%) reduction on the Phase 3 baseline. The reduced improvement in performance in Phase 3 is attributed to installation of the floor membrane (refer to Section 3.1.5).

Although both Phase 3 tests involving retrofits to openings (Stages 12 and 13) did not measure significant changes in AP_{50} in comparison to their Phase 1 counterparts. The Phase 3 measurements did show significant increases on the Phase 3 baseline AP_{50} value. Air infiltration investigation demonstrated issues with the seal around the thresholds and door reveals after the doors were replaced for the Phase 3 opening retrofits. As only the DGUs in the windows were replaced, their air permeability remained constant.

The combined Phase 3 underperformance of the ground floor and openings retrofits compared with Phase 1 of 0.7 $m^3.h^{-1}.m^{-2}$ @ 50 Pa accounts for most of the 1 $m^3.h^{-1}.m^{-2}$ @ 50 Pa discrepancy between the sum of individual measures in Phase 3 and the difference between the Phase 3 piecemeal and retrofit scenarios. Given that the retrofits involved the same installers and materials, the findings highlight the potential variability in airtightness that can occur when installing retrofit measures.

3.1.5 Ground floor airtightness

The ground floor retrofit resulted in the greatest reduction in AP_{50} value in both Phase 1 and Phase 3 of the DEEP tests. Air infiltration identification showed that the installation of the ground floor membrane during the Phase 1 retrofit provided an effective ground floor seal at locations where it was correctly applied and sealed to the perimeter. The air source heat pump internal unit was not removed due to the cost and complexity, so an attempt to seal around the unit was made. This was only partially successful and highlights an issue with perimeter sealing where internal fixtures are not removed for a retrofit. In Phase 3 the ground floor was retrofitted, and the membrane initially left unsealed at junctions with the internal and external walls, thresholds, and door reveals (Stage 15a). Following Stage 15a, the membrane was taped along its perimeter to provide a seal (Stage 15b). Figure 11 shows the impact of the floor membrane during Phase 3.
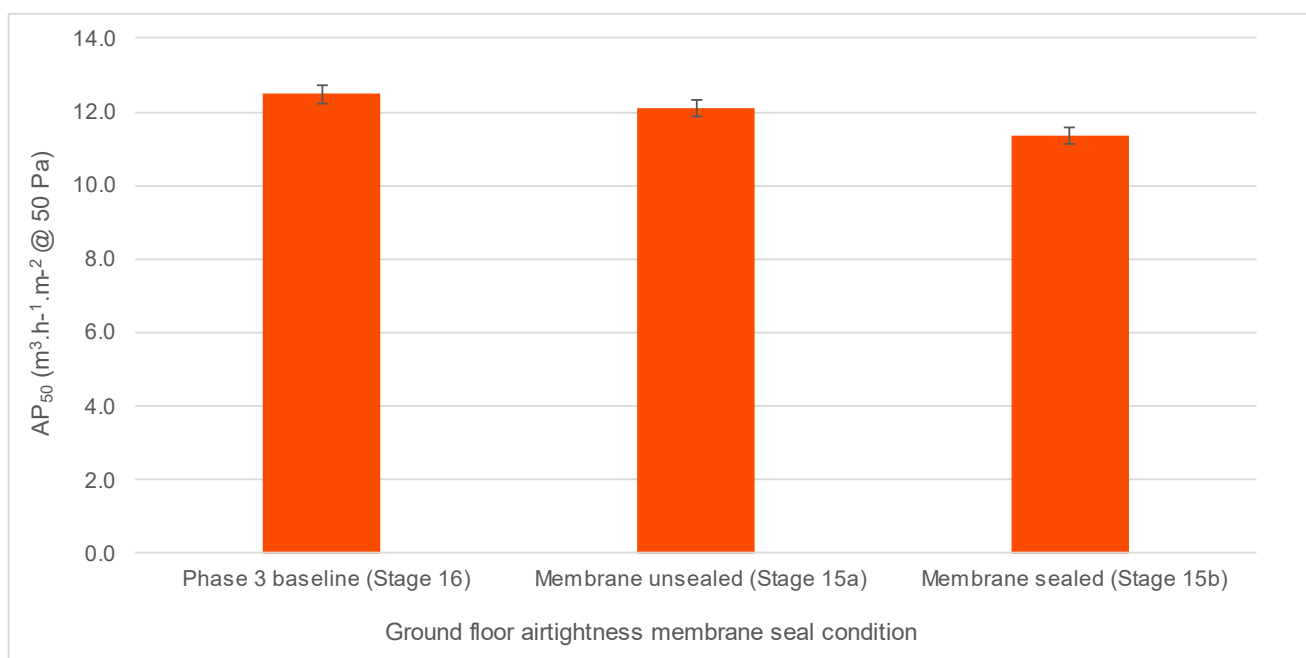
Figure 11: Impact on AP_{50} value due to floor membrane during Phase 3

Installing the ground floor insulation with the membrane left unsealed at its perimeter resulted in an AP_{50} reduction from baseline of 0.4 (±0.3) $m^3.h^{-1}.m^{-2}$ @ 50 Pa (3%). Sealing of the membrane resulted in a further 0.7 (±0.3) $m^3.h^{-1}.m^{-2}$ @ 50 Pa (6%) reduction in the AP_{50} value. The perimeter sealing contributed 64% of the total AP_{50} value reduction resulting from the ground floor retrofit. As the unsealed membrane will have provided some sealing of the interface between the ground floor and adjoining elements, it is therefore likely that the impact of the perimeter sealing is underestimated. The findings suggest that perimeter sealing of the suspended timber ground floor had the single greatest impact on airtightness of any retrofit measure.

Figure 12 compares the reductions in AP_{50} value resulting from retrofits of the ground floor in DEEP with the 2013 Saint-Gobain ground floor retrofit[40].

---

[40] The 2014 Saint-Gobain whole house approach retrofit did not include staged testing, so the AP_{50} change resulting from the ground floor retrofit could not be disaggregated from the fan pressurisation test results.
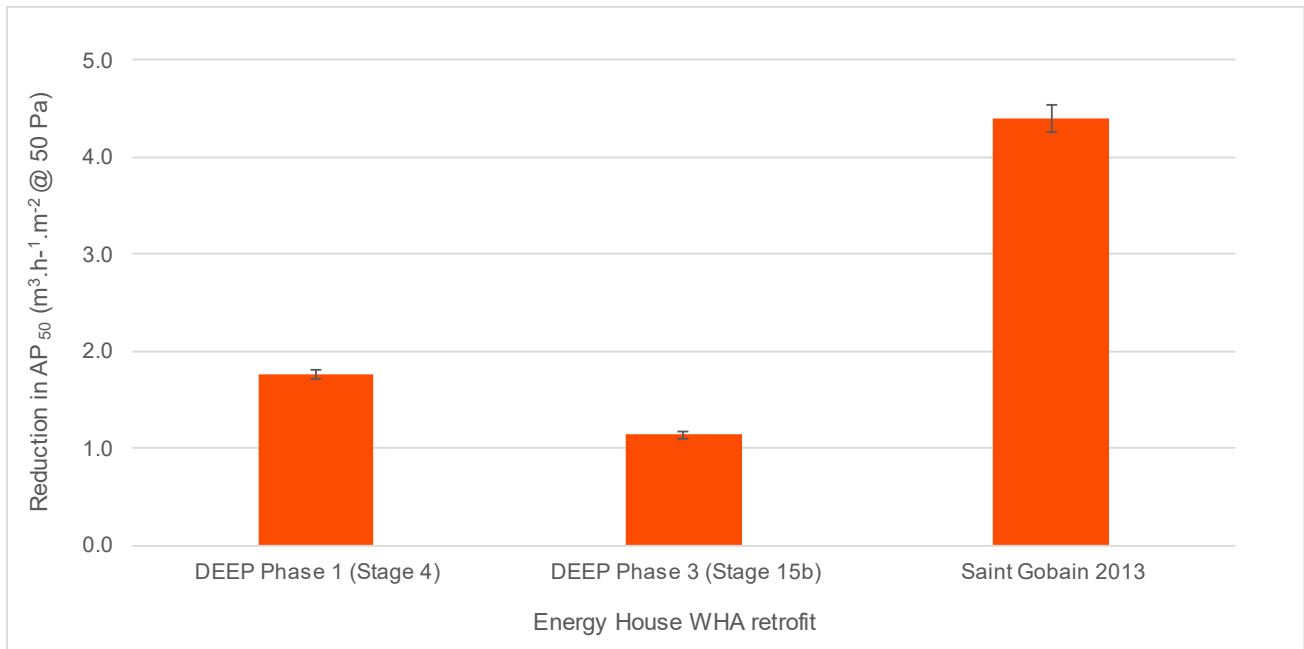
Figure 12: AP$_{50}$ value reductions resulting ground floor retrofits of the Energy House

The pre-ground floor retrofit AP$_{50}$ value of 10.4 (± 0.2) in the 2013 Saint-Gobain test was in good agreement with that measured in Phase 1 prior to the ground floor retrofit (10.8 ±0.2 m^3.h^{-1}.m^{-2} @ 50 Pa). However, the 2013 Saint-Gobain ground floor retrofit delivered a 4.4 (±0.3) m^3.h^{-1}.m^{-2} @ 50 Pa (42%) reduction in the AP$_{50}$ value. The Saint-Gobain retrofit followed a 'best practice' approach that involved a high level of attention to perimeter sealing as well as blower door testing and thermography to identify and rectify discontinuities in the airtightness barrier. Remedial sealing in the 2013 Saint-Gobain test reduced the AP$_{50}$ value by 13% from the original post-retrofit AP$_{50}$ value. During the 2014 Saint-Gobain test, remedial sealing to the ground floor reduced the original post-retrofit AP$_{50}$ value by 16%. This highlights the importance of air infiltration investigation during best practice retrofit.

The contrast between the AP$_{50}$ reductions previously measured at the Energy House and those measured in DEEP again demonstrate the potential for variability in performance from the application of a ground floor membrane and highlights the importance of attention to detail and removal of internal fixtures during their application.

3.1.6 Whole house approach measures

Each whole house approach measure resulted in a non-significant increase in AP$_{50}$ value. The full whole house approach retrofit AP$_{50}$ value measured at Stage 6d was 5% greater than that measured for the full piecemeal retrofit at Stage 5. However, the initial repositioning of the openings in-line with the EWI insulation layer at Stage 6d resulted in a 1 (±0.3) m^3.h^{-1}.m^{-2} @ 50 Pa (11%) increase in the AP$_{50}$ value to 10.3 (±0.2) m^3.h^{-1}.m^{-2} @ 50 Pa. The increase eliminated most of the previous improvement in airtightness. Air infiltration investigation and images taken during the retrofit highlighted the reveals and doors as areas of concern.

1. **Window reveals**. The reveals were treated with plasterboard affixed to the jambs and lintels using dabs of plasterboard adhesive as the contractor deemed it to constitute typical practice. This created an inconsistent seal that allowed air from within the EWI cladding void to circumvent the seal around the window frame and enter the habitable space through gaps within the sealant applied to the perimeter of the plasterboard. Air

infiltration could result in increased cooling of this junction and increase the risk of condensation and mould growth. Additionally, airpaths were also evident between the 10 mm cavity between the two leaves of brickwork within the external wall. This airpath provides the potential for warm air to bypass the EWI layer via the cavity between the two leaves of brickwork in regions of inconsistent mortar fill. Therefore, best practice should involve the entirety of the plasterboard[41] being coated in adhesive rather than just the around the perimeter.

2. **External doors**. Repositioning the external doors in-line with the insulation within the EWI also resulted in thresholds and opening reveals no longer linking with the floor membrane installed during the ground floor retrofit.

Previous issues resulting from 'typical' retrofit practice were left unresolved up to this point during the test programme. However, the primary aim of the test programme was to compare piecemeal and whole house approach retrofits. So, remedial works were performed to resolve issues relating to poor sequencing that are less likely to occur in a whole house approach retrofit. Figure 13 shows the AP_{50} value measured during the final whole house approach retrofit stage remedial works.
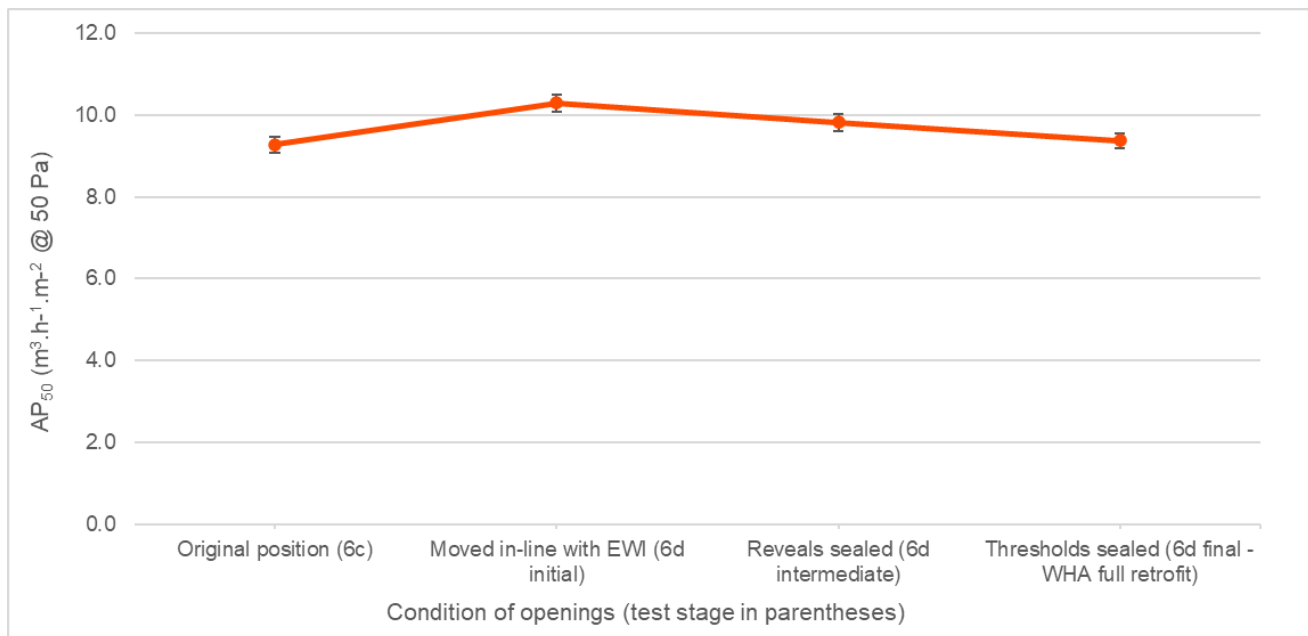
Figure 13: AP_{50} value measured during remedial works at the final whole house approach retrofit stage (6d)

Remedial works to the window reveals resulted in a 0.5 (±0.3) $m^3.h^{-1}.m^{-2}$ @ 50 Pa (5%) reduction in AP_{50} value. The remedial work to the interface between the ground floor membrane and external doors resulted in a further 0.4 (±0.3) $m^3.h^{-1}.m^{-2}$ @ 50 Pa (4%) reduction in AP_{50} value. Following the remedial works the Stage 6d AP_{50} value was 0.1 (±0.3) $m^3.h^{-1}.m^{-2}$ @ 50 Pa greater than that measured at Stage 6c.

These findings highlight a potential unintended consequence of converting a piecemeal full retrofit to a whole house approach retrofit. Consideration must be given to how whole house approach measures interact with previously retrofitted elements.

---

[41] Insulated plasterboard should be used if space allows.

3.1.7 Inter-dwelling air exchange

Table 9 and Figure 14 provide the results of the co-pressurisation tests performed at Stage 15 of the test programme. Testing took place with the ground floor membrane unsealed (Stage 15a) and sealed (Stage 15b) at the perimeter to assess the effectiveness of the ground floor seal at preventing inter-dwelling air exchange. The co-pressurisation tests were performed by Leeds Beckett University (LBU).

Table 9: Co-pressurisation test results and inter-dwelling air exchange

Test stage	Ground floor membrane condition	ATTMA test AP_{50} ($m^3.h^{-1}.m^{-2}$ @ 50 Pa)	Co-pressurisation AP_{50} ($m^3.h^{-1}.m^{-2}$ @ 50 Pa)	Inter-dwelling air exchange ($m^3.h^{-1}.m^{-2}$ @ 50 Pa)	Inter-dwelling air exchange (%)
15a	Unsealed	12.2 ± 0.2	9.1 ± 0.2	3.1 ± 0.3	25
15b	Sealed	11.6 ± 0.2	8 ± 0.2	3.6 ± 0.4	31
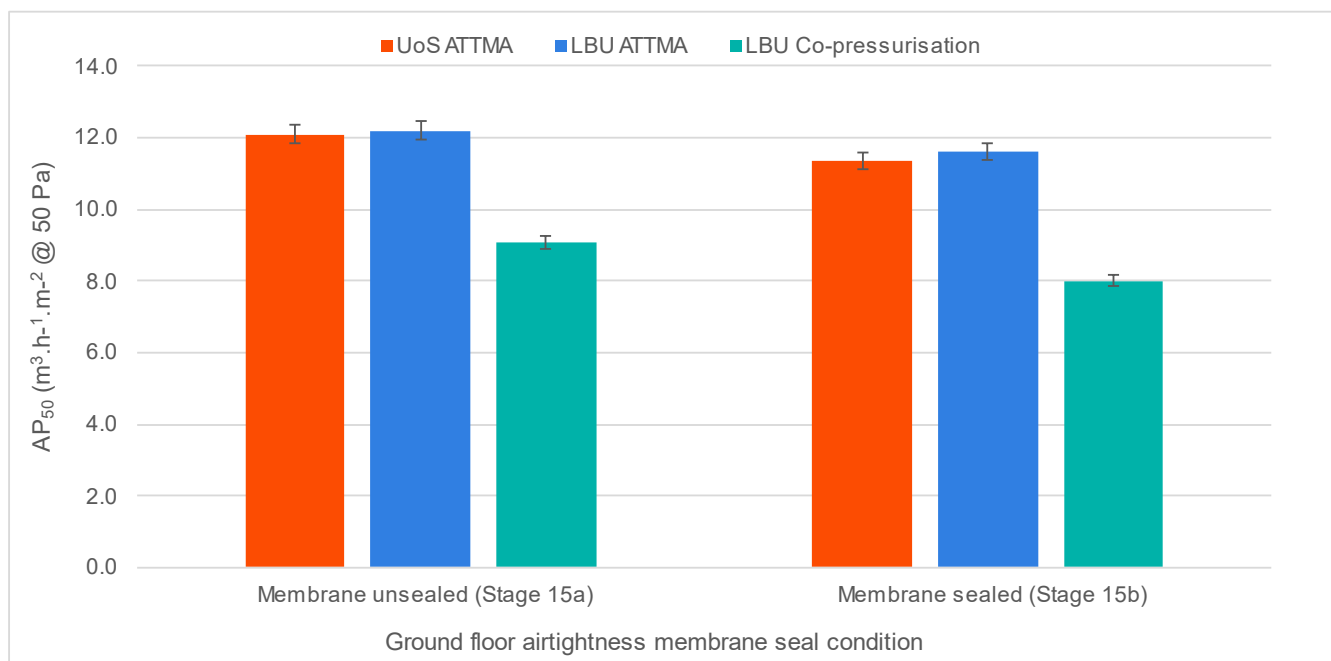
Figure 14: Results of the Stage 15 co-pressurisation tests

The co-pressurisation tests show that a significant proportion of the AP_{50} value measured during the blower door tests can be attributed to inter-dwelling air exchange. Sealing of the ground floor membrane suggested that the proportion of inter-dwelling air exchange increased. This was not expected due to the ground floor perimeter being identified as the primary air infiltration path and the presence of gaps in the party wall brickwork at underfloor void level. CO_2 release in the Energy House during the steady state tests also suggested inter-dwelling air exchange under reduced pressure differentials as CO_2 concentration in the conditioning

void rose soon after release. Figure 15 shows CO_2 concentration in the Energy House, conditioning void, and chamber following CO_2 release in the Energy House.
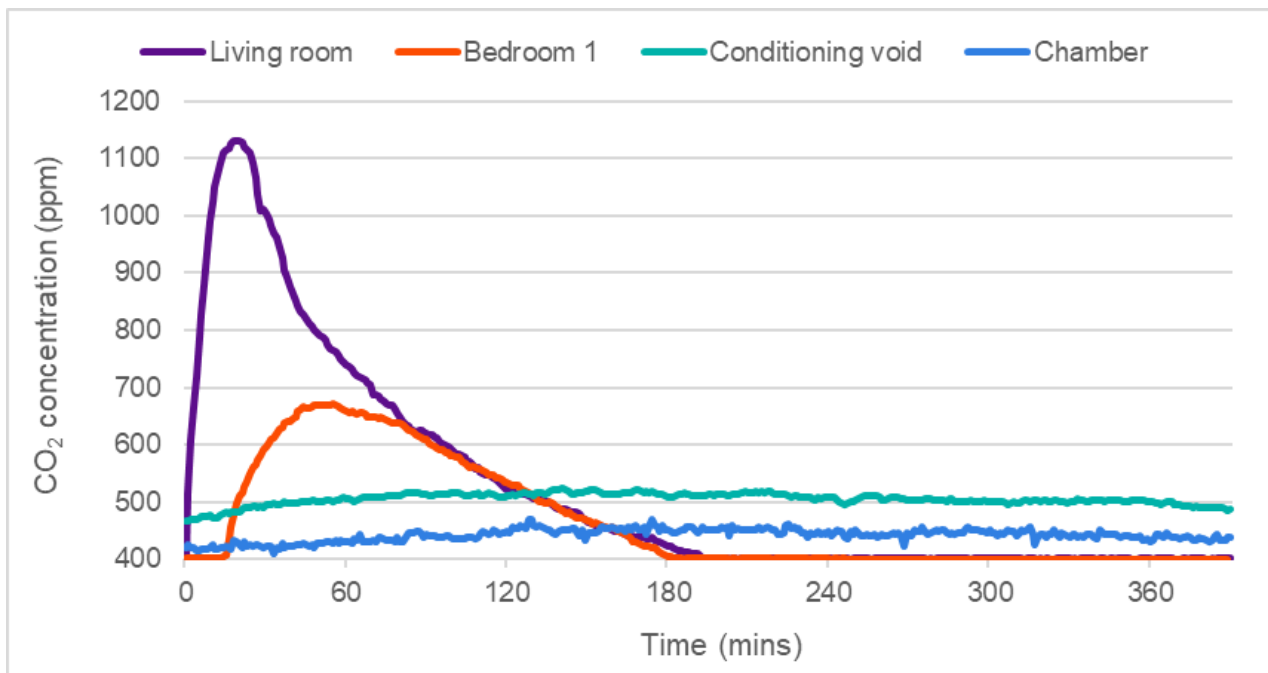
Figure 15: CO_2 concentration in Energy House, conditioning void, and chamber following CO_2 release in Energy House

The findings suggest that inter-dwelling air exchange would not have reduced the AP_{50} value below the 5 $m^3.h^{-1}.m^{-2}$ @ 50 Pa threshold for continuous mechanical ventilation provision at any point during Phases 1 and 2 of the retrofits.

Assuming adjoining dwellings are heated to the same temperature, inter-dwelling air exchange will not result in significant repercussions regarding space heating energy use. However, it does raise the following concerns[42] about:

- exchange of indoor air pollutants and passage of smoke during a fire.

- masking the effectiveness of retrofits that improve air infiltration paths to the external environment when analysing blower door test results.

- ventilation provision based on blower door test results that overestimate air exchange with the external environment.

- overestimation of air infiltration/leakage heat loss rates derived from blower door test results due to exchange of warm air across party elements.

The co-pressurisation tests also showed excellent agreement between UoS and LBU ATTMA AP_{50} measurements. Each test was conducted independently using different brands of blower door test equipment (UoS – Retrotec, LBU – Minneapolis). This finding shows the robustness

---

[42] Some of these concerns have previously been raised by Jones (2015). Jones, B. et al. Assessing uncertainty in housing stock infiltration rates and associated heat loss: English and UK case studies. Building and Environment, [s. l.], v. 92, p. 644–656, 2015.

of blower door tests when undertaken correctly and justifies the use of a lower uncertainty in the sheltered conditions provided by the Energy House chamber.

3.1.8 Air infiltration/leakage ventilation rate (n) and ventilation heat loss rate (H_v)

Table 10 provides the blower door test and CO_2 concentration decay derived values for n and H_v at each stage of the retrofit. For more details on the calculation methods, please refer to Section 2.3.1.6.

Table 10: $n_{50}/20$ and CO_2 decay derived ventilation rate and ventilation heat loss rates

Test stage	Retrofit (cumulative)	n derived from $n_{50}/20$ (ACH)	H_v derived from $n_{50}/20$ (W/K)	n derived from CO_2 decay (ACH)	H_v derived from CO_2 decay (W/K)
1	Baseline	0.45	21.0	0.20	9.4
2	Roof	0.45	21.2	0.21	9.8
3a	Openings	0.46	21.4	0.22	10.3
4	Ground floor	0.38	17.9	0.20	9.4
5	External walls	0.38	17.7	0.19	8.9
6a	Walls below DPC	0.39	18.1	0.19	8.9
6b	Bay window	0.39	18.2	0.19	8.9
6c	Extend eaves	0.39	18.4	0.18	8.4
6d	Openings into EWI	0.39	18.5	0.18	8.4

n and H_v derived from the blower door test results were generally double those derived from CO_2 concentration decay measurements. The large discrepancy was expected as the Energy House chamber provides sheltered test conditions meaning the main driver for air exchange is buoyancy driven stack effect. The test environment means that CO_2 derived H_v was used to disaggregate the fabric and ventilation components of the HTC. Figure 16 shows the relationship between blower door test and CO_2 decay derived n.
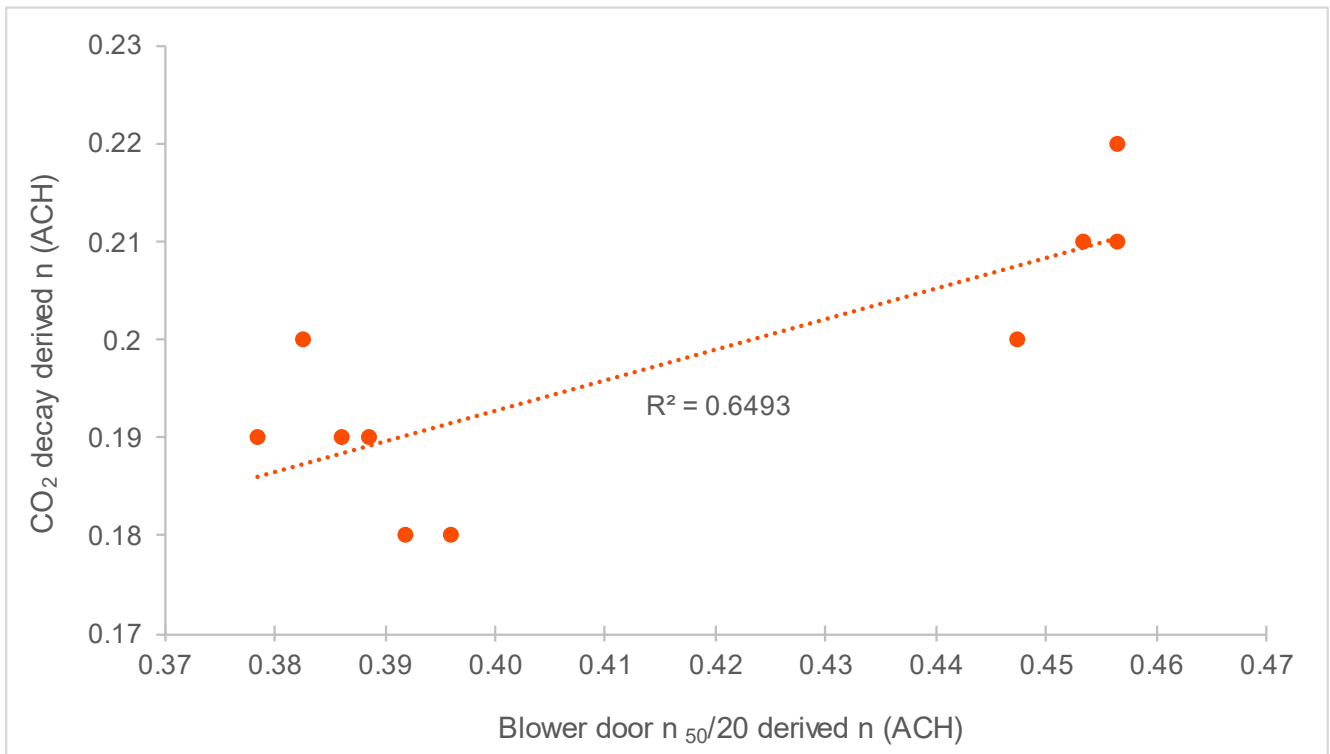
Figure 16: Relationship between blower door n_{50}/20 and CO_2 derived n

CO_2 derived n were reasonably consistent (0.18-0.22 ACH) throughout the retrofit programme, with the lowest CO_2 n measured in the final two whole house approach retrofit stages. A reasonably strong relationship between blower door test and CO_2 derived n was evident (p = 0.005). This provides additional confidence in the CO_2 derived H_v used to disaggregate the HTC.

3.2 Plane elemental performance

3.2.1 Piecemeal retrofit

Table 11 summarises the in-situ U-value measurements obtained during Phase 1 of the DEEP fabric thermal performance testing. Pre-retrofit U-values are based on measurements performed in the test stage immediately prior to each retrofit. For more details on the U-value calculation methods, please refer to Section 2.3.1.4.

Table 11: Summary of in-situ U-value measurements for each thermal element (window (centre pane) and door (panel) in-situ measurements do not represent U-value for entire assembly). *Indicates non-significant difference between target and in-situ retrofit U-values

Element	Pre-retrofit ISO 6946 U-value (W/m²K)	Pre-retrofit in-situ U-value (W/m²K)	Post-retrofit ISO 6946 U-value (W/m²K)	Target in-situ post-retrofit U-value (W/m²K)	Post-retrofit in-situ U-value (W/m²K)	Target & in-situ post-retrofit U-value difference
Roof	0.45	0.29 ±0.01	0.16	0.14	0.13 ±0.01	-7%*
Windows	2.60	2.42 ±0.1	1.60	1.40	1.16 ±0.08	-
Windows (low U)	2.60	2.42 ±0.1	-	-	0.45 ±0.01	-
Doors	3.00	1.02 ±0.07	1.80	0.80	0.51 ±0.03	-
Ground floor	0.68	0.69 ±0.03	0.24	0.21	0.22 ±0.03	5%*
External walls	1.84	1.65 ±0.07	0.30	0.29	0.34 ±0.05	17%

Pre-retrofit in-situ U-values were generally lower than those calculated according to ISO 6946. This resulted in the target retrofit in-situ U-values being lower than the retrofit ISO 6946 calculated U-values. Most retrofits achieved their target retrofit in-situ U-value. The EWI performance gap of 17% between target in-situ retrofit U-value and that measured post-retrofit in Stage 5 was not significant. However, the mean external wall in-situ U-value of all Phase 1 tests (Stages 5-6d) with EWI present was 0.35 W/m²K, which indicates underperformance. Despite the performance gap, external wall heat loss was reduced by 79%. The underperformance of the EWI system is partially attributed to air movement within the solid wall structure (refer to Section 3.2.2.1).

3.2.2 Performance of individual elements

3.2.2.1 External walls

Figure 17 shows the external wall pre- and post- retrofit U-values at locations used in the calculation of the external wall in-situ U-value.
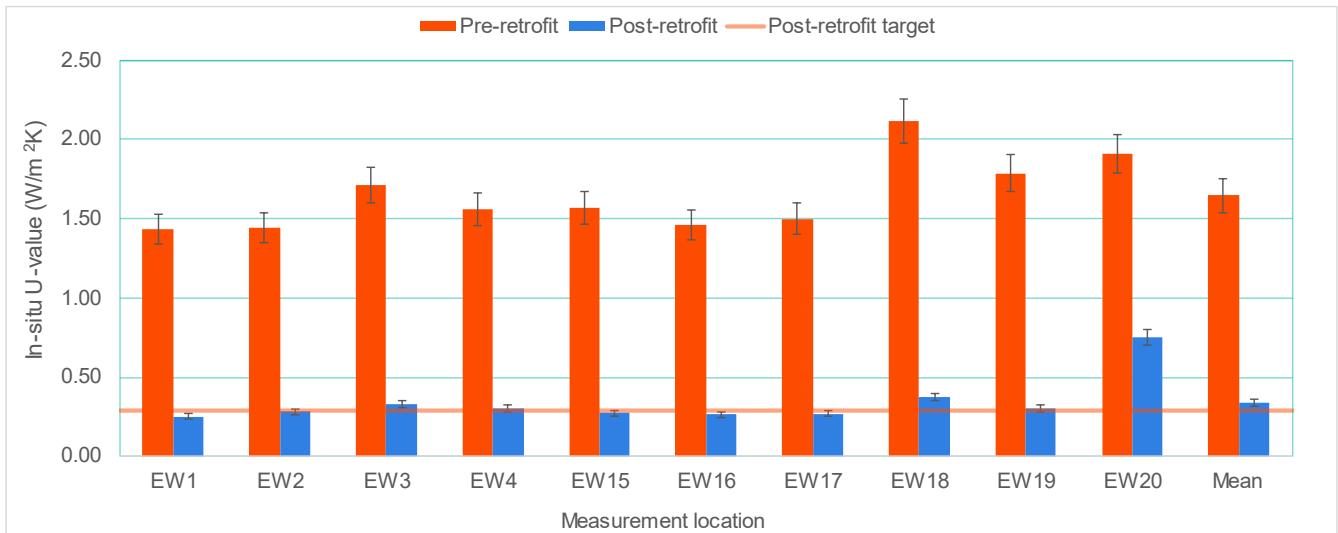
Figure 17: Unbridged external wall in-situ U-value measurements pre- and post-retrofit

The largest pre-retrofit in-situ U-values were measured by HFPs EW18-20 located on the gable wall in Bedroom 2. Post-retrofit performance was in reasonable agreement with the retrofit in-situ U-value target of 0.29 W/m²K at most locations, however the in-situ U-value at EW20 (0.75 (±0.05) W/m²K) was 2.6 times greater than the target in-situ U-value. The post-retrofit in-situ U-value at EW18 of 0.43 (±0.03) W/m²K was ~50% greater than the retrofit in-situ target U-value.

Figure 18 shows the external wall retrofit R-value increase at locations used in the calculation of the external wall in-situ U-value. Change in R-value at each location is not dependent on baseline performance.

Figure 18: External wall retrofit R-value increase at non-bridged locations

38

Figure 18 shows that significant retrofit underperformance was measured at 3/10 of the external wall locations used to calculate the external wall in-situ U-value, most notably at EW20. Inspection of the EWI during its deconstruction in Phase 3 did not reveal any issues with its installation. Underperformance was measured in the 2013 Saint-Gobain tests in the regions around EW3 and EW20. Borescope investigation at the location of EW3 during the 2014 Saint-Gobain study revealed a cavity within the solid wall above an airbrick in the vicinity of EWI allowing chamber air to infiltrate the wall structure. A high-volume smoke air leakage investigation revealed the presence of interconnected air paths within the gable wall at first floor level towards the rear of the Energy House extending to verge level. It was suspected that warm air was bypassing the EWI layer in this region of wall. Prior to the EWI install in DEEP, four HFPs were fixed to the exterior of the external wall at corresponding locations to the location of internal HFPs to assess whether bypassing of the EWI was occurring. Figure 19 shows heat flux measured at locations on internal wall surface and corresponding locations at wall/EWI interface.
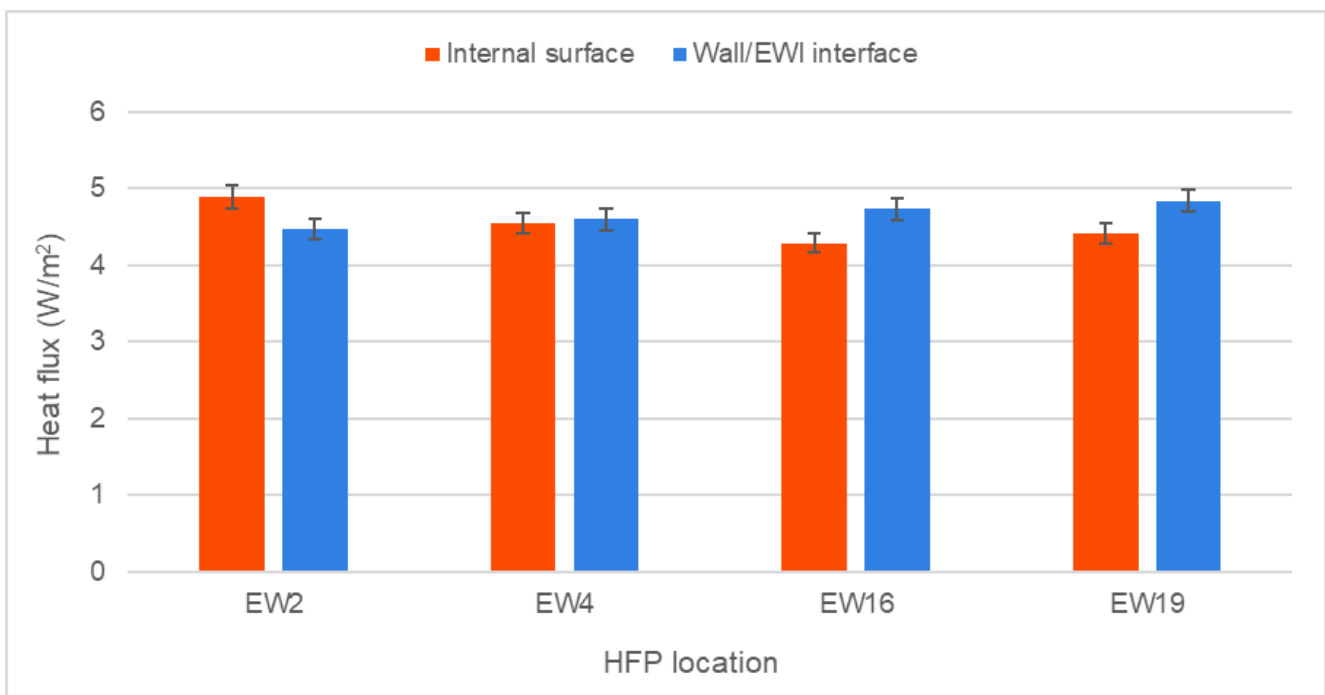
Figure 19: Heat flux measured at locations on internal wall surface and corresponding locations at wall/EWI interface

Bypassing of the EWI would be characterised by significantly greater heat flux on the internal surface than measured by corresponding locations at the wall/EWI interface. Despite significant post-retrofit underperformance at EW18 and EW20, either side of EW19, the heat fluxes measured internally and at the wall/EWI interface were reasonably similar. This suggests that thermal bypassing of the EWI was not taking place at the location of EW19. Further testing of EWI on the gable wall of Bedroom 2 is required to identify the cause of underperformance of two separate EWI installations at this location. Such an investigation may assist retrofit designers and installers in optimising solid wall insulation performance.

3.2.2.2 Roof

Three retrofits of the roof took place during DEEP. The performance of each roof retrofit is provided in Table 12.

Table 12: Roof retrofit in-situ U-value in Phases 1 and 3. * Indicates non-significant difference between target and in-situ retrofit U-values

Test stage	Pre-retrofit in-situ U-value (W/m^{2}K)	Post-retrofit target in-situ U-value (W/m^{2}K)	Post-retrofit in-situ U-value (W/m^{2}K)	Target & in-situ retrofit U-value difference
2	0.29 ±0.02	0.14	0.13 ±0.01	-7%*
12	0.33 ±0.03	0.14	0.15 ±0.02	7%*
14	0.34 ±0.02	0.15	0.14 ±0.01	-7%*

Post-retrofit U-values agreed with their target retrofit in-situ U-values at each stage, indicating good repeatability of this retrofit measure. However, it must be noted that all three retrofits were performed by the same installer to the same specification and the original 100 mm mineral wool between joists remained in place throughout the retrofit process.

Figure 20 shows the in-situ U-value at each location used to calculate the roof retrofit in-situ U-value in each test (RF3 was not measured at Stage 12 due to a sensor error).
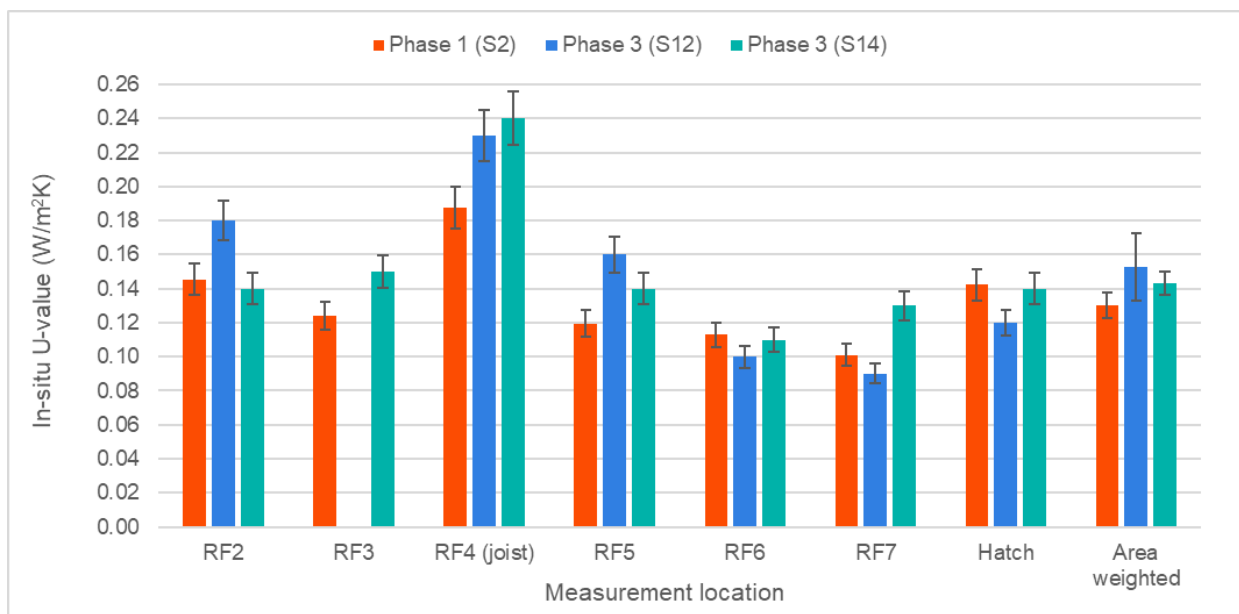
Figure 20: Roof retrofit in-situ U-value at each location for each retrofit

Although the area weighted roof U-values that represent the roof retrofit in-situ U-value were reasonably consistent for each retrofit, variation at individual locations between test stages was evident. This suggests variability in the application of mineral wool insulation across the loft between test stages.

40

Figure 21 compares the R-value of the 170 mm mineral wool (3.86 m^2K/W) applied to the loft during each retrofit with the measured increase in R-value at each unbridged location.
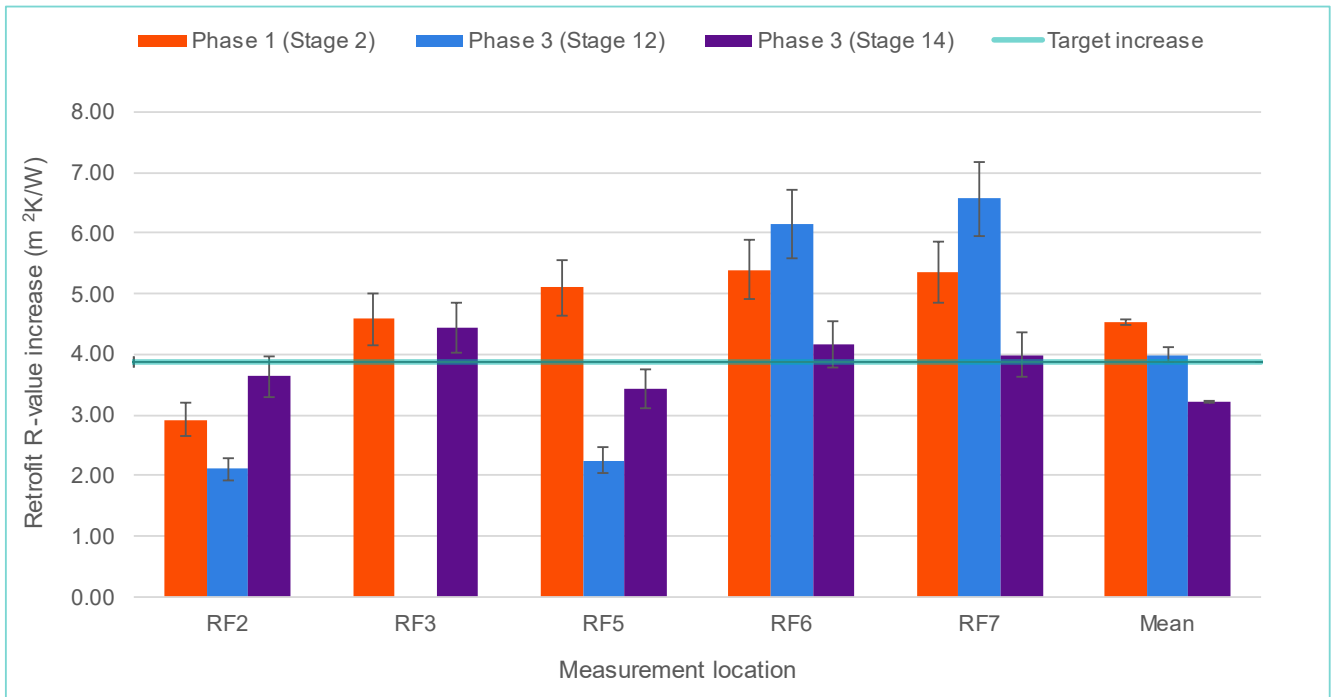
Figure 21: Increase in R-value at each unbridged HFP location on the roof for each retrofit

Variation in retrofit R-value increase at individual locations and between test stages was evident. Some R-value increases greater than target R-value increases were measured. Visual inspection of the loft post-retrofit suggested varying depth of mineral wool across the loft. The installer used the same quantity of insulation for each measure, so underperformance at one location was compensated by overperformance at another. The findings suggest the correct installation of this measure is reliant on installer practice.

Ventilation in the loft space is important for preventing condensation formation. Poor installation of loft insulation can result in ventilation points at the eaves becoming blocked. Blower door tests were conducted with the loft hatch open and closed pre- and post-loft retrofits. The AP_{50} value with the loft hatch open remained the same pre- and post-retrofit for each loft retrofit. This indicated that the loft insulation did not restrict air flow at the eaves during each install.

3.2.2.3 Ground floor

The performance of ground floor retrofits in Phases 1 and 3 is provided in Table 13

Table 13: Ground floor retrofit in-situ U-value in Phases 1 and 3. * Indicates non-significant difference between target and in-situ retrofit U-values

Test stage	Pre-retrofit in-situ U-value (W/m^{2}K)	Post-retrofit target in-situ U-value (W/m^{2}K)	Post-retrofit in-situ U-value (W/m^{2}K)	Target & in-situ retrofit U-value difference
4	0.69 ±0.03	0.21	0.22 ±0.03	5%*
15b	0.59 ±0.03	0.20	0.25 ±0.06	25%*

The ground floor retrofits showed poor repeatability. The Phase 1 retrofit performed in good agreement with the post-retrofit target U-value, whereas the Phase 3 retrofit suggested a 25% performance gap.

Figure 22 shows the in-situ U-value at each location used to calculate the ground floor retrofit in-situ U-value in Stages 4 and 15b.
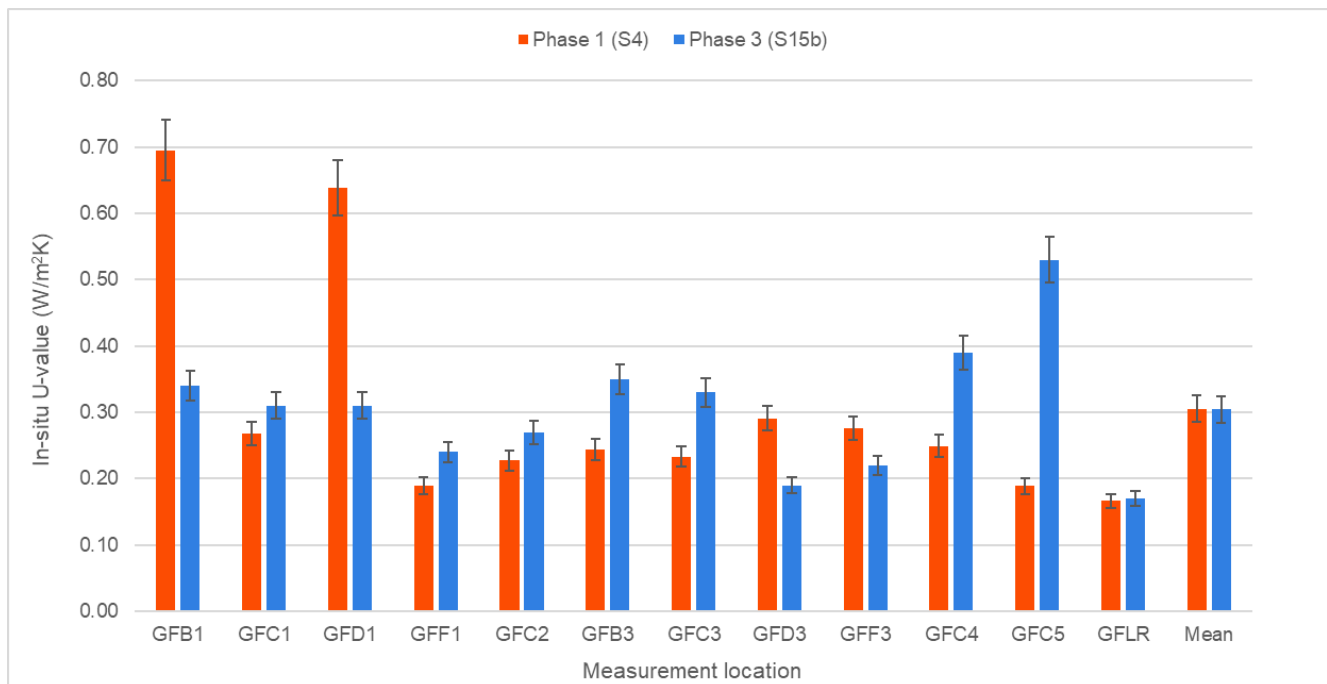
Figure 22: Ground floor retrofit in-situ U-value at unbridged locations for each retrofit

Variation in ground floor in-situ U-values across its surface was anticipated. The 0.3 W/m^{2}K difference in the (non-area weighted) mean of the unbridged in-situ U-values for each test was not significant. However, there was significant variation at most measurement locations in the two retrofits. The in-situ U-values at GFB1 and GFD1 in Stage 4 were approximately double those measured in Stage 15b and *vice versa* at GFC5.

Figure 23 compares R-value of the 150 mm mineral wool (3.41 m^{2}K/W) applied to the ground floor during each retrofit with the measured increase in R-value at each unbridged location.
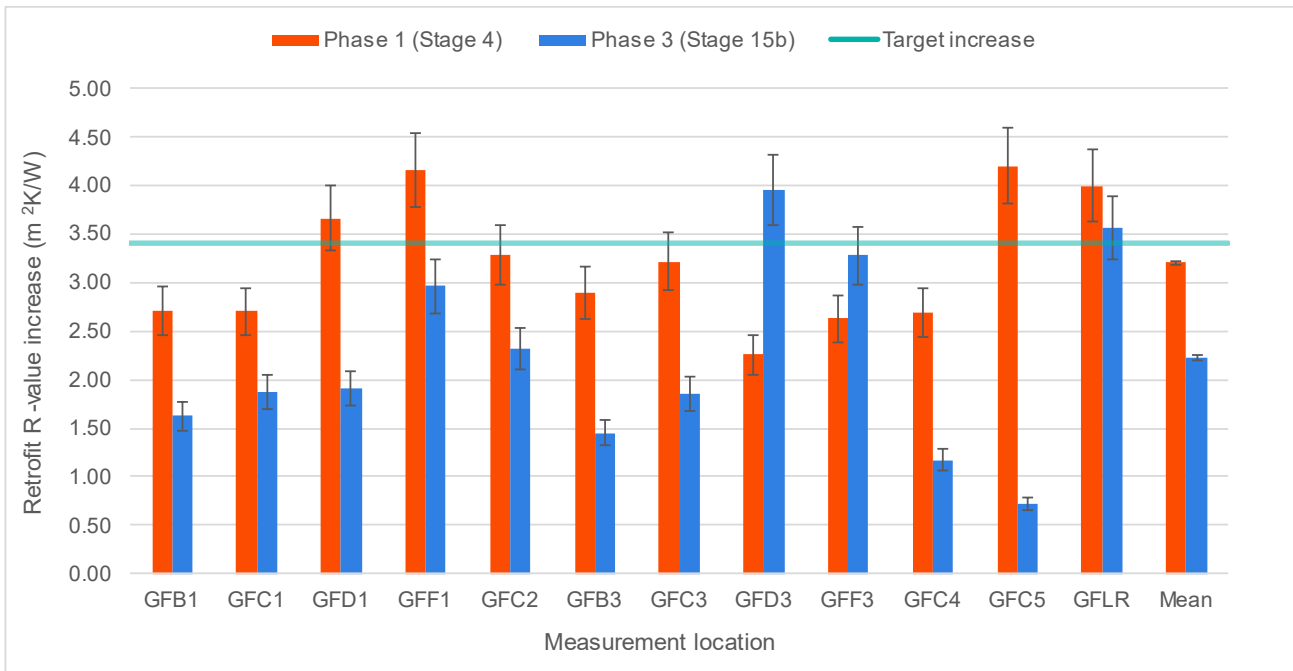
Figure 23: Increase in R-value at unbridged locations on the ground floor for each retrofit

The R-value increase at most ground floor measurement locations in the Phase 1 (Stage 4) retrofit was greater than the Phase 3 (Stage 15b) retrofit. In Phase 1, half of the R-value increases achieved the target R-value increase compared with only one quarter of locations in Phase 3. Visual inspection of the ground floor retrofits revealed inconsistencies in the depth of the ground floor membrane which resulted in variation in insulation contact with the floorboards across the ground floor. The poor airtightness achieved by the Phase 3 retrofit may also have resulted in increased thermal bypassing of the insulation layer. The findings suggest that the performance of this retrofit measure is highly dependent upon installer practice.

3.2.2.4 Openings

Table 11 and Figure 24 provide the pre- and post-retrofit in-situ U-values for the openings during Phase 1. It must be noted that only the original window frames were retained throughout the entire test programme and only the DGUs were changed.
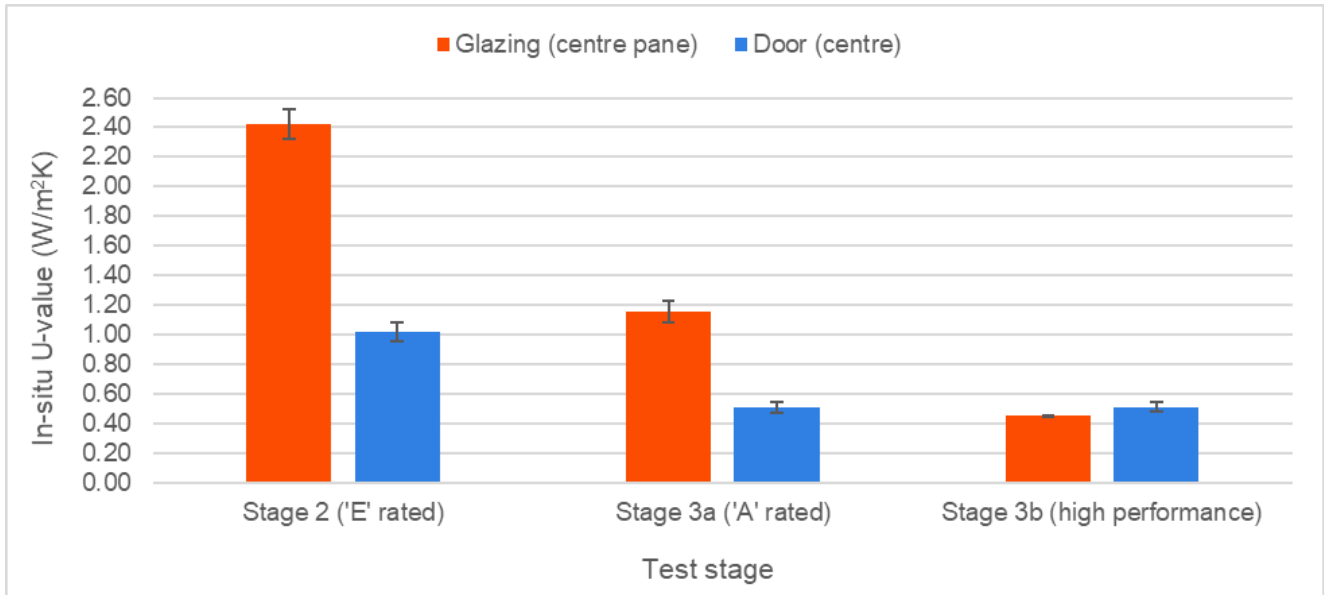
Figure 24: In-situ U-value of openings pre- and post-retrofit

Replacing the 'E' rated DGUs with 'A' rated DGUs reduced the in-situ centre pane U-value by 1.26 W/m^2K (52%). Replacing the 'E' rated doors with 'A' rated doors reduced the in-situ centre door panel U-value by 0.51 W/m^2K (50%).

The high performance DGUs reduced the in-situ centre pane U-value by 1.97 W/m^2K (81%) on an 'E' rated baseline and by 0.71 W/m^2K (61%) on an 'A' rated baseline. The centre pane U-value of 0.45 ($\pm$0.01) W/m^2K for the high performance DGUs is comparable to triple glazing performance.

In-situ U-values in both Phase 1 and Phase 3 were in good agreement, this was due to only the DGUs being replaced.

3.3 Thermal bridging

3.3.1 Whole house thermal bridging heat loss (H_{TB})

Table 14 provides the bridging heat loss (H_{TB}) and y-values derived from thermal modelling at each stage of the retrofit process.

Table 14: H_{TB} and y-value derived from thermal modelling at each stage of the retrofit

Test stage	H_{TB} (W/K)	y-value (W/m^{2}K)	ΔH_{TB} from previous stage (W/K)	ΔH_{TB} from previous stage	ΔH_{TB} from baseline (W/K)	ΔH_{TB} from baseline
1	4.2	0.03	-	-	-	-
2	7.8	0.06	+3.6	+86%	+3.6	+86%
3a	7.8	0.06	0.0	0%	+3.6	+86%
4	13.4	0.10	+5.6	+72%	+9.2	+219%
5	28.3	0.21	+14.9	+111%	+24.1	+574%
6a	27.3	0.21	-1.0	-4%	+23.1	+550%
6b	26.1	0.20	-1.2	-4%	+21.9	+521%
6c	25.2	0.19	-0.9	-3%	+21.0	+500%
6d	22.0	0.17	-3.2	-13%	+17.8	+424%

H_{TB} was also calculated by subtracting plane element heat losses ($\Sigma U*A$) and the CO_2 decay derived H_v from the measured HTC. H_{TB} values derived from disaggregation of the HTC is provided in Table 15.

Table 15: H_TB and y-values derived from HTC disaggregation at each stage of the retrofit process (Stage 3b is change from Stage 2 and Stage 4 is change from Stage 3a)

Test stage	H_{TB} (W/K)	y-value (W/m²K)	ΔH_{TB} from previous stage (W/K)	ΔH_{TB} from baseline (W/K)	H_{TB} disaggregated-H_{TB} modelled (W/K)
1	-1.5	-0.01	-	-	-5.7
2	-4.5	-0.03	-3.0	-3.0	-12.3
3a	3.5	0.03	+8.0	+5.0	-4.3
3b	7.2	0.05	+11.4	+8.7	-0.6
4*	11.4	0.09	+7.9	+12.9	-2.0
5	28.5	0.21	+17.0	+30.0	0.2
6a	26.6	0.20	-1.9	+28.1	-0.7
6b	24.5	0.18	-2.1	+26.0	-1.6
6c	25.7	0.19	1.1	+27.1	0.5
6d	26.6	0.20	+1.0	+28.1	4.6

Figure 25 compares the change in H_{TB} at each stage of the retrofit process obtained through thermal modelling and HTC disaggregation.

Figure 25: H_TB change on previous test stage based on thermal modelling and HTC disaggregation (Stage 3b is change from Stage 2 and Stage 4 is change from Stage 3a)

The H_{TB} value derived from each method were in reasonable agreement throughout most of the retrofit process. This provides a reasonable level of reassurance that the findings from the H_{TB} analysis are robust. The greatest discrepancies occurred at Stages 1 and 2 where negative values that were derived from HTC disaggregation. Negative thermal bridging can occur where the external heat loss area is lower than the internal heat loss area (not applicable for the Energy House) and where internal elements adjoin external elements. In the case of the latter, the fabric of the internal element provides additional resistance than its surroundings. The discrepancy could be due to the modelling not representing as-built junction detailing and/or issues with the HTC disaggregation calculation during these stages. The large change in H_{TB} derived from HTC disaggregation in the Stage 3 tests suggests uncertainty with the Stage 2 H_{TB} value of -4.5 W/K as minimal modifications to the junctions were performed between Stages 2 and 3. The window frames were retained when the glazing was replaced, and the retrofit door frames were fitted in the same positions.

H_{TB} derived from both methods shows that thermal bridging heat losses generally increased throughout the piecemeal retrofit process, in-line with expectations. H_{TB} derived from both methods significantly increased at Stage 5 as the EWI interacts with the greatest number of junctions. However, the in-situ temperature factor (f_{Rsi}) measurements showed that the risk of surface condensation and mould growth only increased at the EW/GF (joists perpendicular) junction after the application of EWI (refer to section 3.3.2).

H_{TB} derived from modelling and HTC disaggregation resulted in respective 6.3 W/K and 1.9 W/K reductions resulting from the conversion of the piecemeal retrofit (Stage 5) to a whole house approach retrofit (Stage 6d). The lower H_{TB} reduction from whole house approach measures derived from HTC disaggregation means that the retrofit was not as effective as predicted by thermal modelling. This could be attributed to issues with the modelling method and/or workmanship. The H_{TB} findings agree with the in-situ f_{Rsi} measurements (refer to section 3.3.2) and suggests that the whole house approach reduces thermal bridging heat losses.

Figure 26 compares the H_{TB} derived from thermal modelling and HTC disaggregation with the H_{TB} calculated using the RdSAP assumed y-value of 0.15 W/m^{2}K.
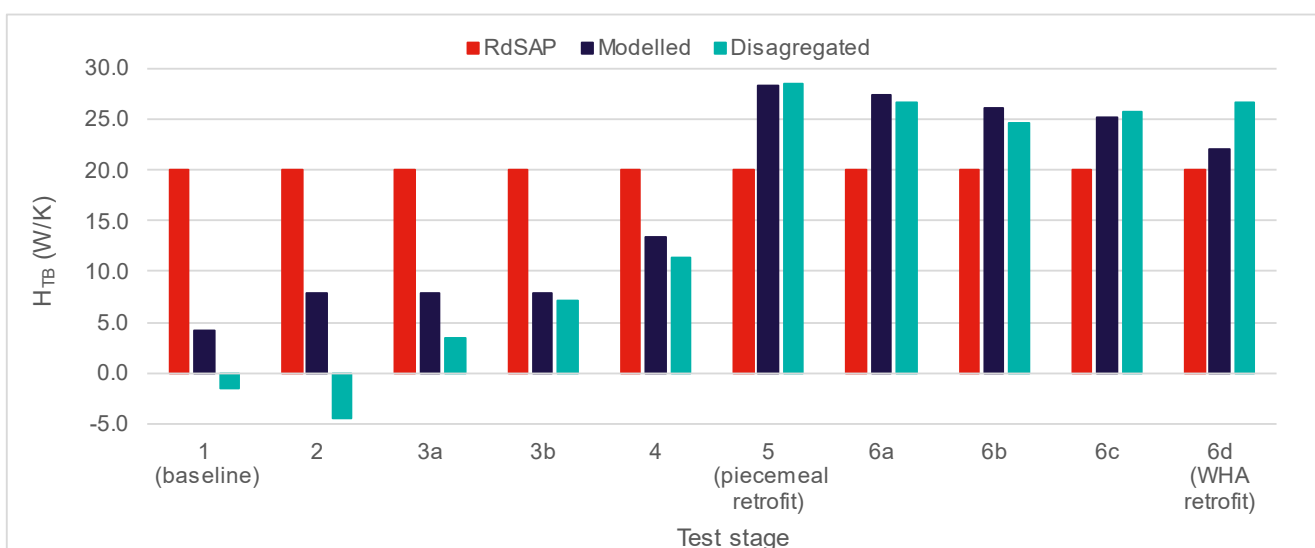
Figure 26: H_{TB} derived from RdSAP, thermal modelling, and HTC disaggregation

47

The RdSAP y-value of 0.15 W/m^{2}K results in a H_{TB} of 19.9 W/K across all retrofit stages. The RdSAP y-value of 0.15 W/m^{2}K is five times greater than that predicted by thermal modelling at the baseline stage. This results in a substantial overestimation of H_{TB} in comparison to other calculation methods until the application of EWI at Stage 5. From Stage 5 onwards RdSAP underestimates H_{TB}, though the discrepancy between the H_{TB} derived from RdSAP and other methods is substantially reduced. This suggests that the RdSAP y-value of 0.15 W/m^{2}K could result in significant overestimation of H_{TB} for relatively uninsulated dwellings. Which in turn could result in retrofits failing to deliver the anticipated reductions in HTC following whole house retrofit.

3.3.2 Temperature factor

Figure 27 shows the number of the Energy House's junctions in each surface condensation and mould growth risk category at the landmark test stages. Although the f_{Rsi} values may not be applicable to all solid wall dwellings due to construction details and materials, the change in behaviour resulting from retrofit is likely to be similar for dwellings with junctions in comparable configurations.
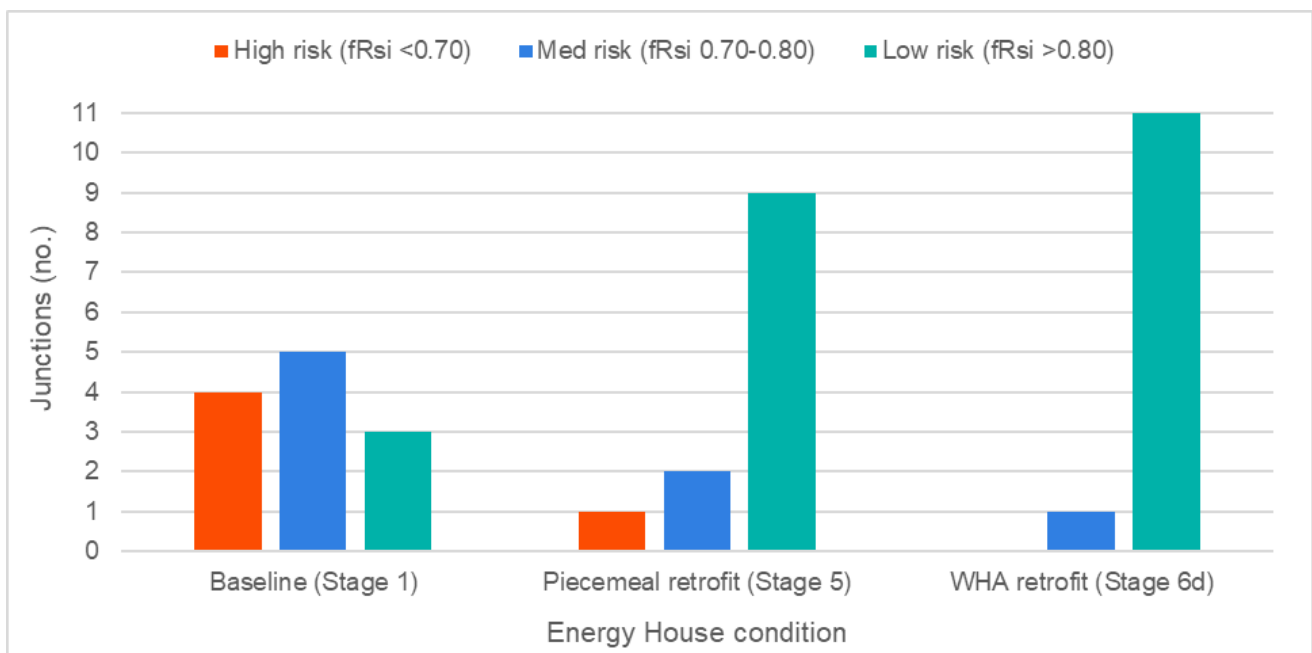
Figure 27: Energy House junctions in each f_{CRsi} risk category

In its baseline condition (Stage 1), three quarters of the Energy House's junctions were deemed to pose a risk of surface condensation and mould growth. At the full piecemeal retrofit stage, one quarter of junctions were considered to pose a risk. The whole house approach measures resulted in only the external wall ground floor junction with joists parallel to the external wall considered to pose a medium risk (0.76 ±0.03). The findings suggest that a whole house approach to retrofit is required to minimise the risk of surface condensation and mould growth, though success is by no means guaranteed.

Figure 28 provides the in-situ f_{Rsi} measurements at each test stage in Phases 1 and 2. Values in bold represent test stages with fabric modifications in the vicinity of the f_{Rsi} measurement. Red denotes high risk of surface condensation and mould growth (<0.70), orange represents a medium risk (0.70-0.79), and green a low risk (≥0.80). Junction identifiers can be found in Table 5.

Detail\Test stage	1 (base)	2	3a	3b	4	5 (PA)	6a	6b	6c	6d (WHA)
EW/GF (par)	0.63	0.67	0.63	0.64	**0.86**	**0.78**	**0.80**	0.80	0.81	0.81
EW/GF (perp)	0.64	0.64	0.64	0.65	**0.65**	**0.73**	**0.73**	0.73	0.75	0.76
EW/IF	0.78	0.78	0.77	0.78	0.76	**0.97**	0.97	0.98	0.98	0.97
EW/RF (eaves)	0.65	**0.69**	0.62	0.62	0.64	**0.65**	0.64	**0.65**	**0.90**	0.89
EW/RF (gable)	0.73	**0.73**	0.74	0.74	0.74	**0.87**	0.87	0.87	0.88	0.88
EW (corner)	0.55	0.61	0.55	0.55	0.55	**0.86**	0.85	0.85	0.87	0.86
EW/PW	0.74	0.72	0.73	0.73	0.72	**0.81**	0.81	0.82	0.80	0.82
Jamb	0.76	0.76	**0.78**	**0.78**	0.76	**0.84**	0.83	0.84	0.84	**0.84**
Sill	0.83	0.80	**0.80**	**0.81**	0.81	**0.81**	0.81	0.82	0.81	**0.81**
Lintel	0.88	0.88	**0.88**	**0.88**	0.86	**0.88**	0.88	0.88	0.91	**0.90**
Bay lintel	0.73	0.74	**0.75**	**0.74**	0.74	0.75	0.75	**0.82**	0.83	**0.86**
PW/RF	0.99	0.99	1.00	1.00	1.00	1.00	1.00	1.00	1.00	1.00
PW/RF (CV)	0.81	**0.80**	0.79	0.80	0.80	0.82	0.81	0.82	0.83	0.83
EW/PW (CV)	0.92	0.92	0.92	0.91	0.91	**0.92**	0.91	0.91	0.92	0.92

Figure 28: In-situ f_{Rsi} measurements at each test stage in Phases 1 and 2

Improvement in the f_{Rsi} at junctions during Phase 1 (Stages 1-5) can be considered incidental rather than intentional. In Phase 1, the risk categorisation of all junctions remained the same until the ground floor retrofit at Stage 4 changed the risk categorisation of the EW/GF (joists perpendicular) junction from high to low. The ground floor retrofit did not improve the EW/GF (joists parallel) junction as the installers had difficulty insulating the narrow gap between the joist running parallel with the wall and the external wall and applying the airtightness membrane at this location. It is likely that a retrofit to 'best practice' principles would have reduced the risk.

The application of EWI at Stage 5 raised the f_{Rsi} of external wall surfaces away from junctions above the f_{CRsi}, thereby removing the risk of surface condensation and mould growth from most of an element that comprises 37% of the entire thermal envelope. It resulted in modifications to all but one junction and produced the most incidental improvements by removing one third of the junctions from the high and medium risk categories. The risk at the EW (corner) junction changed from high to low risk. The EW/IF, EW/RF (gable), EW/PW, and jamb junctions moved from medium to low risk. The reveals were treated with 5 mm XPS, though this only had a measurable impact on f_{Rsi} at the jambs, moving from medium to low risk[43]. The EWI had a deleterious impact on the EW/GF (par) junction with its categorisation moving from low to medium risk. No impact was measured at the eaves junction and the risk remained high prior to extending the eaves as a whole house approach measure at Stage 6c. Figure 29 shows thermography highlighting the impact of EWI on the risk of surface condensation and mould growth on the front and gable wall surfaces and along the eaves junction throughout the retrofit programme.

---

[43] The jambs were deliberately left untreated in the 2013 Saint-Gobain whole house approach retrofit. This resulted in significant thermal bridging heat loss at this location.

Figure 29: Thermography of eaves and front and gable walls at test Stages 2, 5, and 6. Locations below the f_{CRsi} of 0.75 which are deemed to pose a risk of surface condensation and mould growth are highlighted in red (measurements on glazing panels are unreliable)

The whole house approach measures in Phase 2 (Stages 6a-6d) targeted specific junctions, so f_{Rsi} improvements can be considered intentional. The EWI applied to external walls below DPC at 6a reverted the categorisation of EW/GF (par) junction back to low risk following its change to medium risk at Stage 5. However, the EW/GF (perp) junction remained in the medium risk category. As the external walls below the DPC had been insulated, it is suspected that the poor quality of the airtightness membrane at this junction was allowing air from the underfloor void to cool this junction. The retrofit of the bay window at Stage 6b changed the risk categorisation of the bay lintel junction from medium to low. Extending the eaves at Stage 6c changed the classification of EW/RF eaves junction from high to low risk (Figure 29). Repositioning the openings in line with insulation in the EWI system at Stage 6d only had a measurable impact at the junction between the bay window lintel and roof, though it was already considered low risk prior to 6d. The sill and lintel junctions were categorised as low risk throughout the retrofit process. The jamb moved to the low-risk category during the Stage 5 EWI retrofit due to the application of 5 mm XPS on the external reveals. Stage 6d findings suggest that repositioning the openings was unnecessary in this instance. The thermography in Figure 30 suggests that repositioning the openings increased the risk of surface condensation and mould growth in some locations. This agrees with the H_{TB} increase between Stages 6c and 6d derived from HTC disaggregation.
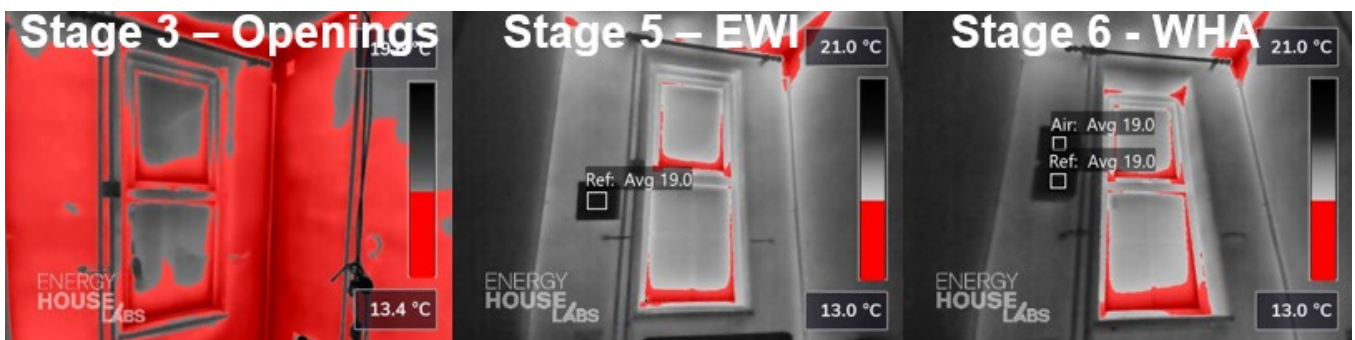
Figure 30: Thermography of rear window and rear and gable walls at test Stages 3, 5, and 6. Locations below the f_{CRsi} of 0.75 which are deemed to pose a risk of surface condensation and mould growth are highlighted in red (measurements on glazing panels are unreliable)

In both Figure 29 and Figure 30 a residual risk of surface condensation and mould growth following the whole house approach retrofit was evident at the eaves/gable interface at the verge on both the front and rear elevations. These locations are highlighted in Figure 31.

Figure 31: Thermography of eaves/gable interface at verge (circled) on both the front (left) and rear (right) elevations after the whole house approach retrofit. Locations below the f_{CRsi} of 0.75 which are deemed to pose a risk of surface condensation and mould growth are highlighted in red (measurements on glazing panels are unreliable)

Figure 32 shows that although some effort was made to insulate the eaves/gable interface, the gap between the rafter and gable wall was too narrow to be insulated. In addition, thermal bridging through the gable brickwork is thought to have contributed to point thermal bridging at this detail.

Figure 32: Hard-to-treat detail at eaves/gable interface at verge resulting in residual risk of surface condensation and mould growth following the whole house approach retrofit

All junctions in the conditioning void were categorised as low risk throughout the retrofit process. The EWI install did not have a measurable impact on the EW/PW junction in the conditioning void.

The Phase 3 EWI only retrofit (Stage 11) resulted in the EW/GF (joists perpendicular) junction moving from the low to medium risk category (f_{Rsi} 0.77). The EW/GF (joists parallel) junction moved from the medium to high-risk category (f_{Rsi} 0.57). This suggests that suspended timber floors should be insulated before EWI is applied or measures put in place to mitigate the risk. EWI below DPC with the ground floor uninsulated was not tested, but it's potential to provide mitigation in this scenario should be investigated.

3.4 Heat transfer coefficient (HTC)

3.4.1 Retrofit HTC reduction

Table 16 provides the measured HTC at each retrofit stage in Phases 1 and 2. The change on previous stage for Stage 3b is based on change from Stage 2. The change on previous stage for Stage 4 is based on Stage 3a.

Table 16: HTC measured at each stage of the retrofit process

Test stage	HTC (W/K)	Change on previous stage (W/K)	Change on previous stage	Change on baseline (W/K)	Change on baseline
1 (baseline)	163.9 ±3.5	-	-	-	-
2	162.7 ±3.1	-1.1 ±4.6	-1%	-1.1 ±4.6	-1%
3a	155.1 ±2.9	-7.6 ±4.2	-5%	-8.8 ±4.5	-5%
3b	151.1 ±1.6	-11.6* ±3.4	-7%	-12.8 ±3.8	-8%
4	148.1 ±3.3	-7.0* ±4.4	-5%	-15.8 ±4.8	-10%
5 (piecemeal)	82.8 ±2.4	-65.3 ±4.0	-44%	-81.1 ±4.2	-49%
6a	82.1 ±1.2	-0.7 ±2.6	-1%	-81.8 ±3.7	-50%
6b	79.5 ±1.2	-2.6 ±1.7	-3%	-84.4 ±3.7	-51%
6c	79.9 ±1.2	0.4 ±1.7	+1%	-84.0 ±3.7	-51%
6d (WHA)	80.3 ±1.8	0.4 ±2.2	0%	-83.6 ±3.7	-51%

The piecemeal retrofit (Stage 5) resulted in a 50% (81.1 ±4.2 W/K) reduction in HTC from baseline (Stage 1). The whole house approach retrofit (Stage 6d) resulted in a 2% (1.8 ±3 W/K) lower HTC than the piecemeal retrofit, a 51% (83.6 ±3.9 W/K) reduction from baseline. As Stages 5 and 6d HTCs were within measurement uncertainty, the whole house approach retrofit failed to deliver any significant HTC reduction benefit over the piecemeal retrofit. Thermal bridging calculations predicted that the whole house approach measures collectively would reduce the HTC by 6.3 W/K from Stage 5, thus resulting in a HTC of 76.5 W/K, a 53% reduction from the Stage 1 baseline. The Stage 6d measured HTC of 80.3 (±1.8) W/K represents a 5% performance gap for the whole house approach measures.

Figure 33 shows the cumulative impact of each retrofit during Phases 1 and 2.
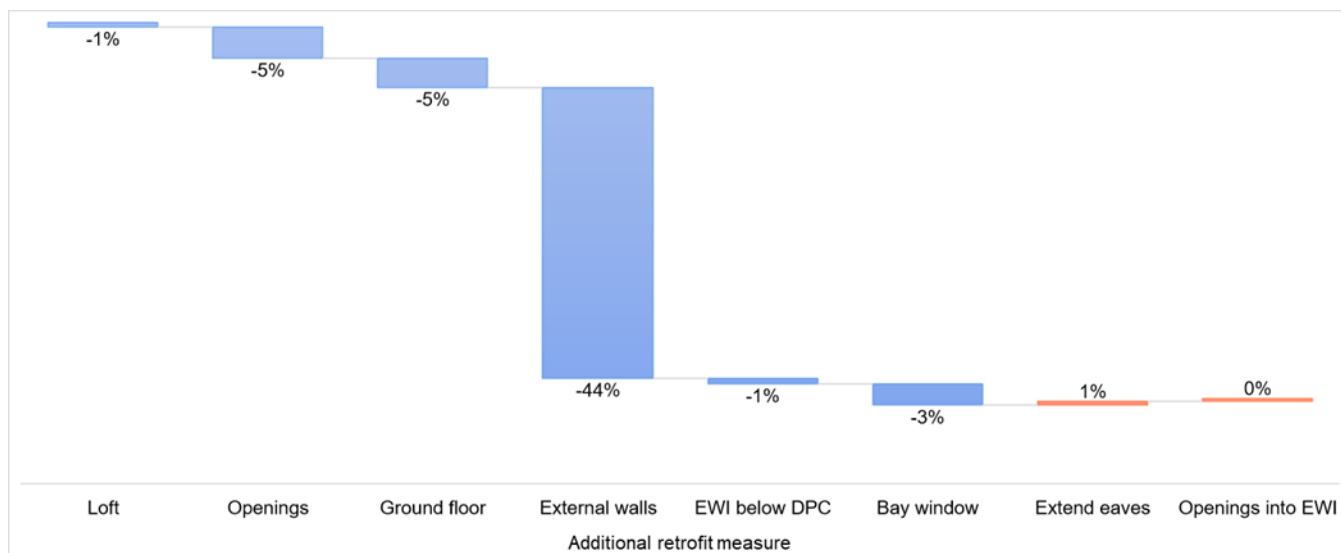
Figure 33: Cumulative impact of retrofits at each stage in Phases 1 and 2

The only retrofits that resulted in measurable reductions in HTC were the openings, ground floor and external walls. The application of EWI at Stage 5 resulted in a 44% (65.3 ±4 W/K) reduction in HTC from Stage 4 and was responsible for 78% of the 83.6 W/K HTC reduction from baseline resulting from the whole house approach retrofit.

The high impact of the external wall retrofit and relatively modest reductions in HTC from other retrofits was partially due to the Energy House being an end-terrace. External walls are 47% of its external heat loss area, openings 10%, and the ground floor and roof 21% each. For a similar mid-terrace, external walls would represent only 26% of the total heat loss area, with openings 14%, and the ground floor and roof 30% each. Table 17 compares the contribution of each fabric retrofit towards the total HTC reduction resulting from the whole house approach retrofit with estimated values based on the Energy House being a mid-terrace[44].

Table 17: Impact of dwelling form on HTC reduction resulting from a whole house approach retrofit

	End-terrace (measured)	Mid-terrace (estimated)	Mid-terrace (estimated)
Standard of openings	'A' rated	'A' rated	High performance
HTC reduction	51%	34%	38%
Roof contribution	1%	3%	3%
Openings contribution	9%	22%	31%

---

[44] Mid-terrace values are based on subtracting the measured external wall U-value multiplied by the party wall area from the measured HTC (HTC-(U_{EW}*A_{PW}))

	End-terrace (measured)	Mid-terrace (estimated)	Mid-terrace (estimated)
Ground floor contribution	8%	19%	17%
External wall contribution	78%	48%	43%
WHA contribution	3%	7%	7%

The relative impact of solid wall insulation and HTC reduction is reduced in the mid-terrace scenario. This demonstrates the importance of dwelling form in the potential improvement that can be achieved by retrofit and specification of retrofits. However, the findings suggest that substantial reductions in the HTC of solid wall dwellings can only be achieved by application of solid wall insulation.

3.4.2 Measured vs. predicted HTCs

Figure 34 compares the measured HTC at each stage of the retrofit process in Phases 1 and 2 with those predicted using calculated U-values and ventilation and thermal bridging heat losses based on SAP/RdSAP assumptions (refer to Section 2.2.5).
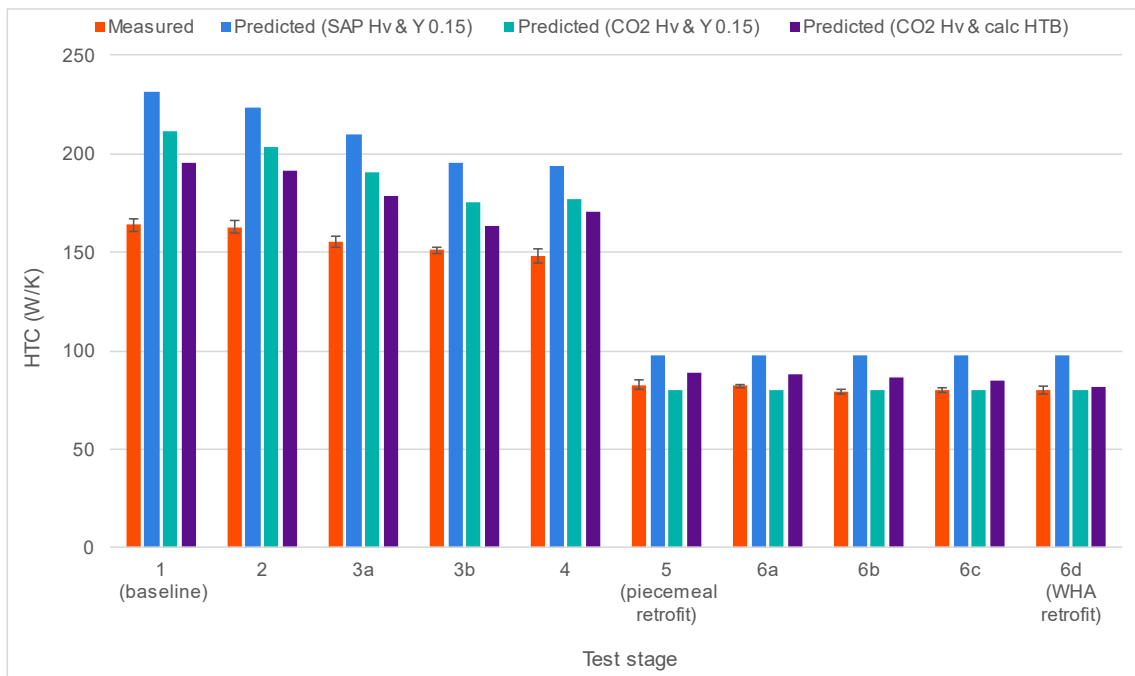
Figure 34: Measured and predicted HTCs at each stage of the retrofit process

The measured HTC reductions of 50% and 51% for the piecemeal and whole house approach retrofits, respectively, were significantly lower than the 58% predicted HTC reduction. The predicted HTC overestimated the measured HTC by 29% at the baseline stage, 15% at the piecemeal retrofit stage (Stage 5), and 18% at the final whole house approach retrofit (Stage 6d). Discrepancies reduced as more calculated U-values were introduced into the predicted

HTC calculation as post-retrofit performance was in reasonable agreement with predicted U-values. This is due to the R-value of retrofit measures providing the majority of the total R-value of each retrofitted element, meaning pre-retrofit R-value assumptions contributed only a small proportion of the total predicted R-value.

Ventilation heat loss is lower at the Energy House than the external environment, so overestimation was anticipated. Substituting SAP derived H_v with the CO_2 decay derived H_v in the predicted HTC calculation resulted in the HTC prediction overestimation of 22% at the baseline stage, a 3% underestimation at the piecemeal retrofit stage, and no discrepancy at the final whole house approach stage. Introduction of H_{TB} values derived from thermal modelling further improved the agreement between predicted and measured HTC for piecemeal retrofits but did not improve HTC predictions for the whole house approach stage.

Assuming retrofits are installed correctly, the findings suggest that inaccuracies in predicted HTC calculations reduce as the total retrofitted surface area increases. However, all methods significantly overestimated the resulting reduction in HTC for both retrofit approaches. This has implications for funding models based on savings in energy bills. Cost-effective fabric performance measurement tools and SMETER technologies could potentially reduce the prediction gap and inform retrofit decision-making processes.

3.4.3 Disaggregated HTC

The disaggregated HTC at each stage of the retrofit process was calculated by summing in-situ U-value measurements ($\Sigma U*A$), H_{TB} values from thermal modelling, and H_v derived from CO_2 concentration decay. Figure 35 compares the coheating test measured HTC and disaggregated HTCs using H_v derived from CO_2 decay and $n_{50}/20$ at each Phase 1 and 2 test stage.
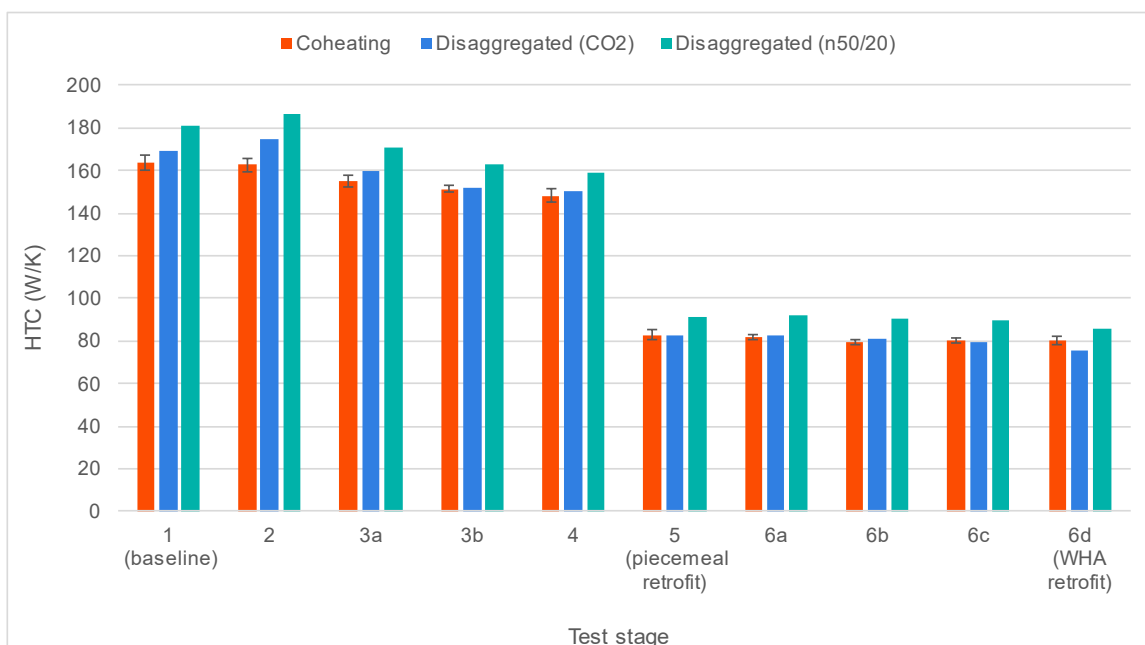
Figure 35: Coheating test measured HTC and disaggregated HTCs using H_v derived from CO_2 decay and $n_{50}/20$

The closer agreement between the measured HTC and disaggregated HTC derived from CO_2 decay measurements suggests this method is more appropriate for HTC disaggregation.

55

Figure 36 shows the disaggregated HTC at each Phase 1 and 2 test stage. Figure 37 shows the proportion of heat losses from each component of the HTC at each stage of the retrofit process.
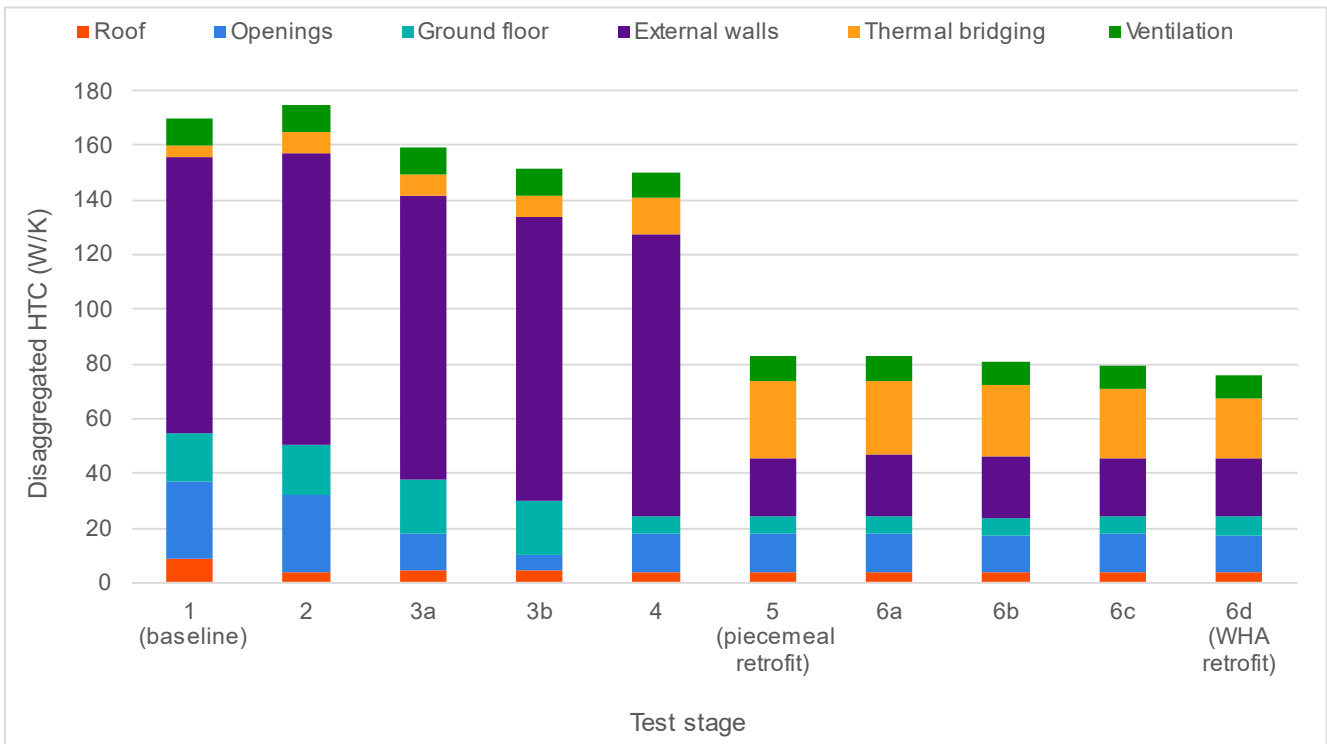
Figure 36: Disaggregated HTC at each stage of the retrofit process
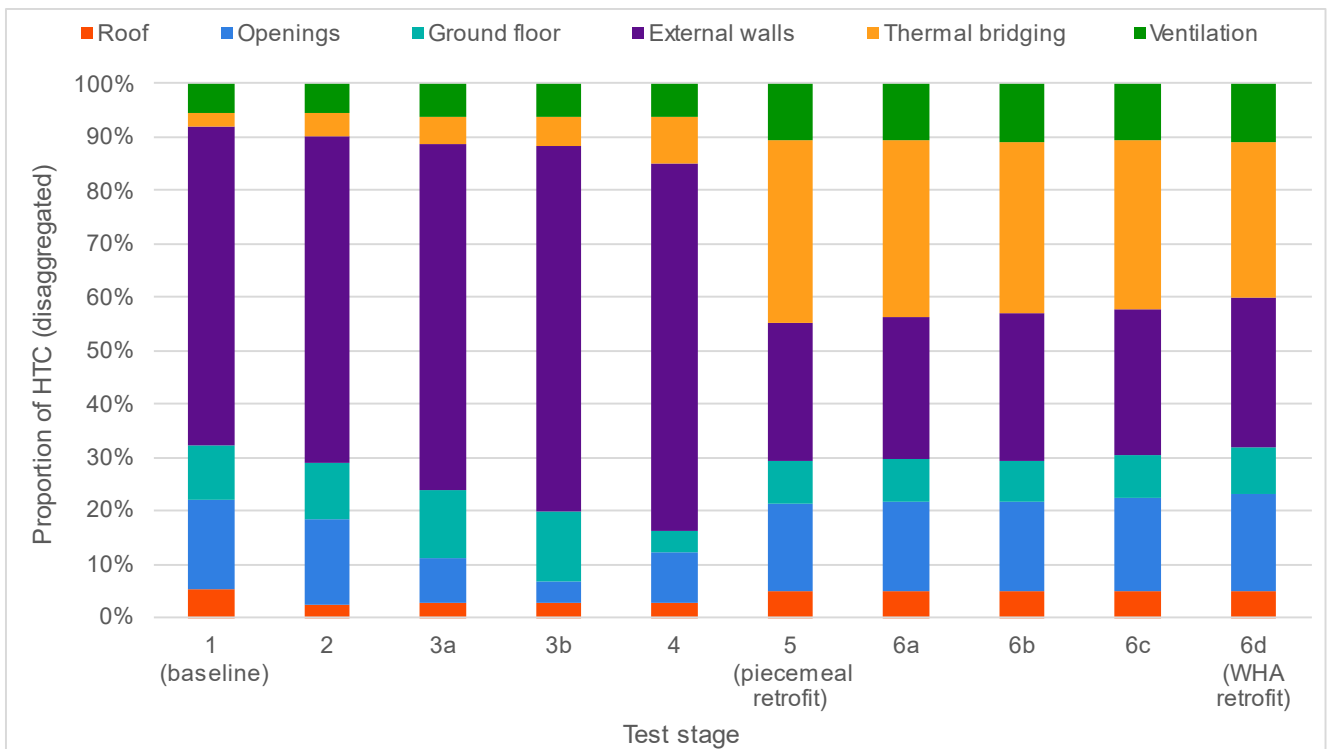
Figure 37: Proportion of heat losses from each component of the HTC at each stage of the retrofit process

Thermal bridging and ventilation heat losses became more prominent after the EWI retrofit at Stage 5, following which, thermal bridging heat losses were responsible for ~30% of the HTC during the remaining test stages. whole house approach measures had a minor impact on the proportion of heat loss attributable to each component of the HTC.

3.4.4 Retrofits to individual elements

Table 18 provides the HTCs measured during Phase 3 where retrofits to individual measures were tested in isolation.

Table 18: HTC resulting from retrofit of individual elements

Test stage	Element retrofitted	HTC (W/K)	Phase 3 HTC reduction (W/K)	Phase 1 HTC reduction (W/K)	Ph3 - Ph1 HTC reduction(W/K)
10	All (piecemeal)	87.5 ±0.8	84.8 ±1.8	81.1 ±4.2	+3.7 ±4.6
11	EWI	107.8 ±1.4	64.4 ±2.1	65.3 ±4.0	-0.9 ±4.5
13	Openings	165.9 ±1.7	6.4 ±2.3	7.6 ±3.4	-1.3 ±5.1
14	Loft	168.8 ±1.8	3.4 ±2.3	1.1 ±4.6	+2.2 ±5.1
15b	Ground floor	165.5 ±2.9	4.4 ±3.3	7.0 ±4.4	-2.6 ±5.5
16	None (baseline)	172.2 ±1.7	-	-	-

The sum of the individual elemental retrofit HTC changes was 78.6 W/K, which is 2.1 W/K lower than the Phase 1 piecemeal HTC reduction, and 6.2 W/K lower than the difference between the Phase 3 piecemeal retrofit (Stage 10) and Phase 3 baseline (Stage 16) of 84.8 W/K. The discrepancies are within measurement uncertainty, so no firm conclusions can be drawn as to whether it is due to differences in thermal bridging at junctions. The differences between Phase 1 and Phase 3 reductions are within measurement uncertainty, so suggest the repeat retrofit measures resulted in similar HTC change.

3.5 Retrofit thermal benefit, cost, and disruption

Table 19 summarises the thermal benefit, cost, and disruption associated with each retrofit measure. It must be noted that the costs and times provided may not be representative of 'real world' costs due to the increased complexity of performing work within a chamber, absence of economies of scale within the procurement process, the lack of consideration that needs to be paid to occupants, and sheltered environment. The whole house approach costs are associated with conversion works rather than works being performed simultaneously. Disruption has been defined for this study as the requirement for work within the habitable space and to adapt services or relocate furnishing during the retrofit.

Table 19: DEEP Energy House retrofit thermal benefit, cost, and disruption (time based on one person except EWI)

Stage	Retrofit	Cost (exc. VAT)	Time (days)	Disruption	HTC change (W/K)	F_{Rsi} risk junctions removed (no)	F_{Rsi} risk junction removed (m)
2	Roof	£720	0.25	Low	-1.1	0	0
3a	Openings	£3,123	1.5	Med	-7.6	0	0
4	Ground floor	£1,978	3	High	-7.0	1	7.6
5	External walls	£14,064	14[45]	Med	-65.3	4	46.5
6a	EWI below DPC	£1,442	0.5	Low	-0.7	1	7.6
6b	Bay window	£1,410	3	Med	-2.6	1	2.3
6c	Extend eaves	£4,827	6	Low	+0.4	1	7.4
6d	Openings into EWI	£4,490	5	Med	+0.4	0	0

All piecemeal works required access to the habitable space. The roof retrofit only required access between the external door and loft hatch and was completed within a couple of hours. The openings retrofit required access to each room, while the replacement doors required new frames. This task was responsible for most of the time taken to perform the retrofit to the openings. As only the window DGUs were replaced, the work was completed within a few hours. Replacing the window frames would have significantly increased the time taken to perform this measure. The ground floor retrofit caused the most disruption. Had the kitchen units and internal furnishings not been removed prior to DEEP, they would have needed

---

[45] 14-day installation period involving between two to four operatives onsite at one time. Confined space thought to have increased installation time.

removing along with the floor coverings and then replaced post-retrofit, adding to the disruption. The EWI install required wastewater pipes to be extended through the EWI and refitted to the surface of the EWI.

The conversion process from piecemeal to whole house approach retrofit resulted in minimal disruption for all measures except repositioning of the openings in-line with the EWI. The application of EWI below the DPC, initial bay window retrofit, and eaves extension required no internal works. Moving openings in-line with EWI required access to the dwelling over multiple days and the bay side windows to be replaced due to the change in geometry.

The Phase 1 (Stages 1-5) retrofit cost was £19,885. The conversion to a whole house approach retrofit increased the cost by an additional £12,169 (61%), resulting in a total cost of £32,054.

The EWI retrofit was the most expensive retrofit measure, representing 71% and 44% of the piecemeal and whole house approach retrofit cost, respectively. However, it provided the overwhelming majority (78%) of the HTC reduction resulting from the entire retrofit process and removed the risk of surface condensation and mould from the greatest number and length of junctions. It was also one of the least disruptive retrofit measures. It must be noted that the impact of EWI on the heat loss and treatment of junctions is likely to be lower than similar installations on mid-terrace dwellings, though the cost of retrofit is also likely be lower.

Extending the eaves reduced the risk of surface condensation and mould growth at this junction and provided effective protection against the ingress of moisture behind the EWI. Including this measure with the EWI installation would have increased the cost of the EWI retrofit cost by ~30%. However, at one location the eaves extension resulted in the existing loft insulation being displaced between ceiling joists which doubled the heat loss at the junction.

Given the limited benefits provided by moving the openings in line with the insulation in the EWI system, expense, disruption, and potential for unintended consequences associated with the works, it could be argued that this could be omitted from a whole house approach retrofit if the existing EWI already provides adequate treatment of reveals. Omission of Stage 6d in DEEP would have saved £4,490. This represents a total retrofit cost saving of 14% and reduced the additional cost of whole house approach conversion measures by 39%.

The installation of EWI below DPC level at Stage 6a could also be considered superfluous due to the limited benefits it provided. A 'best practice' ground floor retrofit may have treated the EW/GF (joists parallel) and removed the risk of surface condensation and mould growth at this junction. Omission of Stages 6a and 6d in DEEP would have reduced total retrofit costs by £5,932. This represents a total retrofit cost saving of 19% and reduced the additional cost of whole house approach conversion measures by 31%.

3.6 Alternative in-situ test methods

3.6.1 HTC measurement

HTC measurements were performed at various stages throughout the DEEP test programme using the Saint-Gobain QUB and Veritherm test methods to assess whether they could accurately quantify the reduction in HTC resulting from retrofit. Figure 38 shows the temperatures and power input during the Stage 1 QUB test, similar behaviour was evident during the Veritherm tests.
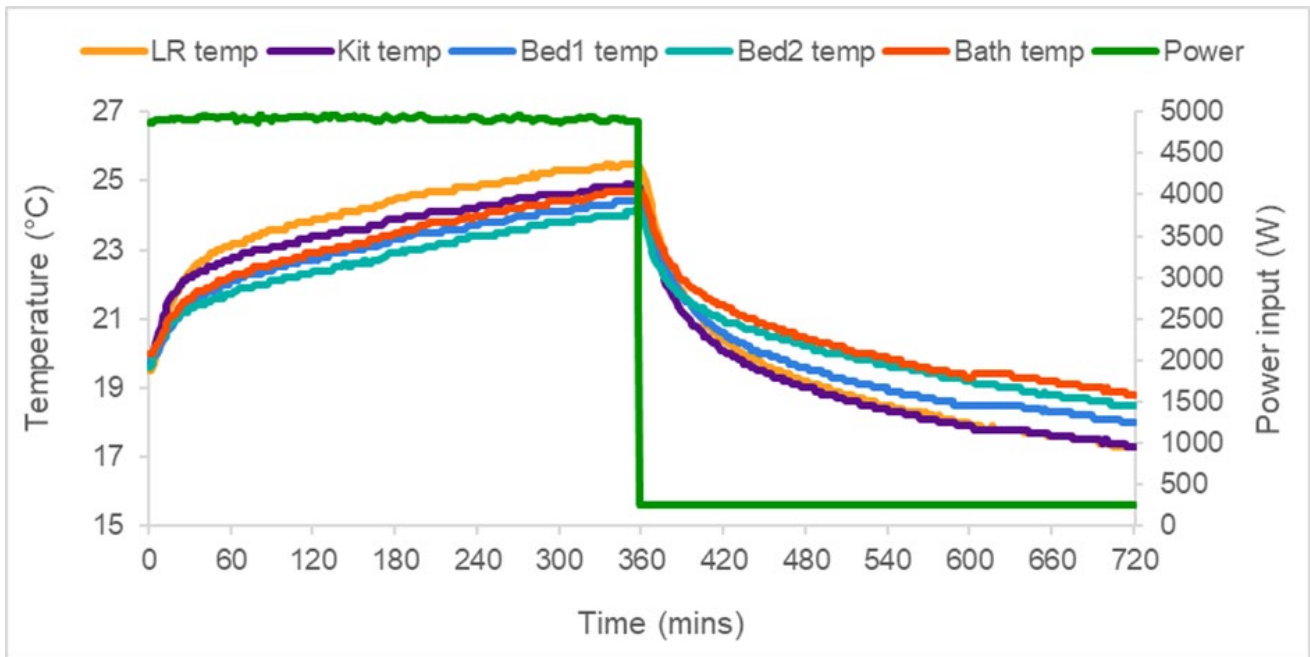
Figure 38: Internal temperatures and power input measured during the Stage 1 QUB test

Veritherm visited the Energy House to perform tests at four stages during Phase 1 of the DEEP test programme. QUB tests were performed at eight stages during DEEP[46]. QUB tests were performed by the UoS research team using UoS heaters and the Energy House monitoring system to perform the tests. Analysis of QUB test data was performed by the UoS research team. The results from the coheating and alternative HTC test methods can be found in Table 20 and Figure 39.

---

[46] Time constraints meant that it was not possible to accommodate QUB and Veritherm tests at each retrofit stage.

Table 20: HTCs measured using the coheating, QUB, and Veritherm tests

Test stage	Coheating HTC (W/K)	QUB HTC (W/K)	Veritherm HTC (W/K)	QUB difference from coheating	Veritherm difference from coheating
1	163.9 ±3.5	166.2 ±5.8	-	1%	-
2	162.7 ±3.1	154.1 ±4.9	$144\,^{-18}_{+24}$	-5%	-12%
3	155.1 ±2.9	153.1 ±4.6	$151\,^{-20}_{+27}$	-1%	-3%
4	148.1 ±3.3	156.8 ±4.1	$154.5\,^{-16}_{+20}$	6%	4%
5	82.8 ±2.4	97.3 ±3.6	$91.2\,^{-10.5}_{+13}$	17%	10%
10	87.5 ±0.8	96.9 ±3.8	-	11%	-
11	107.8 ±1.4	119.6 ±5	-	11%	-
12	158.4 ±1.5	151.6 ±4.1	-	-4%	-
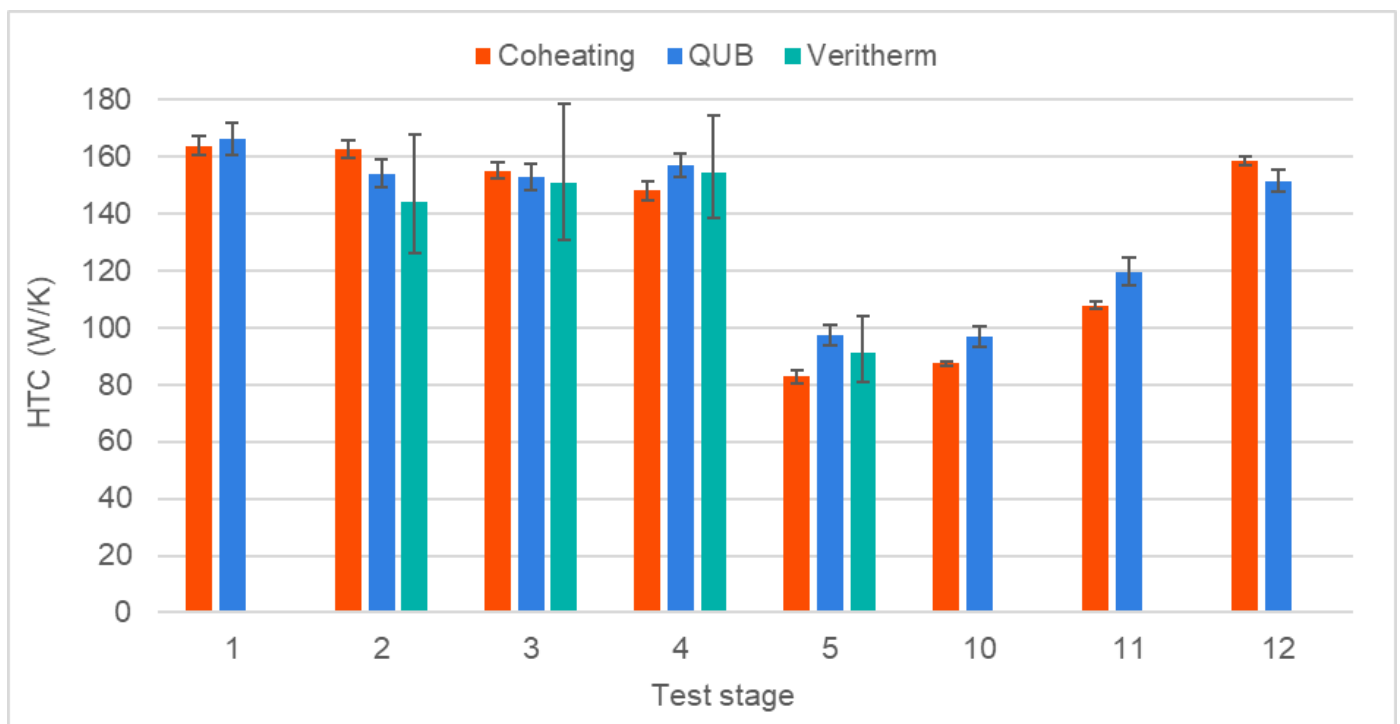
Figure 39: HTCs measured using the coheating, QUB, and Veritherm test methods

The HTCs measured by the alternative methods were generally in good agreement with the coheating test HTCs when measurement uncertainty is considered. Veritherm uncertainty was typically 3-5 times greater than QUB, which resulted in more Veritherm HTCs agreeing with coheating HTCs across the four stages in which tests using all three methods were performed. Both QUB and Veritherm were unable to measure any significant reduction in HTC following retrofits to the openings and ground floor at Stages 3 and 4, respectively. Table 21 shows the change in HTC at each stage of the piecemeal retrofit process measured by coheating, QUB, and Veritherm.

Table 21: Change in HTC at each stage of the piecemeal retrofit measured by coheating, QUB, and Veritherm

Test stage	Coheating change on previous stage (W/K)	QUB change on previous stage (W/K)	Veritherm change on previous stage (W/K)
2	-1.1 ±4.6	-12.1 ±7.6	-
3	-7.6 ±4.2	-1 ±6.7	$+7 \, ^{-26.9}_{+36.5}$
4	-7.0 ±4.4	+3.7 ±6.2	$+3.5 \, ^{-25.6}_{+34}$
5	-65.3 ±4.0	-59.5 ±5.5	$-63.3 \, ^{-19.1}_{+23.9}$

No test method produced a confident estimate of the impact of loft insulation at Stage 2. QUB and Veritherm failed to produce a confident estimate of the impact of the retrofits to openings and the ground floor at Stages 3 and 4, respectively. However, both QUB and Veritherm produced reasonable estimates of the reduction in HTC resulting from the application of EWI at Stage 5.

Early validation of the QUB method took place during the 2013 Saint-Gobain retrofit. Similar issues with measuring relatively small changes in HTC resulting from retrofit were also observed. However, the QUB test provided a reasonable estimation of the impact of solid wall insulation (SWI)[47]. Figure 40 shows the HTCs derived from coheating and QUB tests at each stage of the 2013 Saint-Gobain retrofit.

---

[47] The hybrid solid wall insulation system in the 2013 Saint-Gobain retrofit was similar in performance to the EWI applied in DEEP. For more details of the 2013 QUB tests, please refer to: Alzetto, F., Farmer, D., Fitton, R., Hughes, T. & Swan, W. (2018). Comparison of whole house heat loss test methods under controlled conditions in six distinct retrofit scenarios. Energy and Buildings. 168. 35-41. 10.1016/j.enbuild.2018.03.024
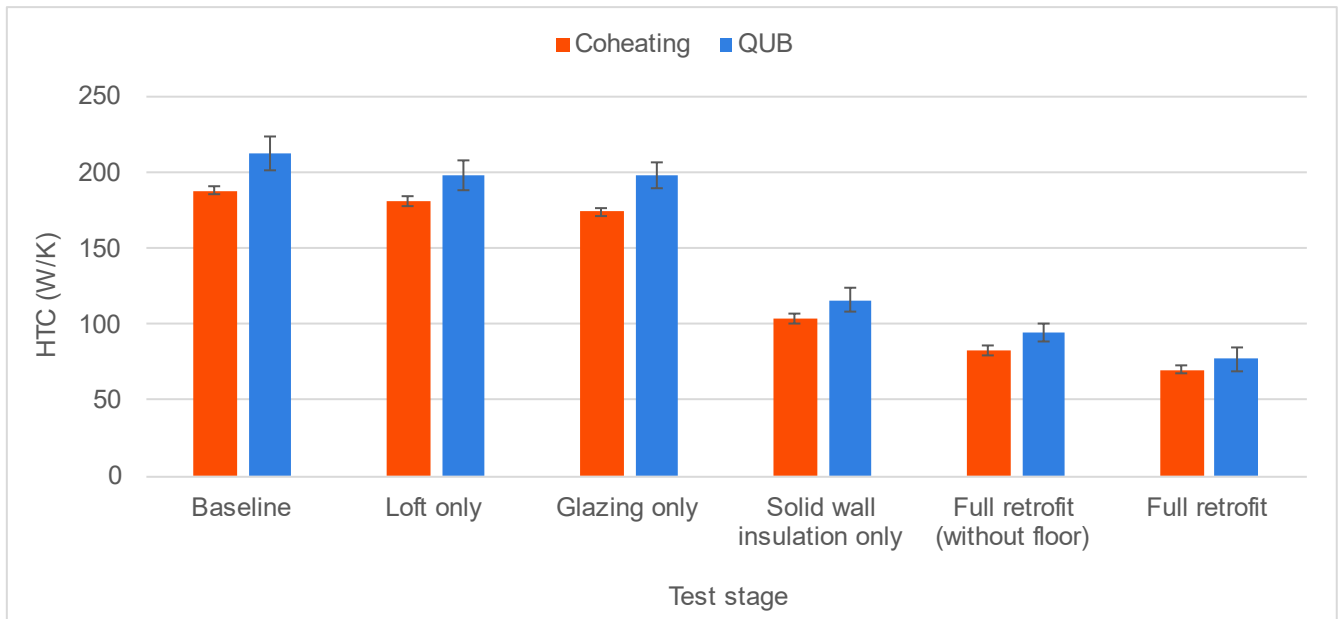
Figure 40: Coheating and QUB HTCs at each stage of the 2013 Saint-Gobain retrofit

It must be noted that all QUB and Veritherm tests were performed with the chamber at a constant temperature of ~4.5 °C. Therefore, conditions at the Energy House during the DEEP project provided a benign test environment in comparison to those experienced in the field due to the absence of dynamic external conditions. However, the findings suggest that QUB and Veritherm are most suited to assessing the impact of retrofit measures that result in substantial reductions in HTC such as the application of SWI. The cost of a Veritherm test currently starts at £500, meaning a pre- and post-retrofit testing total cost of £1,000. Including such testing could significantly increase the cost of retrofit. However, these methods may provide a relatively low-cost method for housing providers to assess the performance of solid wall insulation in pilot retrofit studies.

3.6.2 In-situ U-value measurement

The external wall U-value of the living room was measured in its pre- and post-retrofit conditions using Heat3D. It is an iOS mobile application used for rapid in-situ U-Value measurements (in comparison to ISO 9869) across a predefined area of an external wall. Refer to Section 2.3.1.4 for more details.

Heat3D measurements were compared with the mean of the in-situ U-values measured at EW1 and EW2 on the living room wall. Heat3D only provides the U-value to one decimal place, so three surveys were performed post-EWI retrofit due to the relatively low external wall U-value. The in-situ U-values were 0.2 W/m²K, 0.3 W/m²K, and 0.2 W/m²K. The mean was 0.23 W/m²K with a standard deviation of 0.06 W/m²K. Table 22 provides pre- and post-retrofit in-situ U-values measured using both methods.

Table 22: Pre- and post-retrofit living room external wall in-situ U-value measured using ISO 9869 and Heat3D. *Average of three Heat3D surveys.

Method	Pre- retrofit U-value (W/m²K)	Post-retrofit U-value (W/m²K)	Reduction (W/m²K)	Reduction
ISO 9869	1.44 ±0.09	0.27 ±0.02	1.17 ±0.09	-81%
Heat3D	1.40 ±0.13	0.23* ±0.06	1.17 ±0.14	-83%

It must be noted that the Heat3D tests were performed with the chamber at a constant temperature of ~4.5 °C. Therefore, conditions at the Energy House during the DEEP project provided a benign test environment in comparison to those experienced in the field due to the absence of dynamic external conditions. The findings suggest that Heat3D provides a good estimate of pre- and post-retrofit performance. However, the ability to only measure to one decimal place means resolution becomes more important as U-value decreases. It may be the case that repeated surveys are required to obtain a confident measurement of external walls with a relatively low U-value.

4 Conclusions and recommendations

This case study has provided detailed insight into the thermal performance a of solid wall retrofit. Important findings have emerged relating to the benefits and drawbacks of the piecemeal and whole house approaches to retrofit, the conversion of a pre-existing retrofit, and the repeatability of retrofit measures. The main findings are summarised below.

Benefits and drawbacks of piecemeal and whole house approaches to retrofit

The main benefit of the whole house approach to retrofit was a lower risk of surface condensation and mould growth at junctions. Of the twelve junctions measured in the Energy House, only one was considered a risk following the whole house approach retrofit compared with four after the piecemeal retrofit. The piecemeal retrofit removed most of the risks present at the baseline stage. Though an unintended consequence of the EWI applied during the piecemeal retrofit was the reintroduction of a risk that had previously been removed with the application of ground floor insulation. The residual risk following the whole house approach retrofit was present throughout the retrofit process. This risk was attributed to difficulty installing a piecemeal retrofit measure rather than issues with the design of the whole house approach retrofit or the conversion process. The whole house approach details underperformed by 5%, which was partially attributed to workmanship. The reduction in risk delivered by the whole house approach retrofit shows that it has the potential to provide a healthier internal environment for occupants than a piecemeal retrofit. However, its effectiveness is reliant on material in-situ performance, buildability, and workmanship.

The main drawback of whole house approach retrofit was cost. The whole house approach retrofit was 61% more expensive than the piecemeal retrofit. It reduced the HTC of the Energy House by 51% from baseline. However, the HTC was not significantly different to the 50% HTC reduction resulting from the piecemeal retrofit. If the whole house approach measures performed as predicted, the retrofit would have delivered a 53% HTC reduction from baseline. Therefore, it is unlikely that whole house approach retrofit measures can be funded through payback models that rely on savings in energy bills. Fabric retrofit funding models must also consider the health of an occupant and not just reductions in energy use and CO_2 emissions.

A whole house approach retrofit does not necessarily mean performing all retrofits simultaneously. Retrofits can be undertaking in an elemental fashion with full understanding of future retrofits and adaptations. This principle of forward planning should not only apply to existing dwellings but also the design of new-build dwellings which may require a net-zero fabric retrofit in the future.

Conversion of a pre-existing piecemeal retrofit

The test programme demonstrated that existing piecemeal retrofits can be converted to whole house approach retrofits if required. However, they can also have the unintended consequence of reducing airtightness or increasing thermal bridging if not implemented correctly. The eaves retrofit and repositioning of openings resulted in localised damage to existing airtightness and thermal barriers. Consideration must be paid during their design and implementation to prevent unintended consequences. Both issues were only identified with BPE methods post-retrofit, highlighting the importance of post-retrofit testing.

The openings did not pose a risk of surface condensation and mould growth following the piecemeal retrofit. Moving them in line with EWI did not reduce the risk any further and was unnecessary in this instance. Measures that are often deemed necessary for a retrofit to be considered a whole house approach retrofit may not be required if a junction does not pose a significant risk following a piecemeal retrofit. As whole house approach measures can be disruptive and unlikely to be funded through payback schemes, their application should be targeted according to requirement. The absence of mould growth is not a reliable indicator of thermal performance as the conditions required for it to be present are also influenced by occupant behaviour (e.g., space heating use, ventilation provision, furniture placement). Survey tools are required to assist with identification of at-risk junctions and specification of whole house approach retrofit measures before issues relating to mould growth become manifest.

Airtightness

Elemental retrofits that do not incorporate specific airtightness measures may not improve airtightness. The ground floor retrofit was the only intervention that included a specific airtightness measure and the only retrofit that resulted in a significant improvement in airtightness. However, the two ground floor retrofits in DEEP produced significantly different improvements in airtightness, both of which were significantly lower than two previous ground floor retrofits of the Energy House in a different study. This suggests that workmanship and specification can have a significant impact on potential airtightness improvements. This could pose difficulty when predicting the benefits post-retrofit airtightness of dwellings. Additional retrofits during a piecemeal retrofit can make airtightness worse if interfaces with previous retrofits are not considered. Where possible, fan pressurisation testing with airtightness investigation should be undertaken following retrofit works to identify whether remedial sealing is required and whether a dwelling requires purpose provided ventilation.

External wall retrofit

Retrofit solid wall insulation is likely to provide the single greatest fabric heat loss reduction to solid wall homes. The EWI retrofit provided 78% of the HTC reduction resulting from the entire retrofit process and removed the risk of surface condensation and mould from the greatest number and length of junctions. However, it was also the most expensive measure, representing 71% and 44% of the piecemeal and whole house approach retrofit cost, respectively.

The EWI retrofit did not reduce the risk of surface condensation and mould growth at the eaves. This was addressed by extending the eaves but at significant extra cost. Ideally, these measures should be undertaken concurrently. Alternative low-cost measures are required that not only reduce risk at this junction but also provide effective protection against moisture ingress behind EWI. Existing roof replacements and new-build dwellings should be designed with consideration for future application of EWI.

The 17% EWI performance gap was similar to a previous Energy House EWI retrofit where underperformance was attributed to air movement within the solid wall. Some solid walls have inherent issues that prevents EWI from delivering the anticipated reductions in fabric heat loss. Given that EWI is likely to be the most expensive retrofit measure, the potential for air movement within solid walls to impact EWI and potential mitigation measures requires further investigation.

Roof retrofit

Loft insulation was shown to provide good repeatability of installation, with all three retrofits achieving their target post-retrofit in-situ U-value. However, repeatability at individual locations on the roof was poor. It must be noted that the same installer undertook all three retrofits. The small reductions in HTC resulting from the loft retrofit could be due to the pre-existing 100 mm of loft insulation and the law of diminishing returns for thermal insulation. This means that top-ups of lofts with pre-existing insulation will have longer payback times. The point thermal bridge at the eaves/gable interface at the verge was difficult to treat and requires extra attention during a retrofit.

Ground floor retrofit

Retrofitting suspended timber ground floors can significantly improve airtightness as well as reduce fabric heat loss. However, the two ground floor retrofits resulted in significantly different performance in terms of fabric transmission and airtightness. The presence of internal fixtures resulted in inconsistent perimeter sealing on each occasion. Predicting the performance of suspended timber floor retrofits could be difficult due to their reliance on workmanship to achieve effective sealing and consistency of insulation. The narrow gap between the perimeter floor joist and external wall was difficult to treat with insulation. This resulted in a risk of surface condensation and mould growth that was not removed with EWI below DPC level. Care must be applied to ensure insulation is fitted between floor (and roof) joists running parallel and in close proximity to walls.

Openings retrofit

The openings retrofits produced relatively small HTC reductions. This was attributed to the relatively small proportion of heat loss area and the uninsulated frame not being replaced. Their impact was estimated to be greater for mid-terrace dwellings where openings represent a larger proportion of the surface area. The high-performance double glazing units tested had similar performance to triple glazing and could have contributed 31% of the HTC reduction of a similar mid-terrace retrofitted to the same standard. The manufacturer did not provide a cost for the high-performance glazing. The cost-effectiveness of high-performance windows and glazing for dwellings with a high proportion of glazed areas should be investigated. Replacing DGUs rather than replacing the frames reduced cost and installation time. The potential for changing DGUs rather the entire window assembly should also be investigated.

Thermal bridging calculations

The RdSAP y-value of 0.15 W/m^{2}K can result in a significant overestimation of thermal bridging heat losses for relatively uninsulated dwellings. Which in turn could result in retrofits failing to deliver the anticipated reductions in HTC following whole house retrofit. A wider selection of y-values are required that can be applied to different building typologies across a range of fabric retrofit standards.

Appendix A: Energy House construction

Table A1 provides construction details for the Energy House in its baseline condition.

Table A1: Construction details for the Energy House in its baseline condition

Thermal element	Construction
External walls	Solid wall – 222.5 mm brick arranged in English bond (5 courses) with 9 mm lime mortar and 10.5 mm British Gypsum Thistle hardwall plaster with a 2 mm Thistle Multi-Finish final coat. The ground and intermediate floor joists are built-in to the gable wall.
Roof	Purlin and rafter cold roof structure with 100 mm mineral wool insulation (λ 0.044 W/mK) at ceiling level between 100x50 mm ceiling joists. Ceiling joists run parallel to the gable wall at 400 mm centres above lath (6 mm) and plaster (17 mm) ceiling
Ground floor	Suspended timber ground floor above a ventilated underfloor void (20 mm depth). 150x22 mm floorboards fixed to 200x50 mm floor joists at 400 mm centres. Floor joists run between the gable and party wall with joists ends built into masonry walls.
Windows	4-20-4 'E' rated double glazing units in uninsulated PVCu frames.
Doors	Front – 'E' rated PVCu

Rear – 'E' rated half glazed PVCu. |
| Party wall | Solid wall – as external walls but with plaster finish on both sides. |

Appendix B: Energy House floor plans

Ground Floor Plan

First Floor Plan
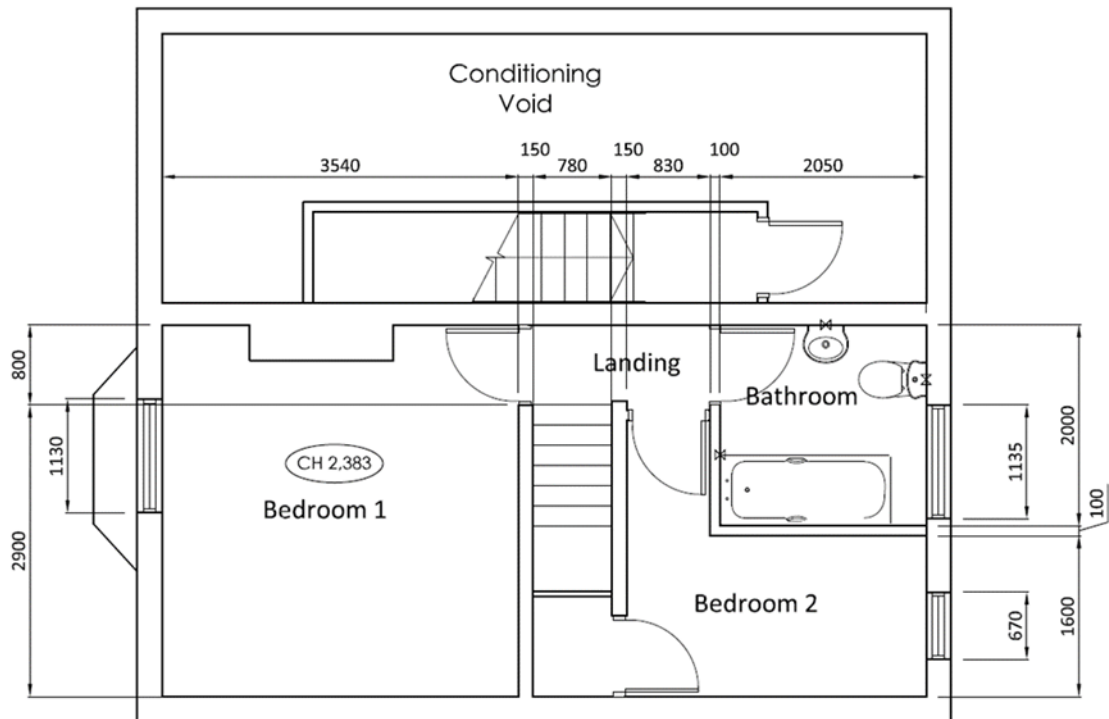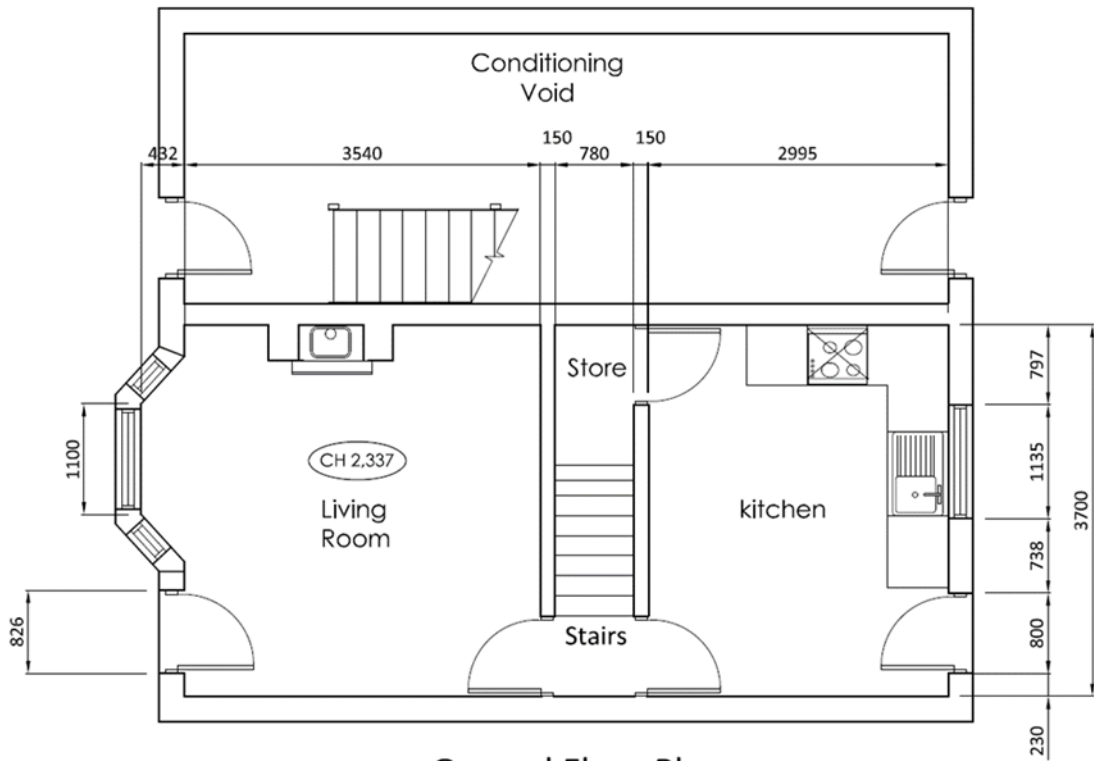
Appendix C: Energy House monitoring

The Energy House test facility is equipped with a monitoring system that records a comprehensive array of parameters used to assess both fabric and heating system thermal performance at one-minute intervals. Additional monitoring equipment can be incorporated into the system if required. Table C1 provides details of the monitoring equipment permanently installed in the Energy House test facility.

Table C1: Energy House monitoring equipment

Measurement	Details
Air temperature	15 locations in each room – three heights in each corner and in centre
	Conditioning void – each zone
	Environmental chamber – mid-storey on each elevation
	Underfloor void and loft
Ground floor slab temperature	Surface
	Below ground at three depths
Black globe temperature	Centre of each room
CO_2 concentration	GF and FF of Energy House
	Conditioning void
	Environmental chamber
Relative humidity	Centre of each room in Energy House
	Each zone in conditioning void
	Environmental chamber – mid-storey on each elevation
Heat flux density	Each thermal element (including party wall)
	Ten locations on ground floor slab

Measurement	Details
Electricity consumption	Each circuit
	Electric heating supply (e.g. IR) to each room
	Selected sockets
Natural gas	Volume
	Flow rate
Central heating (gas & ASHP)	Boiler heat metering (power, energy, flow rate, volume, flow and return temperatures)
	Radiator heat metering (power, energy, flow rate, volume, flow and return temperatures)
	Corrosion rate and pressure monitoring (Resus RisyCor)
	OpenTherm monitoring

Appendix D: HFP locations and identifiers
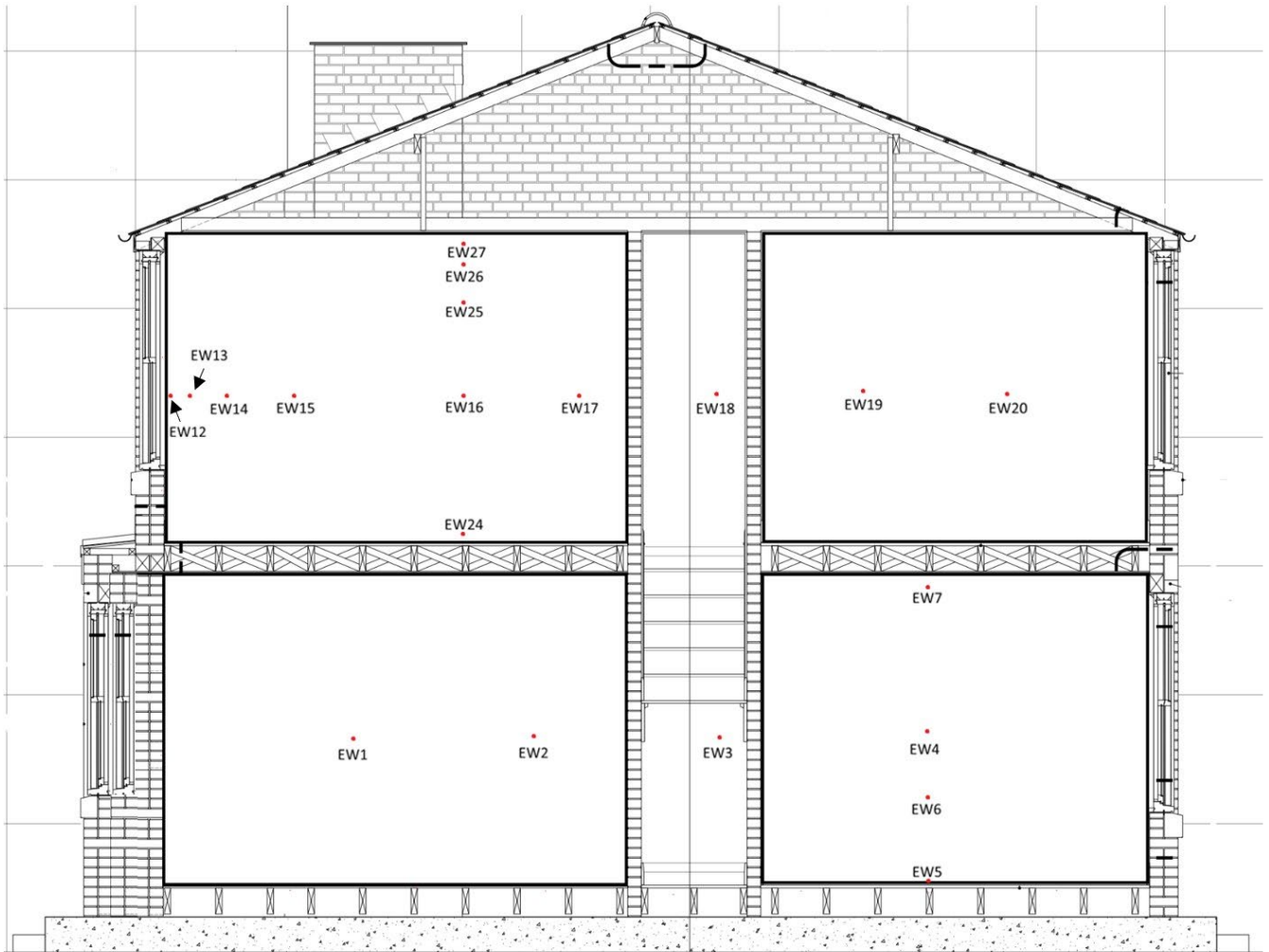
Figure D1: External (gable) wall HFP locations and identifiers
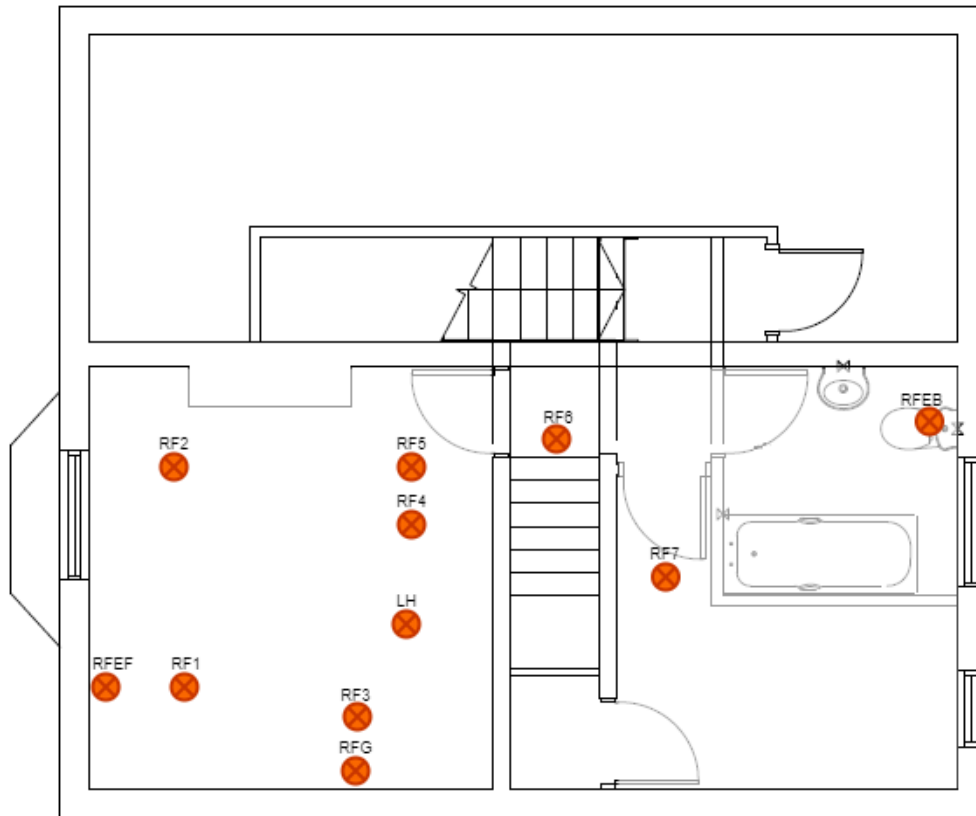
Figure D2: Roof HFP locations and identifiers
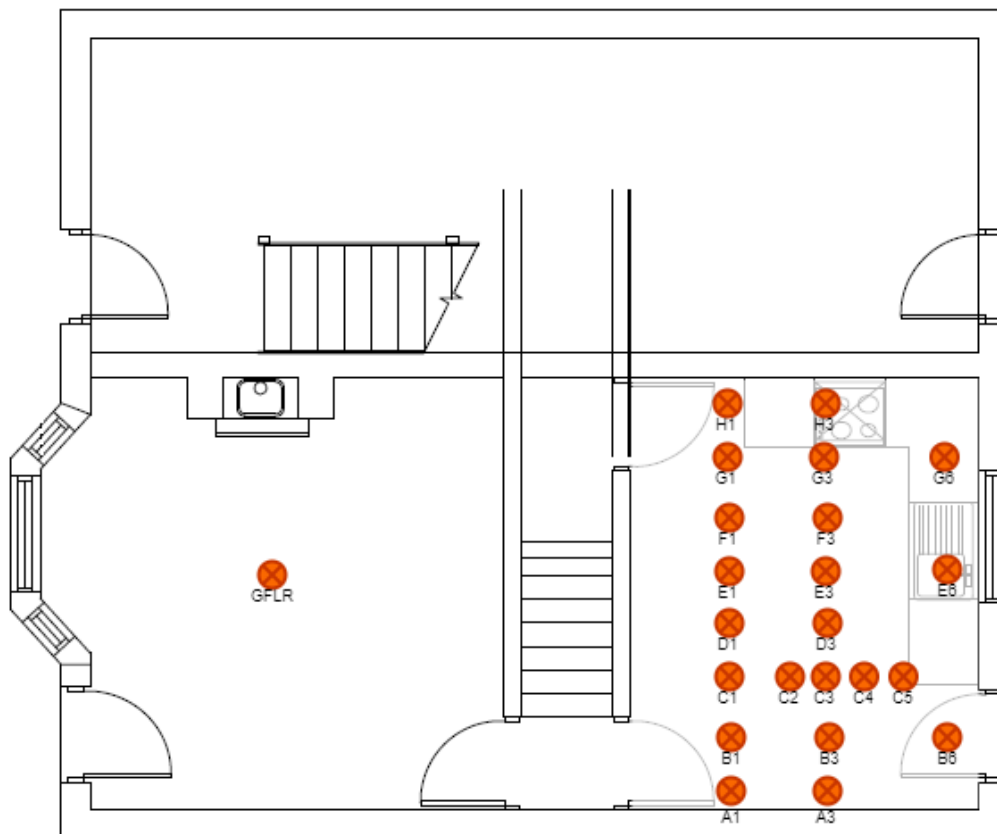
Figure D3: Ground floor HFP locations and identifiers

Appendix E: HTC uncertainty

HTC uncertainty was calculated by considering type A and type B uncertainties.

Type A uncertainty

Type A uncertainty considers statistical variation in the recorded data. To calculate this, the following methods were followed.

Power (Q)

Space heating power input is inherently noisy due to multiple electrical resistance heaters, the limited number of power settings for the heaters, and the sensitivity of their thermostatic controllers. To minimise noise, heaters were placed on the lowest power setting that prevented them being permanently in operation to ensure that the fabric was close to steady state and PID thermostatic controllers were used. The 24-hour averaging period minimises the impact of variation over each aggregation period. However, the standard deviation based on minutely power data over a 24-hour period can overestimate the uncertainty. The "sma()" function from the "smooth" R programming language package is used to create a simple moving average of the power data. This package optimises the moving average by varying the averaging period. It allows uncertainty to capture whether power input over a 24-hour period was significantly different to a previous 24-hour period. The standard deviation of the smoothed data is calculated and taken as the type A power uncertainty.

Volume weighted average internal temperature (T_{i_vw})

The T_{i_vw} is first calculated for every minute of data, using the proportions in Table E2.

The deviation of each individual temperature sensor to the T_{i_vw} is then calculated, denoted by θ.

The standard deviation of all these variations is then calculated and taken as the type A T_{i_vw} uncertainty.

Average external temperature (T_e)

Calculated through a simple mean of the three external temperature sensors located on the front, gable, and rear elevations.

The type A uncertainty of T_e is calculated as the standard deviation of the average external temperature.

Type B uncertainty

Type B uncertainty considers the uncertainty attributed to the accuracy of the measurement device.

The accuracy and standard uncertainty of equipment used in the HTC calculation are stated in Table E1.

Table E1: Accuracy and standard uncertainty of equipment used in the HTC calculation

Variable	Device	Accuracy	Probability distribution	Divisor	Standard Uncertainty
Q [W]	Siemens 7KT PAC1200 digital power meter	1% of measurement	-	-	1% of measurement
T_i [°C]	I.C. sensor	0.4	normal	2	0.20
T_e [°C]	I.C. sensor	0.4	normal	2	0.20

The type B uncertainty of total power input is calculated by taking the 24h average power input (based on cumulative energy data) and multiplying by the stated accuracy (1% of measurement).

The type B uncertainty of both the T_{i_vw} and the average external temperature is calculated using Table E2 and Table E3. The standard uncertainty of each individual temperature sensors is scaled by the same coefficient used in the volume weighting equation. These are then summed following the RSS method.

Table E2: T_{i_vw} type B uncertainty

Zone	Weighting	I.C sensor uncertainty	Scaled uncertainty
Living room	0.252	0.20	0.05
Hall	0.028	0.20	0.01
Kitchen	0.209	0.20	0.04
Bedroom 1	0.237	0.20	0.05
Landing	0.052	0.20	0.01
Bathroom	0.077	0.20	0.02
Bedroom 2	0.105	0.20	0.02
Bedroom 2 cupboard	0.016	0.20	0.00

Zone	Weighting	I.C sensor uncertainty	Scaled uncertainty
Understairs	0.025	0.20	0.01
	Quadrature sum (k = 1)	**0.60**	
	k = 2	**1.20**	

Table E3: T$_e$ type B uncertainty

Elevation	Weighting	I.C sensor uncertainty	Scaled uncertainty
Front	0.333	0.20	0.0667
Gable	0.333	0.20	0.0667
Rear	0.333	0.20	0.0667
	Quadrature sum (k = 1)	**0.09**	
	k = 2	**0.18**	

Combined Uncertainty

The Type A and Type B uncertainty attributed to each measurement are combined through the RSS method prior to error propagation in the HTC calculation.

$$u_{combined} = \sqrt{u_A^2 + u_B^2}$$

Uncertainty Propagation

The uncertainty propagation of the HTC calculation is given by the following equation:

$$u_{HTC} = \sqrt{\left(\frac{u_Q}{\Delta T}\right)^2 + \left(\frac{Q^2}{\Delta T^4}\right) \cdot \left(u_{T_i}^2 \cdot u_{T_e}^2\right)}$$

Expanded Uncertainty

All prior uncertainties have been given as k=1. When stating the uncertainty on plots, the expanded uncertainty (k=1.96) is stated, such that:

$$U = k \cdot u$$

Such a coverage factor should result in a 95% confidence interval.

Figure E1 shows the 24-hour HTCs with uncertainty measured during Stage 1 baseline steady state measurement period test. The dashed line denotes ±5% of the final HTC measurement. The HTC measured in the final 24-hour period of each steady state measurement is reported for each stage.
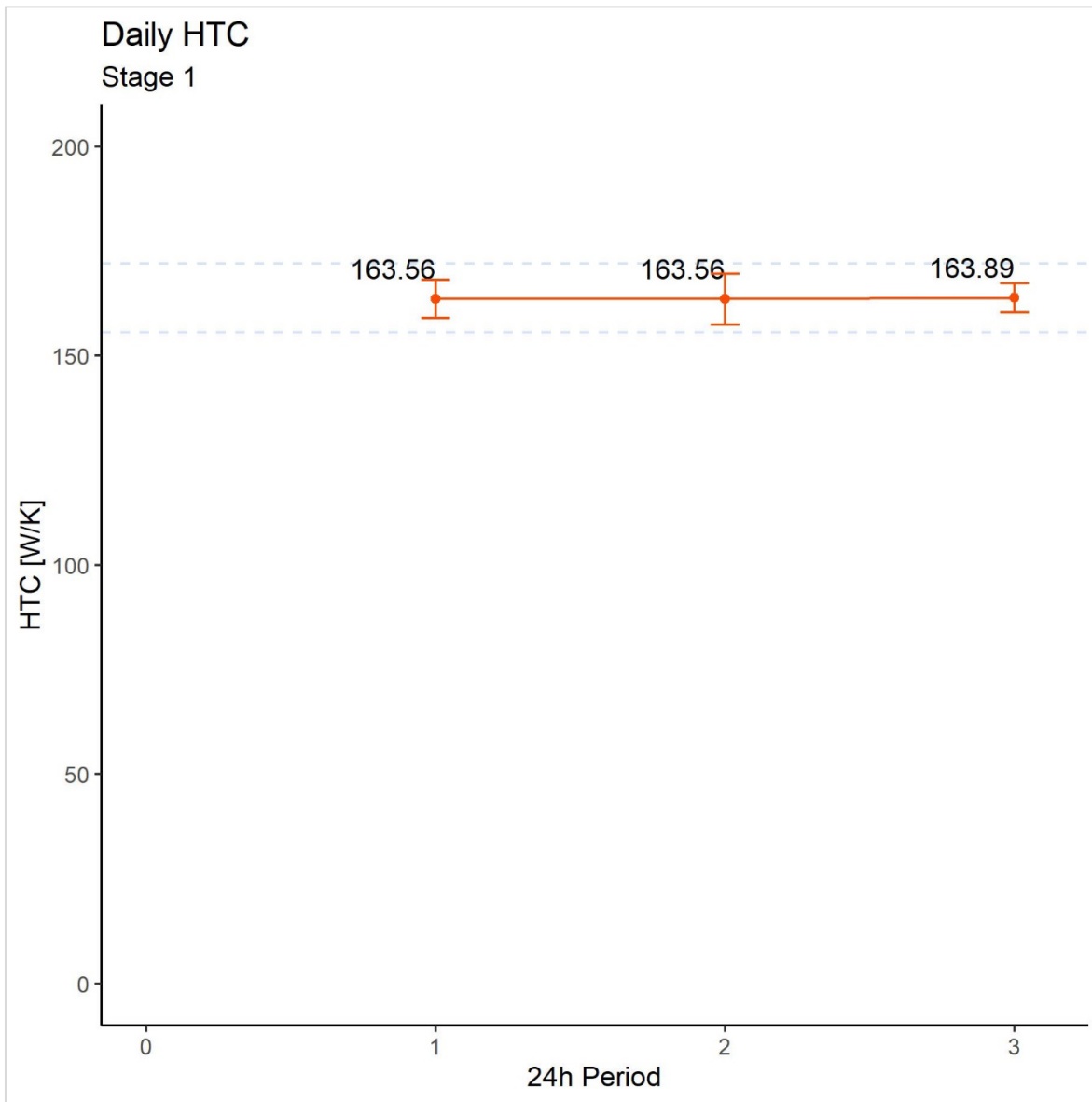
Figure E1: 24-hour HTCs with uncertainty measured during Stage 1 baseline steady state measurement period test

Appendix F: In-situ U-value uncertainty

ISO 9869 applies an uncertainty value of 14-28% to in-situ U-value measurements. However, this uncertainty is based on measurements undertaken in the field without control of external conditions. The ISO 9869 uncertainty calculation was modified for the controlled environment and to include type A and type B uncertainties.

Type A uncertainty

Type A uncertainties consider the statistical variation in the recorded data.

Heat Flux (q)

To reduce noise caused by the operation of electric resistance heaters and fans. the "sma()" function from the "smooth" R programming language package is used to create a simple moving average of the heat flux data. This package optimises moving average by varying the averaging period.

The standard deviation of the smoothed data is calculated and taken as the type A heat flux uncertainty.

T_i and T_e

All U-Value measurements considered a single local internal temperature sensor and a single local external temperature sensor. The standard deviation over a 24-hour period for each sensor was calculated and taken as the type A uncertainty.

Type B uncertainty

Type B uncertainties are based on the sources of uncertainty listed in ISO 9869. Table F1 lists the measurement uncertainties provided by ISO 9869 and modifications that were made for DEEP based on the apparatus and test environment. It must be noted that many of the assumptions regarding sources of uncertainty contained within ISO 9869 are not accompanied with background information as to how they have been derived.

Table F1: Measurement uncertainties provided by ISO 9869 and modifications made for DEEP

ISO 9869 consideration	Notes	% error	Absolute error
Apparatus - Logger	Based on logger accuracy and offset value and DEEP steady state ΔT and heat flux for a U-value of 0.09[48] W/m^{2}K	0.3	

---

[48] U-value of 0.09 W/m^{2}K is the lowest U-value reported in DEEP and associated with a logger uncertainty of 0.3%. As U-value increases logger uncertainty decreases, therefore the maximum logger uncertainty has been applied to all U-value measurements.

ISO 9869 consideration	Notes	% error	Absolute error
Apparatus - HFP	Hukesflux HFP01 datasheet	2	
Apparatus - I. C. temperature sensor	Based on DEEP steady state ΔT	1.8	0.3
HFP contact	ISO 9869 - unadjusted	5	
Isotherm modification	ISO 9869 - unadjusted	2	
Variation in temp & heat flow	ISO 9869 ~10%. Removed as steady state measurement reported. **Captured in type A uncertainty**	0	
Variation in air (T_i) & radiant (T_r) temperature differences	ISO 9869 suggests 5%. Value halved as air circulation fans increase homogeneity & typical 1-2 °C between T_r and T_a at most locations	2.5	
Type B uncertainty	**Quadrature sum**	**6.5**	

Combined Uncertainty

The Type A and Type B uncertainty attributed to each measurement are combined through the RSS method prior to error propagation in the HTC calculation.

$$u_{combined} = \sqrt{u_A^2 + u_B^2}$$

Expanded Uncertainty

All prior uncertainties have been given as k=1. When stating the uncertainty on plots, the expanded uncertainty (k=1.96) is stated, such that:

$$U = k \cdot u$$

Such a coverage factor should result in a 95% confidence interval.

Appendix G: Temperature factor uncertainty

A temperature factor (f_{Rsi}) below the critical temperature factor (f_{CRsi}) of 0.75 is considered a risk of surface condensation and mould growth. Each DEEP in-situ f_{Rsi} measurement is associated with an uncertainty of ±0.03. This value was derived using uncertainty propagation of the temperature measurements and applies to the entire range of f_{Rsi} measurements in DEEP. Therefore, a location with an f_{Rsi} of 0.77 could also be considered a potential risk.

The surface temperature of each junction in the Energy House and condition void was only measured using a thermocouple at one location. Thermography was used to identify measurement locations that were deemed representative of each junction. However, the selection of a representative location is also associated with uncertainty. Figure G1 shows a thermogram of the eaves junction in Bedroom 1 at Stage 2 of the DEEP retrofit.

Figure G1: Thermogram of the eaves junction in Bedroom 1 at Stage 2 of the DEEP retrofit. Location of surface temperature thermocouple circled

The thermogram was used to calculate the in-situ f_{Rsi} at each pixel along the eaves junction. The distribution is seen in Figure G2.
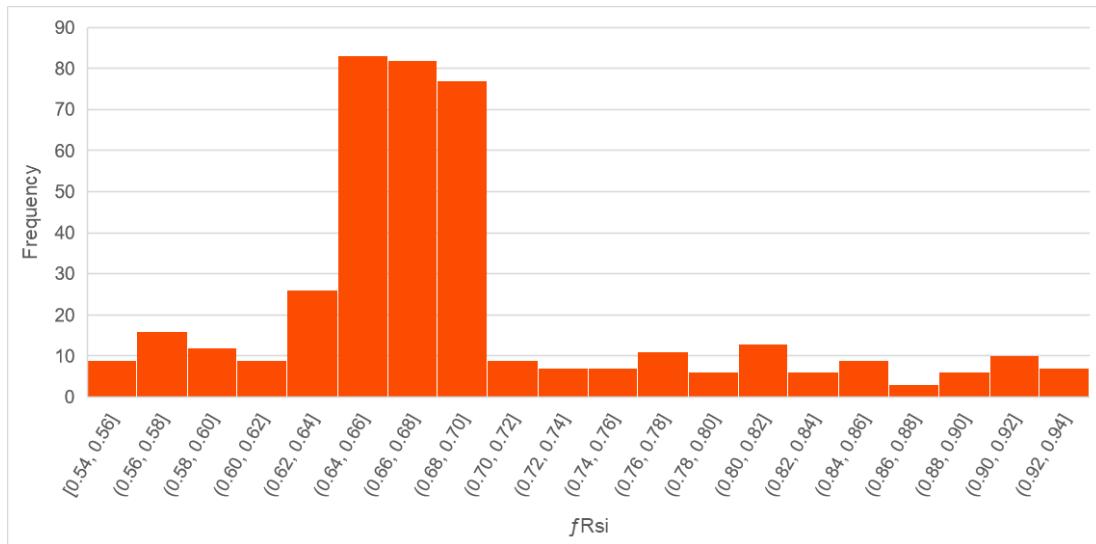
Figure G2: Frequency distribution of eaves in-situ f_{Rsi} measurements obtained using thermography

The f_{Rsi} distribution ranges from 0.54 to 0.93 with a mean of 0.69 and a standard deviation of 0.08. The mean is in good agreement with the f_{Rsi} measured at the location of the surface temperature thermocouple of 0.69 (±0.03). This suggests the surface temperature thermocouple was situated in a representative location. However, the thermogram also include locations with joists, surface conduit, sensor cables, and the reflective tape used to mount the surface temperature thermocouple. Therefore, the mean cannot be considered representative. Figure G3 shows a box plot of the in-situ f_{Rsi} measurements derived from thermography.
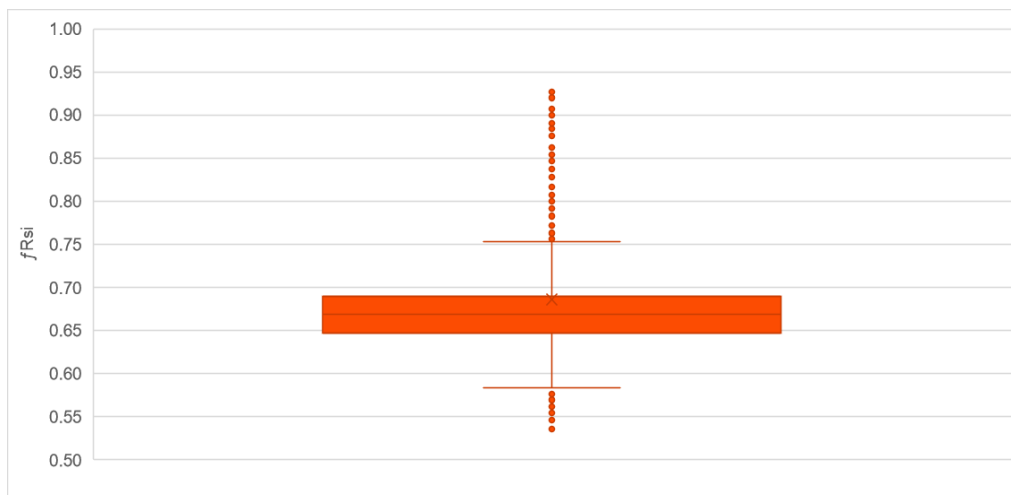
Figure G3: Box plot of the in-situ f_{Rsi} measurements derived from thermography

The median in-situ f_{Rsi} derived from thermography of 0.67 could be considered more representative of the eaves junction as it is less influenced by outliers. To account for uncertainty due to sensor placement, location uncertainty was calculated using difference between the median (0.67) and upper (0.69) and lower (0.65) quartiles. This resulted in a location uncertainty of ±0.02.

To account for the DEEP f_{Rsi} measurement uncertainty of ±0.03 and surface temperatures and ±0.02 location uncertainty, the f_{CRsi} of 0.75 was expanded to include in-situ f_{Rsi} measurements between 0.70-0.079. f_{Rsi} <0.70 is deemed high risk and ≥0.80 is considered low risk.

81

This publication is available from: https://www.gov.uk/government/publications/demonstration-of-energy-efficiency-potential-deep

If you need a version of this document in a more accessible format, please email: alt.formats@energysecurity.gov.uk
Please tell us what format you need. It will help us if you say what assistive technology you use.